Development and Characterization of Electrically Conductive Thermoplastic Based Composite Materials for Fuel Cell Bipolar Plates

by

Muhammad Tariq

A thesis submitted to the
School of Graduate and Postdoctoral Studies in partial
fulfillment of the requirements for the degree of

Doctor of Philosophy in Mechanical Engineering

Department of Mechanical and Manufacturing Engineering/Faculty of Engineering and
Applied Science

University of Ontario Institute of Technology (Ontario Tech University)

Oshawa, Ontario, Canada
August 2022

© Muhammad Tariq, 2022

ABSTRACT

Thermoplastic composites exhibit multiple attractive attributes, such as lightweight, low cost, ease and speed of manufacturing, and ability to recycle, which make them ideal for a wide range of applications. Composites containing conductive fillers have lower resistivity and better ability to conduct heat and electricity, which make them potential candidates for fuel cell bipolar plates. The purpose of this study is to develop electrically conductive thermoplastic composites that can be used for the manufacturing of fuel cell bipolar plates. Graphite, Carbon Fiber (CF), Multi-walled Carbon Nanotubes (MWCNT), Carbon Black (CB), and Expanded Graphite (EG) were used as conductive fillers. These fillers were added to three different polymer matrices: Polypropylene (PP), Nylon, and Thermoplastic Polyurethane (TPU). The composites were prepared using the melt-compounding technique in a twin-screw extruder. Thermogravimetric Analyzer (TGA), Differential Scanning Calorimetry (DSC), Digital microscope, and Scanning Electron Microscope (SEM) were used for thermal and morphological characterization. The flexural strength testing of the composites was carried out by using a Dynamic Mechanical Analyzer (DMA). The conductive fillers were added to the polymer in binary, ternary, and quaternary configurations. A full factorial design of L-27 Orthogonal Array (OA) was used as a Design of Experiment (DOE) to evaluate the effect of the filler and the possibility of any interactions between them. The experimental data were interpreted by the Analysis of Variance (ANOVA) to evaluate the significance of each secondary filler. The material formulation with 4 wt.% MWCNT, 5 wt.% CB, 30 wt.% EG, and 25 wt.% PP was the best formulation in terms of material properties, having an electrical conductivity of 124.7 and 39.6 S/cm in in-plane and through-plane directions, and flexural strength of 29.4 MPa. Furthermore, statistical modeling was performed by Response Surface Methodology (RSM) to predict the properties of the, which demonstrated an average accuracy of 83.9% and 93.4% for predicting the values of electrical conductivity and flexural strength, respectively. Also, the bipolar plates were manufactured by sheet extrusion process to examine the processability of electrically conductive thermoplastic composites.

Keywords: Bipolar plates, thermoplastic composites, graphite, MWCNT, carbon black, expanded graphite, optimization

AUTHOR'S DECLARATION

I hereby declare that this thesis consists of original work of which I have authored. This is a true copy of the thesis, including any required final revisions, as accepted by my examiners.

I authorize the University of Ontario Institute of Technology (Ontario Tech University) to lend this thesis to other institutions or individuals for the purpose of scholarly research. I further authorize University of Ontario Institute of Technology (Ontario Tech University) to reproduce this thesis by photocopying or by other means, in total or in part, at the request of other institutions or individuals for the purpose of scholarly research. I understand that my thesis will be made electronically available to the public.

MUHAMMAD TARIQ

STATEMENT OF CONTRIBUTIONS

The experimental work described in this thesis was performed at the Dick McLaughlin Manufacturing Design Lab (ACE-3030A Lab), Ontario Tech University, under the supervision of Dr. Ghaus Rizvi and Dr. Remon Pop-Iliev

Some parts of this thesis have been published in the following research publications:

- M. Tariq, N.A. Syed, U. Utkarsh, A.H. Behravesh, R. Pop-Iliev, G. Rizvi, Synergistic enrichment of electrically conductive polypropylene-graphite composites for fuel cell bipolar plates. Int J Energy Res. 2022;1-10. doi:10. 1002/er.7898

- M. Tariq, Utkarsh, N.A. Syed, A. Baten, A.H. Behravesh, G. Rizvi, R. Pop-Iliev, Effect of Filler Content on the Electrical Conductivity of Graphite Based Composites, in: Proceedings of SPE ANTEC 2021, United States, 2021.

- M. Tariq, N.A. Syed, U. Utkarsh, A.H. Behravesh, R. Pop-Iliev, G. Rizvi, Investigation of different bonding matrices for the development of electrically conductive thermoplastic composites, in: Polymer Processing Society (PPS-37), Fukuoka, Japan, 2022.

I carried out the experimental work (manufacturing and characterization of composites) along with the writing of the manuscript

A part of the work described in Chapter 4 is in correspondence as:

M. Tariq, N.A. Syed, U. Utkarsh, A.H. Behravesh, R. Pop-Iliev, G. Rizvi, Optimization of Filler Compositions of Electrically Conductive Polypropylene Composites for the Manufacturing of Bipolar Plates. Composite Science and Technology (under review)

I carried out the experimental work (manufacturing and characterization of composites) along with the writing of the manuscript

TABLE OF CONTENTS

List of Figures

LIST OF TABLES

LIST OF ABBREVIATIONS AND SYMBOLS

ANOVA   Analysis of Variance

ASTM   American Society for Testing and Materials

CB   Carbon Black

DMA   Dynamic Mechanical Analyzer

DOE   Design of Experiments

DSC   Differential Scanning Calorimetry

EG   Expanded Graphite

IPEC   In-Plane Electrical Conductivity

MWCNT   Multi-Walled Carbon Nanotubes

PA-6   Polyamide-6

PP   Polypropylene

PVA   Polyvinyl Alcohol

PVC   Polyvinyl Chloride

PVDF   Polyvinyl Difluoride

PVP   Polyvinylpyrrolidone

RPM   Revolutions Per Minute

RSM   Response Surface Methodology

SEM   Scanning Electron Microscope

SSE   Single Screw Extruder

TGA   Thermogravimetric Analyzer

TPEC   Through-Plane Electrical Conductivity

TPU   Thermoplastic Polyurethane

ϕ Filler weight fraction

σ Electrical conductivity

Chapter 1: Introduction

The chapter provides the background and introductory information related to PEM fuel cells, bipolar plates, materials available for the manufacturing of bipolar plates, and electrically conductive thermoplastic composites. Moreover, the motivation, thesis objectives, and thesis novelties are also described

1.1 Background

Thermoplastic resins usually have very high electrical resistivity and are commonly used for insulation on electric wires. The addition of carbon fillers changes their nature from insulator to conductor and allows them to be used in totally different applications. Thermoplastics are lightweight, cheaper, non-corrosive, and most importantly, easy to process compared to most materials, including metals and thermosets. These benefits have been motivating industries to replace metals and thermoset composites with thermoplastics in many applications over the last three decades. However, the insulating behavior of polymer materials is the main barrier to replacing metal with plastic in applications that require the conduction of heat and electricity. Adding conductive fillers overcomes this restriction and lets such composites compete with the metals and alloys for such applications.

One potential market for electrically conductive thermoplastic materials is that of fuel cell bipolar plates. A fuel cell converts the chemical energy of the fuel into electricity by electrochemical reactions. Fuel cells exhibit higher operational efficiency than internal combustion engines since they directly convert chemical energy into electrical energy without undergoing a combustion reaction and do not contain any moving parts that produce noise and friction during the operation. In addition, hydrogen fuel cells emit only water and a small amount of heat without producing carbon dioxide. Therefore, a fuel cell is an environmentally friendly, silent, reliable, and fuel-efficient power source. Proton Exchange Membrane (PEM) fuel cells have a relatively low operating temperature and can be used as eco-friendly power sources in a variety of applications, including homes, data centers, portable communication towers, cars, buses, and trains. The National Aeronautics and Space Administration (NASA) also considered the PEM fuel cells leading candidates to replace old alkaline fuel cells for future space shuttles.

The commercialization of fuel cells in transportation and other industries has been obstructed by the weight, cost, and size of the fuel cell stack. A PEM fuel cell stack is an assembly of multiple PEM fuel cells formed by connecting a series of bipolar plates with a proton exchange membrane between them. Bipolar plates play a significant role in the operation of PEM fuel cells by distributing hydrogen and oxygen, passing electrons between cells, preventing gases from leaking, and removing the excess heat generated during the electrochemical process. Bipolar plates, on the other hand, account for 45-60% of a fuel cell's stack cost, 70-80% of its total weight, and a significant portion of its volume. Due to the high material costs and time-consuming processes involved in the fabrication of fuel cell bipolar plates, PEM fuel cells are significantly expensive, heavy, and bulky. The fuel cell industry has made substantial efforts to minimize the material cost, weight, and size of bipolar plates, as well as to find convenient and cost-effective ways to manufacture them.

The conductive polymer composites are considered to be better potential candidates for bipolar plates. Different types of conductive fillers are commercially available in the market and are divided into two main groups: metal-based and carbon-based fillers. Stainless steel fibers, aluminum fibers, copper fibers, and flakes of silver and copper are the usual metallic fillers. The most commonly used carbon-based conductive fillers are synthetic graphite, natural graphite flakes, carbon black, and carbon nanotubes. The conductivity of the composites depends on the type, shape, and amount of filler inside the polymer matrix. However, in the case of binary or ternary filler formations, the synergistic effects of fillers also determine the conductivity. The electrical conductivity values (S/cm) for some materials are given in Table 1.1.

Table 1.1: Electrical Conductivity of materials[1].

Materials	Electrical Conductivity (S/cm)
Silver	6.3×10^5
Copper	5.9×10^5
Aluminum	3.7×10^5
Steel	10000
Carbon (amorphous)	300
Polymers	10^{-7} to 10^{-14}

1.2 Motivation

A hydrogen fuel cell is an environmentally friendly power source that can be used in a wide range of applications. Similar to Internal Combustion Engine (ICE) cars, fuel cell cars can be refueled in a matter of minutes and can power the vehicle for hundreds of kilometers on a single fill. Fuel cells are more efficient than ICEs as they convert fuel into electricity without converting fuel into heat. Therefore, a fuel cell-powered vehicle can travel more than a gasoline vehicle on the same calorific amount of fuel. In contrast to ICE, fuel cells do not have moving parts, which makes maintenance much cheaper and easier. Batteries can also be replaced by fuel cells in the backup power systems and other power stations since fuel cells provide direct current continuously and do not need to be recharged for a long period of time. The use of electrically conductive polymer composites will reduce cost, weight, and size, as well as make the production process easier and cost-efficient. The production of low-cost and compact-sized fuel cells can induce power industries to replace ICE with fuel cells. Widespread use of fuel cells can help combat global warming and lower greenhouse gas emissions. Therefore, the main motivation of this research is to reduce the overall cost of fuel cells by developing thermoplastic composites for cost effective and faster manufacturing of bipolar plates.

1.3 Problem Statement

A number of comprehensive studies have been published in the literature that investigates conductive polymer composites and their applications in various industrial applications [18,19]. There has been increased interest in electrically conductive composite materials over the past few years, leading researchers across the globe to examine the feasibility of using plastic resins for manufacturing bipolar plates [14–17]. For producing good quality bipolar plates, these composites should be electrically and thermally conductive, have good flexural strength, have good corrosion resistance in the acidic environment, and also have low gas permeability [1,2]. Table 1.2 shows the technical targets set by the US Department of Energy for fuel cell bipolar plates.

Many companies have adopted thermoset composites for manufacturing fuel cell bipolar plates. The low viscosity of thermoset resin enables the fabrication of composite at high filler compositions [1]. At higher filler loadings, the thermoset composites usually

have better bending strength and toughness than the thermoplastic composites [1]. However, a major concern with thermoset bipolar plates is their low production rate due to the manufacturing processes used. Another drawback is that thermosets are not recyclable, which makes them environmentally unfavored.

The feasibility of producing bipolar plates with the thermoplastic matrix has also been studied in the literature [20–22]. It is challenging to fabricate highly filled thermoplastic composites because of the higher viscosity of the resin, which causes poor dispersion of particles in the matrix resulting in lower strength and conductivity. The properties of thermoplastic composite bipolar plates are heavily influenced by the type of conductive filler, the total filler content, and the bonding between the filler and the matrix. Increasing the filler content improves electrical conductivity but reduces mechanical strength [1]. Filler loading must be optimized to achieve better electrical conductivity and flexural strength for bipolar plates [2]. Electrons need adequate through-plane electrical conductivity to travel from one cell to another. It has been observed that the electrical conductivity of the composite material in the through-plane direction is many times lower than that in the in-plane direction [23,24].

A number of researchers have investigated the use of graphite [15], carbon nanotubes [25], carbon black [26], carbon fiber [23], and expanded graphite [27] as conductive fillers for thermoplastic composites. Studies have also been conducted on polymers such as polypropylene [11,15], polyethylene [28], polyphenylene sulfide (PPS) [11], nylon [16], polyvinylidene fluoride (PVDF) [29] as matrix materials for conductive composites. However, a comprehensive study investigating the synergistic effects of these fillers in binary, ternary, and quaternary filler configurations has not been well documented in the literature. Also, comparing the electrical and mechanical properties of composites developed from different thermoplastic matrices to understand how the bonding matrix affects the composites' overall properties has not yet been well documented in the literature. Furthermore, there is a need for optimization studies to obtain a filler composition that would optimize electrical conductivity and flexural strength.

Table 1.2: Technical targets of US Department of Energy for fuel cell bipolar plates [5,30].

Property	Units	Target
Cost	$/kW	3
Weight	kg/kW	0.4
Electrical Conductivity	S/cm	>100
Flexural Strength	MPa	>25
Corrosion resistance	$\mu A/cm^2$	<1
Hydrogen Permeation Coefficient	$cm^3/sec.cm^2$	1.3×10^{-14}

1.4 Objectives

This research focuses on the development of electrically conductive thermoplastic composites that can be used for the manufacturing of fuel cell bipolar plates. The composite bipolar plate materials available in the market are mostly made from thermoset resin which can not be processed through the high production rate manufacturing processes. This research intends to develop thermoplastic composites by adding multiple conductive fillers in three different thermoplastic resins and compare the properties with the commercially available thermoset bipolar plates. This thesis is also concerned with the optimization study to achieve the optimum values of electrical conductivity and flexural strength. Additionally, this thesis examines the fabrication of thermoplastic composite bipolar plates by sheet extrusion process. The following are the objectives of this research,

- **To develop electrically conductive thermoplastic-based composite materials for fuel cell bipolar plates that satisfy the requirements of electrical conductivity and flexural strength.**

  The main objective of this research is to produce a thermoplastic composite that can be used for the manufacturing of fuel cell bipolar plates. It involves the development and characterization of electrically conductive thermoplastic composites based on different conductive fillers and thermoplastic resins.

- **To develop composites at different material formulations to study the effects of filler content and bonding matrix on the electrical conductivity and flexural strength of electrically conductive thermoplastic composites.**

  One of the objectives of this study is to investigate the effect of filler content on the properties of the composite material. This includes (a) manufacturing of single filler composites and examination of the electrical and mechanical performance of the composites at different filler compositions, (b) incorporation of binary fillers to the single filler composites, and investigation of the synergistic effects of binary fillers on the electrical conductivity and flexural strength, and (c) development of thermoplastic composites by using three different thermoplastic resins and analyzing how inherent properties of the bonding matrix affect the overall properties of the composites.

- **To develop a statistical model to optimize the filler formulation to achieve the optimum values of electrical conductivity and flexural strength of the composites.**

  There is a need for optimization studies to obtain a filler composition that would provide the most suitable value of electrical conductivity and flexural strength of the composites. This includes: (a) mixing of Graphite, CB, MWCNT, and EG with the polymer matrix in binary, ternary, and quaternary filler formulation, (b) analyzing the effect of filler combinations on electrical conductivity and flexural strength, (c) development of the Design of Experiments to carry out the experiments and collect data for optimization study, (d) processing of experimental results by ANOVA to analyze the significance of each conductive filler, and (e) statistical modeling by using RSM to predict the values of electrical conductivity and flexural strength of the composites.

- **To examine the processability of electrically conductive thermoplastic composites**

  This study investigates the feasibility of using the sheet extrusion process to manufacture thermoplastic composite bipolar plates. This involves sheet extrusion

of highly filled thermoplastic composite material and fabrication of gas flow channels on the surface of composite sheets.

- **To investigate the feasibility of using thermoplastic resin for the manufacturing of bipolar plates by comparing the properties of the thermoplastic composites with the commercially available thermoset bipolar plates**

  The low viscosity of thermoset polymer makes it easier to manufacture highly filled composites. Also, the toughness of the highly filled thermoset composites is better than the thermoplastic composites. However, the main issues are the availability of the manufacturing processes and the processing time required to produce thermoset bipolar plates. This research has the goal of assisting fuel cell manufacturers in switching from thermoset to thermoplastic bipolar plates. This includes (a) development and characterization of electrically conductive thermoplastic composites, (b) data collection on the properties of the thermoset bipolar plates currently on the market, and (c) comparison of experimental results of this thesis with those of the thermoset bipolar plates.

1.5 Novelties

The original work in this thesis is described below:

- Development of thermoplastic composites by adding different conductive fillers in binary, ternary, and quaternary formulations, and investigation of synergistic effects of filler interaction on the properties of electrically conductive thermoplastic composites.
- Development of thermoplastic composites by using different polymer resins and the investigation of the effect of bonding matrix on the properties of electrically conductive thermoplastic composites.
- Development of an empirical model to predict the values of electrical conductivity and flexural strength of the thermoplastic composites by utilizing ANOVA and RSM.

1.6 Thesis Outline

The thesis consists of six chapters. The first chapter provides a basic introduction to bipolar plates, the availability of materials for the manufacturing of bipolar plates, and the advantages of producing bipolar plates from electrically conductive thermoplastic composites. Furthermore, the motivation of this research, problem statement, thesis objective, novelties, and thesis outline are also discussed in this chapter.

Chapter two is based on the theoretical background and a comprehensive literature review of the PEM fuel cells, bipolar plates, manufacturing of bipolar plates, material selection of bipolar plates, and conductive polymer composites. Furthermore, the chapter discusses the problems associated with using graphite bipolar plates, metallic bipolar plates, and thermoset composite bipolar plates and the advantages of manufacturing bipolar plates with thermoplastic composites. In closing, this chapter summarizes past research studies on the development of electrically conductive thermoplastic composites and identifies major research gaps.

Chapter three provides the details of the experimental procedure and equipment used for the manufacturing and characterization of electrically conductive thermoplastic composites. The manufacturing part of this chapter describes the details of the material used in this research and their properties, the equipment, and the methodologies used for the manufacturing and processing of composite materials. The instruments and techniques used for the electrical, mechanical, thermal, and morphological characterization of the composites are described in the characterization section.

Chapter four discusses the results obtained through material testing and characterization. This chapter is mainly divided into three different studies. The first part investigates the effects of filler composition on the electrical and mechanical properties of the composites. This investigation study includes single filler and binary filler composites. Graphite was added to the polypropylene at different compositions to produce single filler PP/graphite composites. The synergistic effects of adding binary fillers on the electrical and mechanical properties of the composites were evaluated in the second step, where CB and MWCNT were added as binary filler to the single filler PP/graphite composites. The second part of this chapter examines the effects of polymer matrix on the properties of

electrically conductive thermoplastic composites. PP, nylon, and TPU were used to develop thermoplastic composites. The graphite was added to these polymer matrices to produce single filler PP/graphite, nylon/graphite, and TPU/graphite composites. The CB was added to the single filler composites to produce binary filler composites. The effects of polymer matrices were investigated by comparing the properties of PP, nylon, and TPU composites. The last part of this chapter includes an optimization study in which the compositions of the conductive filler were optimized to obtain the optimum value of electrical conductivity and flexural strength. Graphite was used as a primary filler, whereas MWCNT, CB, and EG were added as secondary fillers. The parametric evaluation of the secondary filler compositions has been carried out to achieve the most suitable value of electrical conductivity and flexural strength. The significance of each secondary filler was evaluated by ANOVA. An empirical model was also developed by using RSM to predict the values of electrical conductivity and flexural strength of the composites.

Chapter 5 discusses the feasibility of fabricating bipolar plates out of electrically conductive thermoplastic composites using sheet extrusion. The process involved in the sheet extrusion of highly filled thermoplastic composites has been described in detail. The method of forming gas flow channels on the surface of composite sheets has also been explained.

Chapter 6 is the last chapter which summarizes the experimental investigations conducted in this thesis. This chapter provides the summary of the study, as well as recommendations for future work.

Chapter 2: Theoretical Background

This chapter provides a detailed literature survey and theoretical background of the PEM fuel cells, bipolar plates, manufacturing of bipolar plates, material selection of bipolar plates, and conductive polymer composites. Also, the advantages of manufacturing bipolar plates with thermoplastic composites are discussed in this chapter.

2.1 Fuel Cell

A Fuel cell is an electrochemical device that produces power by converting chemical energy into mechanical energy without undergoing any combustion reaction. It is considered a clean energy source that can be used in automobiles and portable and stationary power stations [5,31]. The concept of fuel cells was first introduced by the Welsh scientist William Robert Grove in 1839 [5]. He electrolyzed the water by passing an electric current through it. After the separation of oxygen and hydrogen, he replaced the current source with an ammeter. The hydrogen and oxygen started to recombine again after the removal of the power source from the circuit. This reversed electrolysis reaction produced water and a small amount of electric current measured by the ammeter. The first fuel cell system was developed by Grove in 1843, which he called a "gas battery"[5]. Later on, the term "fuel cell" was introduced by Charles Langer and Ludwig Mond in 1889. Hydrogen gas is used as a fuel in hydrogen fuel cells that combine with oxygen to generate electricity and produce water as a primary byproduct [32], as shown in Figure 2.1.
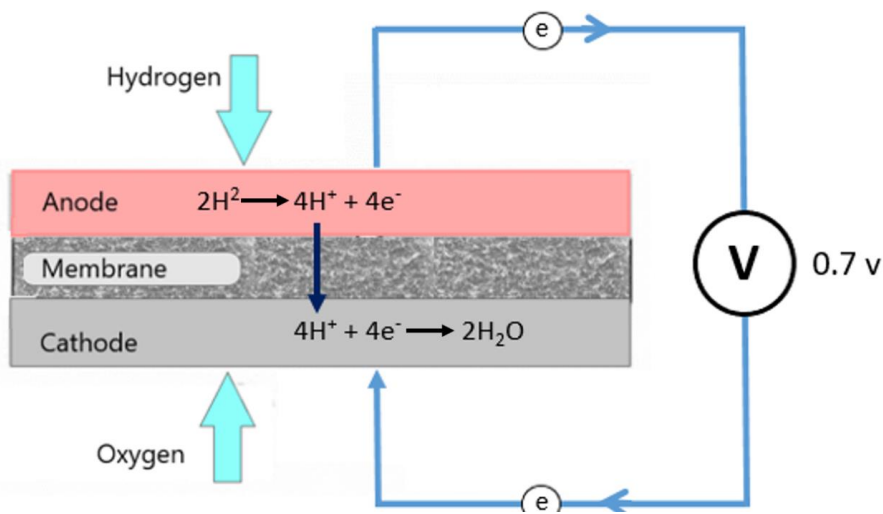
Figure 2.1: Schematic diagram of PEM fuel cell.

2.2 Types of Fuel Cells

The fuel cells are divided into different categories according to the electrolytes used inside them. The types of fuel, catalyst, chemical reaction, and operating temperature range of the fuel cell are determined by the types of electrolytes used inside the fuel cell. Each fuel cell type has a different operating temperature range, applications, advantages, and also limitations [5]. Table 2.1 summarizes the data of each type of fuel cell. This research focuses on the electrically conductive composites material that can be used in a proton exchange membrane (PEM) fuel cell.

Table 2.1: Properties of different types of fuel cells [5].

Type	Electrolytes	Temperature range (℃)	Fuel	Power output (W)
Alkaline fuel cell	KOH solution	50 - 200	Hydrogen gas	1k - 10k
PEM fuel cell	Solid ion exchange membrane	60 - 120	Hydrogen gas	1 - 1M
Direct methanol fuel cell	Solid ion exchange membrane	50 - 140	Methane gas	1 - 100
Phosphoric acid fuel cell	Phosphoric acid	220	Hydrogen gas	10k - 1M
Molten carbonate fuel cell	Li_2CO_2 / K_2CO_3	650	Hydrogen or Methane	100k - 10M
Solid oxide fuel cell	Yttria-stabilized zirconia	950-1050	Hydrogen or Methane	2k - 10M

2.2.1 Proton Exchange Membrane Fuel Cell

Proton Exchange Membrane (PEM) fuel cells use a solid polymer as the electrolytes; thus, they are also known as polymer electrolyte membrane fuel cells. Their electrodes are made up of porous carbon with a platinum catalyst. They operate at around 80 ℃, which is comparatively lower than the other types. A low operating temperature range aids them in starting promptly and makes them more durable. The low operating temperature and quick start ability make them the most promising environmentally friendly power source for locomotives and portable power applications [4,5,33].

The operation of the PEM fuel cell is basically a reverse electrolysis process in which hydrogen combines with oxygen to generate an electric current and produce water as a byproduct. Hence, the emission of PEM fuel cells is water and a slight amount of heat [4,5]. They can rapidly adjust their power output to meet the power demand and can also deliver different combinations of current and voltage. As compared to the other types of fuel cells, they have a better power-to-weight ratio and high power density[4].

Hydrogen
flow field

e^-

Air and
water out

Bipolar Plate
(Anode)

Bipolar Plate
(Cathode)

$2H_2 \rightarrow 4H^+ + 4e^-$

$O_2 + 4H^+ + 4e^- \rightarrow 2H_2O$

Hydrogen
outlet

Air (oxygen)
flow field

Anode
backing

Cathode
backing

Membrane/
Electrode
Assembly
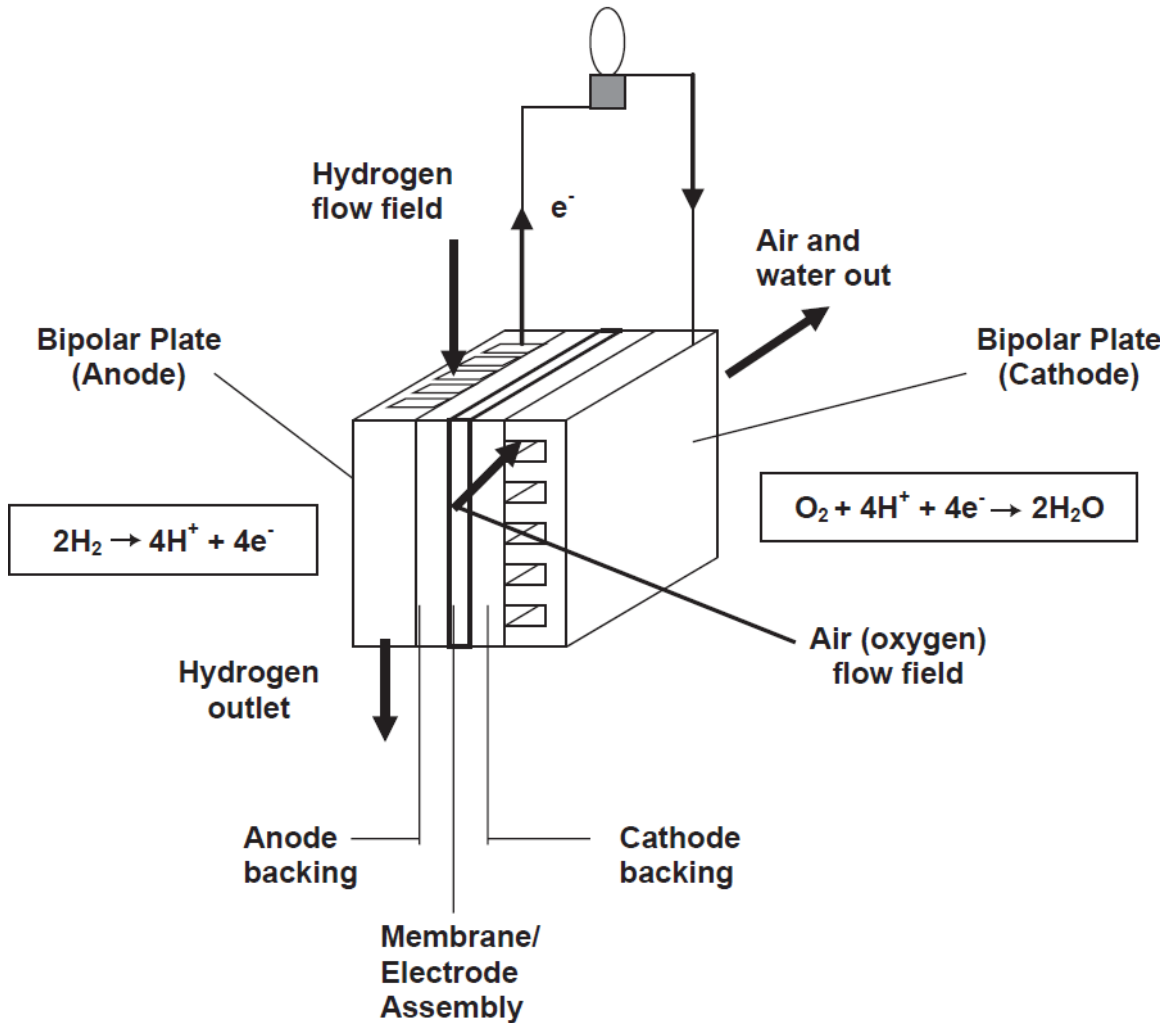
Figure 2.2: PEM fuel cell assembly. Rep. with permission [2].

The PEM fuel cells have three main components: the bipolar plates, backing plates, and proton exchange membrane assembly, as shown in Figure 2.2. Hydrogen gas passes through the anode and strikes with a platinum catalyst to separate electrons and protons. The Proton exchange membrane is designed in such a way that it will only allow protons

to pass through it; thus, electrons have to travel from anode to cathode through the outer circuit. This movement of the electron generates the electric current. Oxygen gas, which flows through the cathode side, reacts with these protons and electrons to produce water as a byproduct [5].

2.3 Bipolar Plates

Bipolar plates play a vital role in PEM fuel cells. Hydrogen gas passes through the anode bipolar plate and interacts with the catalyst to break into electrons and protons. The Proton exchange membrane only allows protons to pass through it; therefore, electrons travel through the outer circuit and generate the electric current [5]. Oxygen gas flows through the cathode bipolar plate, reacts with these protons and electrons, and produces water as a byproduct. Thus, these bipolar plates are responsible for distributing oxygen and hydrogen, passing electrons from one cell to another, keeping reactants separate, and removing the excess amount of heat and water that is generated during the process [2,5]. A fuel cell stack is a series of fuel cells connecting in series. Each cell of the fuel cell stack consists of two bipolar plates (anode and cathode). However, these bipolar plates are also accountable for 70-80% of fuel cell weight, 45-60% stack cost, and a significant portion of fuel cell volume [2,9–11,34]. The purpose of this research is to develop a material that can reduce the material and manufacturing cost, production time, as well as weight of bipolar plates.

2.4 Materials for Bipolar Plates

The material and manufacturing cost of the fuel cells is one of the main hurdles in promoting fuel cells in the commercial sectors. Fuel cell manufacturers are working extremely hard to reduce the weight and cost of bipolar plates, which will make fuel cells more commercially viable in many applications. Efforts are also being made to develop less time-consuming, easier, and cheaper manufacturing processes for bipolar plates [2,9]. As shown in Figure 2.3, the bipolar plates that are commercially available in the market can be classified according to their material into three categories.

1. Graphite bipolar plates
2. Metallic bipolar plates
3. Composite bipolar plates
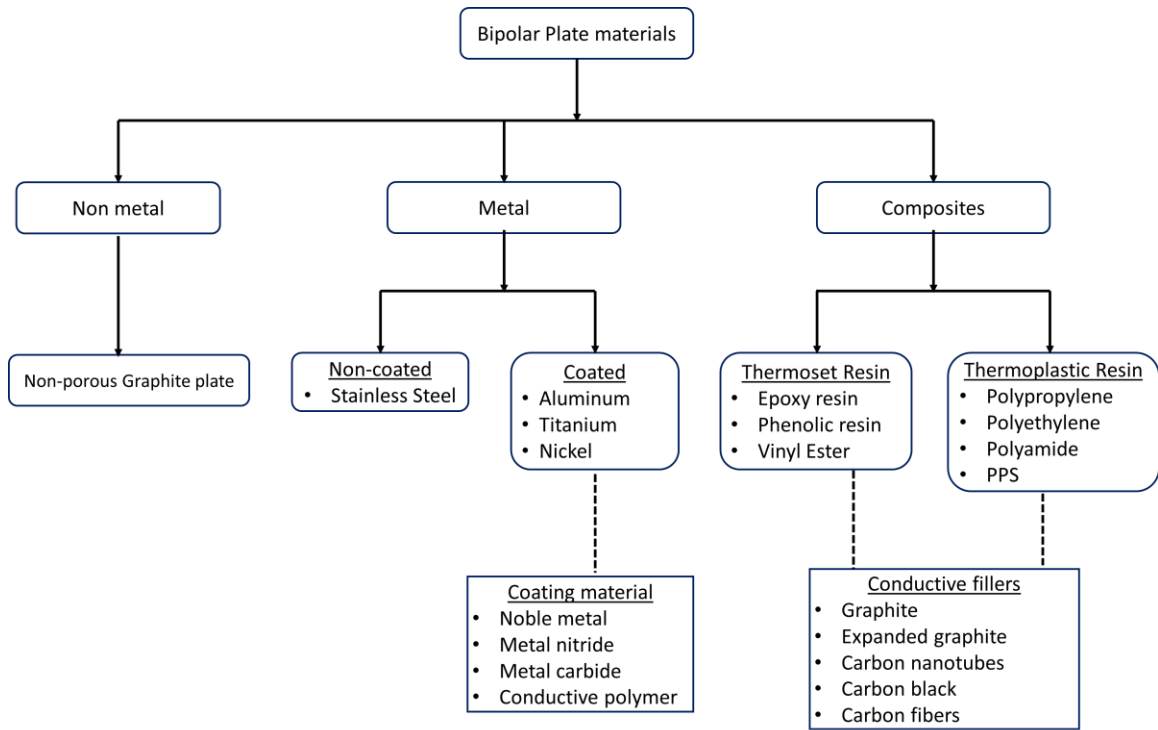
Figure 2.3: Materials for bipolar plates.

2.4.1 Graphite Bipolar Plates

The most common traditional material for bipolar plates is graphite. The graphite bipolar plates offer excellent corrosion resistance and chemical stability in the acidic environment of fuel cells and also have high electrical conductivity. However, the high material cost, poor mechanical strength, and complicated manufacturing processes for machining the gas channels are the core issues associated with these bipolar plates [2]. A comparatively thicker bipolar plate is required to compensate for the mechanical strength, increasing the overall weight and volume of the stack. Also, the porous structure of graphite requires an impregnation process for making non-porous plates to make the surface gas impermeable. Considering these issues, the fuel manufacturers are reluctant to use graphite bipolar plates for automotive, and other portable applications and are looking for an alternate material [1].

2.4.2   Metallic Bipolar Plates

Metallic bipolar plates have very high electrical and thermal conductivities and good mechanical strength. Sheet metals can easily be shaped through die stamping, making the fabrication of flow channels significantly easier, faster, and cheaper. Also, high mechanical strength allows the manufacturer to produce thinner plates, resulting in smaller and lighter fuel cell assembly [1,9]. These benefits make the metal a potential candidate for bipolar plate material. However, the PEM fuel cell's operating environment is acidic in nature, with a PH level between 2 to 3. These metallic bipolar plates are likely to suffer from corrosion and dissolution when they are exposed to the fuel cell environment at a temperature around 80 C to 120 C [35,36]. The formation of oxide layers on the surface of metallic bipolar plates increases the electrical resistance, reduces the power output, and makes them less efficient for industrial applications[37]. Moreover, the dissolved metal ions are harmful to the electron membrane and reduce the ionic conductivity. To solve these issues, a protective layer is applied to some metals to prevent them from corrosion. Hence, these metallic bipolar plates are further classified into non-coated metals and coated metals.

2.4.2.1 Non-coated

Stainless steel is the only metallic material that can survive the corrosive environment of fuel cells without any protective coating. Research studies on the stainless steel bipolar plates show a low corrosion rate and constant fuel cell power output of thousands of hours [38,39]. However, the contact resistance of stainless steel is comparatively high, affecting the overall fuel cell performance. Austenitic and ferritic stainless steels with high chromium content have better corrosion performance[40,41]. Though, they still need improvement in corrosion and contact resistance to be used for bipolar plates[2].

2.4.2.2 Coated

Metals like aluminum, titanium, nickel, and some grades of stainless steel are prone to corrosion in the acidic environment of fuel cells. They need a coating of a protective layer on their surface[2,12]. These protective coating should be conductive in nature in order to avoid any performance losses. These coating materials are fundamentally divided into two types: metal-based and carbon-based. The metal-based coating includes metal nitrides and

metal carbides, whereas graphite and conductive polymers are used as carbon-based coatings [12,13].

These coated bipolar plates are not a feasible solution. The difference in the thermal expansion rate of coating material and base metal generates micro-pores and micro-cracks[2]. One researcher has investigated gold-plated stainless-steel plates in a study. The performance of the gold-plated stainless steel plate was almost identical to the graphite bipolar plates[37]. However, these gold plating treatments and other processing make these bipolar plates difficult to meet the cost requirement.

2.4.3 Composite Bipolar Plates

Polymers are lightweight and easy to mold into any shape and size. Mixing conductive fillers with the polymer forms an electrically conductive composite material. The ability to conduct electricity, along with other benefits of polymer material, makes these composites the most promising materials for the manufacturing of bipolar plates[1,2,9,15,16,42]. Metal-based fillers and carbon-based fillers can be added to the polymer matrix to increase electrical conductivity. Metal-based fillers are very conductive, but due to their very high density and corrosion issues in the acidic environment of fuel cells, they are not suitable for composite bipolar plates[2]. The polymer resins are also divided into two fundamental categories. These are thermoset bipolar plates and thermoplastic bipolar plates.

2.4.3.1 Thermoset Resins

The possibility of manufacturing bipolar plates from thermoset composites has been examined in many research studies. The electrical properties mainly depend on the amount of filler loading and types of filler inside the polymer matrix. The viscosity of thermoset plastic is comparatively lower than the thermoplastic material, which allows the manufacturer to produce highly filled composite material [1]. Also, the toughness and the bending strength of thermoset composites are better than those of thermoplastic composites [1]. However, the main issue in producing the bipolar plates with thermoset resin is the time taken by the manufacturing processes. The thermoset composites cannot be produced by using high production rate processes such as injection molding and sheet extrusion. The processing of thermoset composite is also time-consuming due to the long curing times required. Vinyl ester can be cured in ten minutes, but the mechanical properties of vinyl

ester are inferior to epoxy resin [43]. The composite bipolar plates manufactured from vinyl ester and epoxy resin are currently available in the market. Table 2.2 shows the list of commercially available composite bipolar plates and their properties. Moreover, thermoset composites cannot be recycled, so they are not environmentally friendly. Therefore, researchers are exploring the possibilities of producing bipolar plates with thermoplastic-based composites.

Table 2.2: Properties of commercially available thermoset composite bipolar plates.

Manufacturer/ Patent	Polymer	Filler Graphite (wt.%)	Electrical Conductivity (S/cm)		Flexural Strength (MPa)
			In-plane	Through-Plane	
LANL (US) [43]	Vinyl Ester	68	60	-	30
Premix Inc. [43]	Vinyl Ester	68	85	-	28.2
BMC [43]	Vinyl Ester	69	30	-	27.9
BMC940-15252A	Vinyl Ester	-	133	25	56
Plug Power [44]	Vinyl Ester	68	55	-	40
DuPont [1]	Vinyl Ester	-	-	25-33	53
SGL [1]	-	-	100	20	40
GTI (US) [45]	Phenolic	77.5	53	-	-
ORNL (US) [46]	Phenolic	Carbon Fiber	200	-	-

2.4.3.2 Thermoplastic Resins

The electrically conductive thermoplastic composites are potential candidates for the manufacturing of bipolar plates as they are more versatile in terms of manufacturing processes. Thermoplastics composites can be recycled, remelted, and manufactured by the fastest and most cost-effective production processes like injection molding [47]. However, it is challenging to manufacture bipolar plates from thermoplastic composites because of their high viscosity, making uniform mixing difficult. The properties of thermoplastic composite bipolar plates are heavily influenced by the type of conductive filler, the total filler content, and the bonding between the filler and the matrix. Increasing the filler content improves electrical conductivity but reduces mechanical performance [1]. Thus, one of the most important challenging issues is to enhance electrical properties while maintaining the mechanical properties in acceptable ranges. Hence, filler contents must be optimized to achieve optimal electrical conductivity and flexural strength for bipolar plates [2]. Adequate through-plane electrical conductivity is required for electrons to travel from

one cell to another in a fuel cell stack. The electrical conductivity of the composite material in the through-plane direction is many times lower than that in the in-plane direction [23,24].

The feasibility of using thermoplastic resins including polypropylene (PP) [11,15], polyethylene (PE) [28], polyphenylene sulfide (PPS)[11], polyamide 6 (PA6) [16], polyvinylidene fluoride (PVDF) [29], polyethylene terephthalate (PET) [29], and liquid crystalline polymers [48] have been investigated in the literature. There are many factors that determine the characteristics of composite bipolar plates. As the filler loading increases, the conductive paths inside the composite increase, but the mechanical performance of the composite is reduced due to poor wetting of the filler with the resin. The trade-off between flexural strength and electrical conductivity is the main challenge for scientists[1]. The thermoplastic composite bipolar materials found in the literature have a filler composition between 50 wt.% to 80 wt.%. Increasing the filler content over 80 wt.% compromises the mechanical properties while decreasing the filler content below 50 wt.% reduces the electrical conductivity below the desired level [1,9]. Researchers are making continuous efforts to obtain a balance between electrical conductivity and mechanical strength.

Lawrence [49] added the graphite in PVDF by varying the graphite content from 74 wt.% to 94 wt.%. He achieved the electrical conductivity of 277 S/cm in the in-plane direction at 86 wt.%. However, the flexural strength was only 1350 psi (9.3 MPa) due to a very high filler loading. This research work was further continued by Balko et al. [50] by reinforcing the composite with carbon fibers. They successfully increased the flexural strength to 42.7 MPa by adding 64 wt.% graphite and 16 wt.% of carbon fiber in PVDF, but the electrical conductivity was reduced to 98 S/cm. Researchers also used PPS as a polymer matrix. Li-gang Xia et al.[51] mixed 80 wt.% of graphite in PPS and achieved the in-plane electrical conductivity of 118.9 S/cm with a flexural strength of 52.4 MPa. Cunningham et al. [23] used a wet lay-up process to make PPS composites for bipolar plates. The compositions of graphite and carbon fiber were 70 wt.% and 6 wt.%, respectively. The electrical conductivity in in-plane and through-plane directions was recorded as 325 S/cm and 30 S/cm with a flexural strength of 34.4 MPa.

Dweiri et al. [52] used a combination of 55 wt.% of graphite and 25 wt.% of carbon black in PP and recorded an in-plane electrical conductivity of 36.4 S/cm. Adloo et al. [26] recorded the in-plane electrical conductivity value of 14.92 S/cm and bending strength of 50.9 MPa by adding 6 wt.% of CB and 66 wt.% of graphite to the PP matrix. Mighri et al.[11] investigated the effects of adding graphite and carbon black in PP. They added 38.5 wt.% of graphite with 16.5 wt.% of Carbon black and observed the electrical conductivity of 3 S/cm with a flexural strength of 45 MPa. The electrical conductivity was low due to a low filler loading. The electrical properties of Nylon 6,6 composites were also studied by Heiser et al. [42]. They added a combination of 5 wt.% of carbon black, 30 wt.% of graphite, and 20 wt.% of carbon fiber to Nylon 6,6 by melt-compounding in a twin-screw extruder. They recorded an electrical conductivity of 9.34 S/cm in the through-plane direction[42]. Alo et al. [24] used Polypropylene/epoxy blend as the binding matrix for the composites and recorded the value of in-plane and through-plane electrical conductivity as a function of total filler content. They observed that the in-plane and through-plane electrical conductivities at 50 wt.% filler contents were 49.26 S/cm and 0.37 S/cm, respectively, while at 85 wt.% filler content, these results were 90.34 S/cm and 9.34 S/cm, respectively.

The feasibility of using expanded graphite and carbon nanotubes has also been investigated in the literature. Bairan et al.[53] investigated the effects of multi-filler loading into the polymer matrix. A combination of 49 wt.% of graphite, 25 wt.% of carbon black, and 6 wt.% of carbon nanotubes were used in this study. This filler combination was added to the PP, and an electrical conductivity value of 158.32 S/cm was recorded in the in-plane direction with a flexural strength of 27 MPa. Yan et al. [54] mixed carbon nanotubes with polypropylene at different compositions and recorded the electrical conductivity of the composites as a function of CNT content. Dhakate et al. [27] investigated the effects of EG on the in-plane electrical conductivity of the composites. Herrera et al. [55] investigated the mechanical properties of polypropylene composites and found considerable improvement in flexural strength and tensile strength on adding MWCNT and carbon nanofibers to the polypropylene matrix. Krause et al.[56] used EG as a conductive filler and added it to the PP matrix. They observed an electrical conductivity of 5.26 S/cm in the

through-plane direction. Similarly, Rzeczkowski et al.[57] mixed 80 wt.% of expanded graphite with PP and achieved an electrical conductivity of 15.6 S/cm.

Selamat et al. [58] conducted an optimization study on the compression molding parameters to obtain optimum electrical conductivity and flexural strength of the polypropylene composites. Roncaglia et al. [59] used a two-level-full-factorial design to optimize pressure, mold temperature, and time for manufacturing graphite-epoxy composites to maximize electrical conductivity. San et al. [60] analyzed the effects of surface contact angle and surface roughness of composite bipolar plates on the performance of PEM fuel cell performance by response surface methodology. King et al. [15] conducted the optimization study for the filler content by adding carbon black, graphite, and carbon nanotubes to the polypropylene at different levels. They observed the maximum through-plane electrical conductivity of 38.31 S/cm at the combination of 6 wt.% carbon nanotubes, 2.5 wt.% CB, and 65 wt.% of synthetic graphite. Table 2.3 lists the properties of the thermoplastic composite materials found in the literature survey.

Table 2.3: Properties of electrically conductive thermoplastic composites.

Polymer resin	Filler (wt.%)					Electrical Conductivity (S/cm)		Flexural strength (MPa)
	GR	CB	CF	CNT	EG	In-plane	Through-Plane	
PVDF [49,50]	86	-				277	-	9
PVDF [50]	74					119	-	20
PVDF [50]	64		16			109	-	42.7
PPS [11]	43.8	8.5	4			-	10	84
PP [11]	38.5	16.5				-	3	45
PP [52]	55	25				36.4	-	-
PP [52]	80					7	-	-
PPS [51]	80					118.9	-	52.4
PPS [23]	70		6			325	30	34.4
PP [53]	49	25		6		158.32	-	27
PP [26]	66	6				14.92	-	50.89
Nylon 6,6[42]	30	5	20			-	9.34	-
PP [15]	80					-	11.11	-
PP [15]				15		-	2.5	-
PP [15]	65	2.5		6		-	38.31	-
HDPE [28]					5	-	1E-6	-
PP [57]					80	-	15.9	-
PP [56]					60	-	5.26	-

2.5 Research Gap

Based on the comprehensive literature review, several key gaps were identified in the literature that need to be addressed. There is very little or no literature regarding use of multiple fillers for manufacturing electrically conductive thermoplastic composites. Many well-documented research studies have focused on developing thermoplastic composites using graphite, CF, CB, MWCNT, and EG as conductive fillers. However, a detailed investigation of the filler combinations, and the interaction of EG with other conductive fillers when added to binary, ternary, and quaternary configurations is not well-documented in the literature.

There exists another research gap regarding the investigation of the effects of polymer matrix on the properties of the composites. The feasibility of using different thermoplastic resins for the development of electrically conductive thermoplastic composites has also been investigated in the past. The literature, however, does not provide a detailed comparison of the electrical conductivity and the flexural strength of different thermoplastic resins when loaded with identical filler configurations.

Another research gap is the lack of optimization studies for electrical conductivity and flexural strength. Increasing the filler content improves electrical conductivity but exhibits adverse effects on flexural strength. Optimization studies on the processing parameters of the manufacturing of bipolar plates are available in the literature. However, an optimization study to determine the filler formulations that would optimize the electrical conductivity and flexural strength is not well documented in the literature.

The purpose of this work is to address the research gaps found in the literature. The synergistic effects of filler interactions on the properties of the composite material have been investigated by combining the fillers in different configurations. Multiple combinations of five different carbon-based fillers were added to the thermoplastic resin in binary, ternary, and four filler configurations, and the properties of the composites were recorded as a function of filler content. The effects of polymer resin on the properties of composites were investigated by studying the properties of different thermoplastic resins under the same filler configurations. The carbon-based fillers were added to three different polymer matrices, and the properties of the composites were compared to evaluate the

influence of the inherent properties of the thermoplastic resins on the composite material. An optimization study has also been conducted to develop a composite with optimum electrical conductivity and flexural strength. CB, MWCNT, and EG were added as secondary fillers at different configurations to observe their effects on the electrical conductivity and flexural strength. A DOE was developed by using a full factorial design approach to thoroughly investigate the effects of filler interactions. The impact of each secondary filler was examined by ANOVA. The outcomes of DOE were processed by RSM to develop an empirical model for predicting the electrical conductivity and flexural strength of the composites at different filler compositions.

Chapter 3: Material and Experimental Set-up

This chapter provides the details of the experimental procedure and equipment used for the manufacturing and characterization of thermoplastic composites. The first part of this chapter describes the details of the material used to manufacture composite materials. The second part deals with the equipment and methodologies used for the development and characterization of thermoplastic composites.

3.1 Materials

There are two main categories of materials used for the development of electrically conductive thermoplastic composites: polymer resins and conductive fillers.

3.1.1　Polymer Resins

The research study examined four types of thermoplastic resins. Most of the research work has been carried out on a homopolymer grade of PP, PP-3620WZ by Total Petrochemicals USA Inc, with a melt flow rate of 12 g/10 min. A copolymer grade of polypropylene, PP-5082 by Bapolene®, with a melt flow rate of 35 g/10 min, was also used to compare the properties of homopolymer and copolymer PP composites. It was anticipated that the use of nylon as a bonding matrix would improve the flexural strength of the composites. The nylon resin used in this study was Nylon6, Nylon (PA6)-1013NW8, procured from UBE®. Some of the experiments were also carried out on TPU resin with the intention of improving the toughness of the composites. Table 3.1lists the properties of the polymer matrices provided by the suppliers.

3.1.2　Conductive Fillers

In all experimental configurations, graphite was used as a primary filler, prepared by combining 10wt.% of synthetic graphite (Asbury carbons® A99) and 90wt.% of natural graphite flake (Asbury Carbon® GP3243). The particle size of synthetic graphite and flake graphite was 20 and 45 microns, respectively. The synthetic micro graphite particles increase the packing factor by filling the gap between flake graphite. The properties of synthetic and natural graphite are mentioned in Table 3.2. The CB material used in this study was a highly branched carbon black Ketjenblack EC-600JD by Azko Noble®. This CB is highly suitable for electro-conductive applications and has a very high surface area of 1400 m^2/g. Table 3.3 lists the properties of CB. To avoid the dispersion issues of

MWCNT, a PP-MWCNT masterbatch CNT-PP-25, with the MWCNT weight composition of 25%, was purchased from CTI Materials Inc. The details of the MWCNT are provided in Table 3.4. The expandable graphite flake (#808121) was received from Sigma-Aldrich®. The expandable graphite was expanded in the lab furnace at 700°C for a period of 15 min. Table 3.5 contains the details for the expandable graphite. Chopped CF with a fiber length of 6 mm was purchased from ZOLTEK®. The properties of CF are listed in Table 3.6.

Table 3.1: Properties of polymer resins [61–63].

Properties	Homopolymer PP	Copolymer PP	Nylon (PA6)	TPU
Supplier/trade name	PP-3620WZ by Total Petrochemicals Inc.	PP-5082 by Bapolene®	Nylon (PA6)-1013NW8 by UBE®	EHC
Melt Flow (MFR)	12	35	-	195
Density (g/cc)	0.905	0.9	1.14	1.23
Melting Point (°C)	165	-	215~225	195~200
Tensile Strength (MPa)	37	24.1	85	26
Elongation (%)	10%	5% (at yield)	20%	660%
Tensile Modulus (MPa)	1725	-	3200	12
Flexural Strength (MPa)	-	-	110	-
Flexural Modulus (MPa)	1585	1280	2700	-
Hardness (Rockwell R)	107	95	120	85
Izod Impact (J/m)	27	107	62.5	-

Table 3.2: Properties of natural and synthetic graphite.

Characteristics	Description	
Supplier	Asbury carbons®	Asbury carbons®
Trade name	GP3243	A99
Electrical resistivity	0.036 Ω.cm	0.047 Ω.cm
Carbon content	99%	99%
Particle size	60% - 325 mesh	20 μm
Surface area	3.0 m^2/g	6.5 m^2/g

Table 3.3: Properties of CB material.

Characteristics	Description
Supplier	Azko Noble®
Trade name	Ketjenblack EC-600 JD
Electrical resistivity	0.01-0.1 Ω.cm
Specific gravity	1.8
Bulk density	100-120 kg/m3
Particle size	30-100 nm
Surface area	1400 m^2/g

Table 3.4: Properties of MWCNT.

Characteristics	Description
Supplier	CTI material
Trade name	CNT-PP-25
Electrical Conductivity	>100 S/cm
Length	10-30 um
Diameter	5-10 nm
Specific surface area	110 m^2/g
Ture density	~2.1 g/cm^3
Bulk density	0.28 g/cm^3

Table 3.5: Properties of expandable graphite.

Characteristics	Description
Supplier	Sigma-Aldrich®
Trade name	Expandable graphite 808121
Expansion ratio	270 to 350
PH	5-10
Solubility	water insoluble
Particle size	+50 mesh (>300μ, ≥75% minimum)

Table 3.6: Properties of carbon fibers.

Characteristics	Description
Supplier	ZOLTEK®
Trade name	PX35
Electrical Resistivity	0.00155 ohm-cm
Fiber length	6 mm
Density	1.81 g/ml
Fiber Diameter	7.2 microns
Carbon content	95.00%

3.2 Manufacturing of Electrically Conductive Thermoplastic Composites

3.2.1 Twin-Screw Extruder

A co-rotating twin-screw extruder, Leistritz ZSE18HP-40D, with a screw diameter of 18 mm and length to diameter ratio of 40, is used for the melt compounding of graphite with the polymer. It has two feeding ports and eight heating zones. The polymer pellets were inserted in Zone 1 through the main feeder, while graphite was introduced in Zone 4 through the side feeder [Figure 3.1(a-b)]. In the case of MWCNT composites, the MWCNT was added from the main feeder in the form of PP-MWCNT masterbatch. For CB-based composites, the CB was dry mixed with the graphite and supplied through the side feeder. The CF was dry mixed with the polymer pellets and fed through the main feeder. The processing of EG composites was carried out in two steps. The first step is the formation of single filler EG composites or a PP/EG masterbatch in which EG was supplied through the side feeder. The formation of binary filler EG composites was done in the second step, in which the masterbatch of EG was dry mixed with the polypropylene pellets and sent to the main feeder.

The materials were mixed in the extruder, forming a composite material strand extruding from the die orifice. At the beginning of the extrusion process, only the material from the main feed was supplied to the extruder, and the side feeder remained off. Once the material is extruded out from the die, the side feeder is turned on to add the filler to the polymer. The composite strand was cooled down in the water bath and then pelletized by the pelletizer. After the melt-compounding process, the pelletized composite material was oven-dried to remove the moisture.
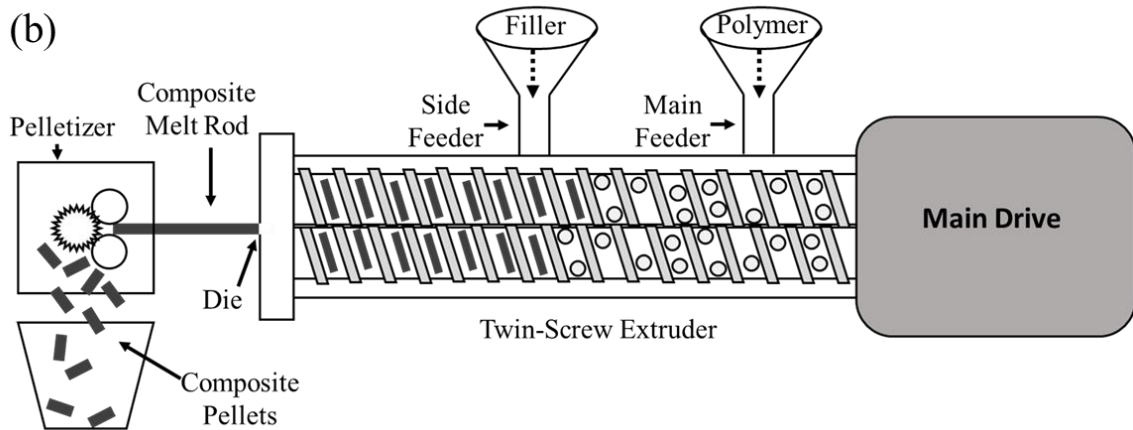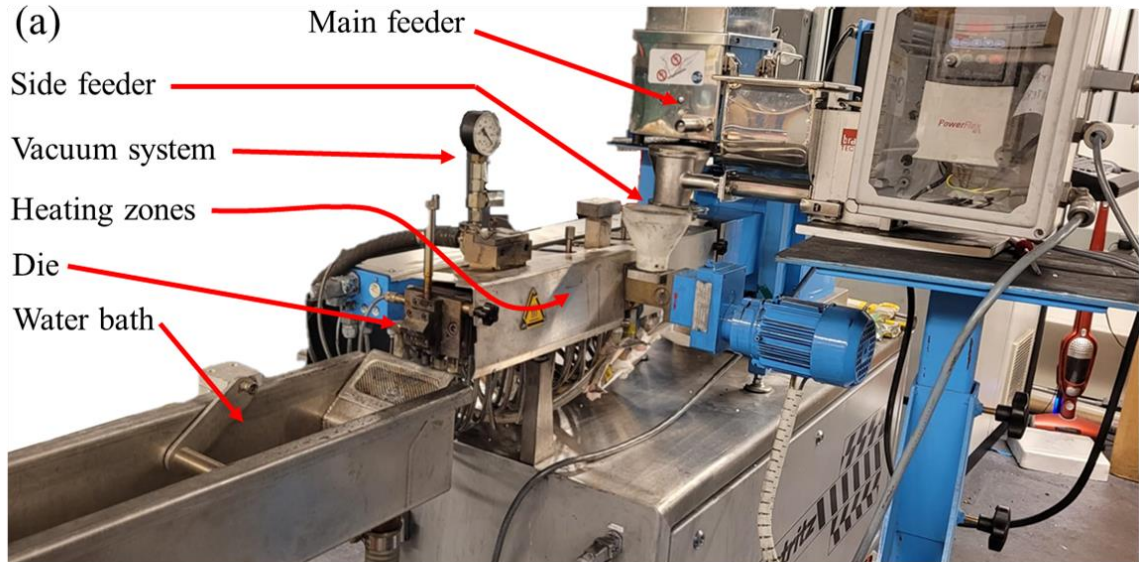
Figure 3.1: Twin-Screw Extruder for melt-compounding process: (a) experimental set-up (b) schematic diagram.

3.2.2   Compression Molding

After the extrusion process, the material was oven-dried for two hours at 100˚C and prepared for the compression molding process. A Carver press was used for the compression molding process in this study. A five-inch diameter disc with a thickness of 1.5 mm has been produced for each composite. The processing temperature for PP, nylon, and TPU were 190˚C, 240˚C, and 215˚C, respectively. The pressure was set to 1000 psi for all types of composites. At the beginning of the process, the press was preheated to the processing temperature of the material, and then the mold was placed inside the preheated press. The heat was provided for 15 minutes to maintain the temperature, then the mold

was set for cooling, whereas the pressure of 1000 psi was maintained until the mold temperature was cooled down to 100℃.

3.3 Characterization of Electrically Conductive Thermoplastic Composites

3.3.1   Thermo-Gravimetric Analysis (TGA)

The actual filler content of the extruded material depends on the accuracy of the melt-compounding process. The errors in adjusting the feed rates of the feeders differ the actual filler content of the composite from the calculated one. The final filler content of all the composite materials used in this research was verified by the Thermo-Gravimetric Analyzer (TGA) Q50 by TA Instruments, USA. The weight of composite material decreased with an increase in the temperature, which can be attributed due to the PP degradation. The thermo-gram of the PP/graphite composite with 84 wt.% filler content is shown in Figure 3.2. Above 500℃, the polymer content of the composite was observed to be completely degraded, leaving behind the residue, which clearly indicates the filler content of the composite. The TGA analysis confirmed that the actual filler composition of the composite was 84.09 wt.%, which was very much close to the planned composition.
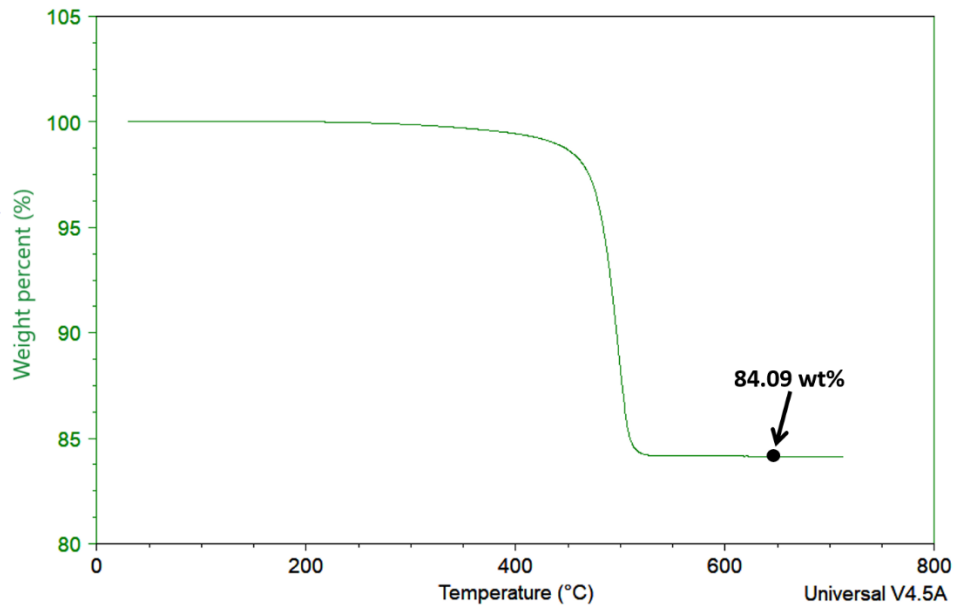
Figure 3.2: TGA thermo-gram of 84 wt.% graphite filled composite.

3.3.2 Differential Scanning Calorimetry (DSC)

Differential Scanning Calorimetry (DSC) is a thermal characterization technique that measures the heat flux of the sample and records it as a function of temperature. DSC determines the heat flow rate of the sample and compares it with reference material. The comparison of heat flow rate is used to evaluate material properties such as melting temperature, crystallization temperature, specific heat capacity, and glass transition temperature. A differential scanning calorimeter, DSC Q20 by TA Instruments (USA), was used to determine the melting point of the polymers. The information obtained from the DSC analysis was used to set the heating zone profile of the twin-screw extruder.

3.3.3 Through-Plane Electrical Conductivity (TPEC) Testing

TPEC of the composites was measured according to the US Fuel Cell Council through-plane electrical conductivity testing protocol [64]. Two gold-plated copper plates are used as the electrodes. The electrode size is 4 inches by 4 inches, with a thickness of 0.25 inches. Toray carbon paper TGP-H-120 is used as a gas diffusion layer—the sample is placed between carbon papers to provide better contact between the sample and gold-plated copper plates. As shown in Figure 3.3, the assembly is installed inside a Carver press, and a pressure of 1000 psi is applied to the sample during the test. Two plastic plates are used as an insulator between electrodes and the platens. A current of 100 mA passes through the circuit, and the voltage across the electrodes is recorded for each sample. The sample size is 1-inch by 1-inch, and five samples of each graphite composition are cut from compression-molded plates.

Before testing the specimens, the system resistance is determined by using reference material. The system resistance of the setup is a combination of circuit resistance and contact resistance. The reference material is POCO graphite DFP-1 with an electrical resistivity of 1.5 mΩ.cm. The reference material's size is the same as the size of the sample (1 inch by 1 inch) so that the equal contact area will produce equal contact resistance. The circuit resistance and contact resistance are calculated by equations (3.1) and (3.2).

$$R_{measured} = R_{POCO} + R_{Circuit} + R_{Contact} \qquad (3.1)$$

$$R_{POCO} = \frac{\rho_{POCO} \cdot t}{A} \qquad (3.2)$$

Where $R_{measured}$ is the resistance measured by placing the reference material between the electrodes, R_{POCO} is the resistance of the reference material, $R_{Circuit}$ is the circuit resistance, $R_{Contact}$ is the contact resistance, ρ_{POCO} is the resistivity of the reference material, t is the thickness of the reference material, and A is the area of reference material.
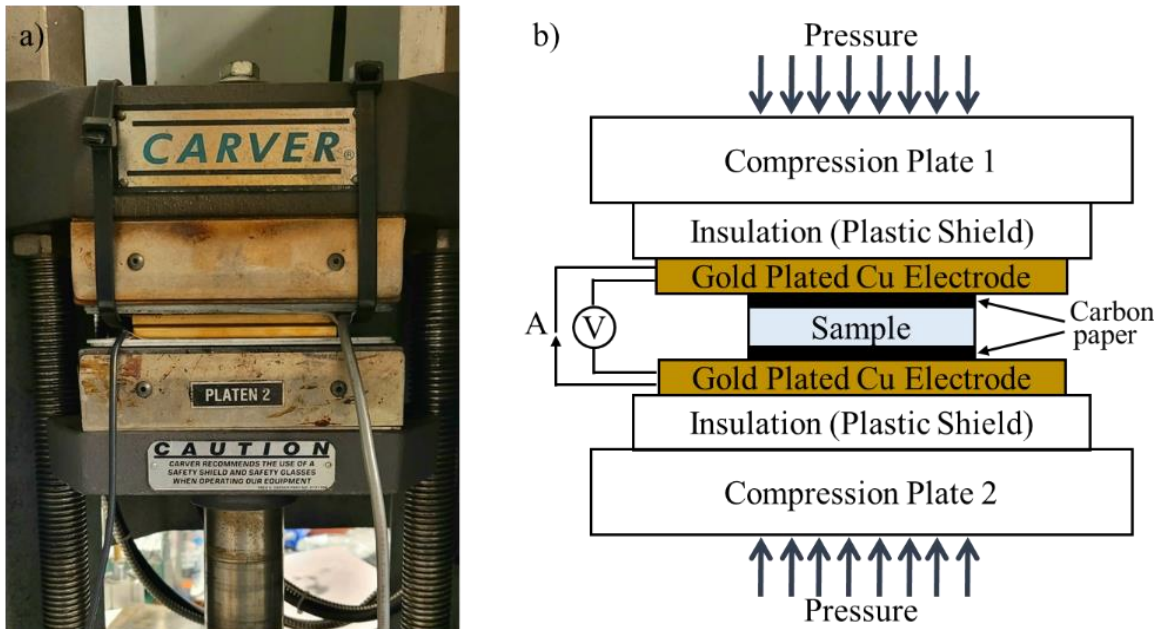
Figure 3.3: Description of through-plane electrical conductivity testing; (a) Lab-scale experimental set-up (b) Schematic illustration.

3.3.4   In-Plane Electrical Conductivity (IPEC) Testing

The IPEC of the composites was measured by the four-point probe method. The equipment used for the electrical conductivity testing was Pro4-L by Signatone Corporation. The setup was pre-wired and ready to connect to the Keithley 2450 source meter. The system was connected to a computer, and the data was collected by using Pro4

software. Multiple points were measured on each sample to determine electrical conductivity. A total of five readings were taken for each composite formulation.

3.3.5   Flexural Strength Testing

A 3-point bending test was performed to determine the flexural strength of the composites. A Dynamic Mechanical Analyzer, DMA Q800 by TA instruments, was used to perform flexural strength testing. The width and thickness of the specimens were 12.7 mm and 1.5 mm, respectively. The support span of the DMA 3-point bending clamp was 50 mm, as shown in Figure 3.4. ASTM D790 protocol was used to calculate the crosshead speed, which was 2.8 mm/min. The samples for the flexural strength testing were cut from the compression molded disc. A total of five samples of each composition were tested, and the average value was recorded.
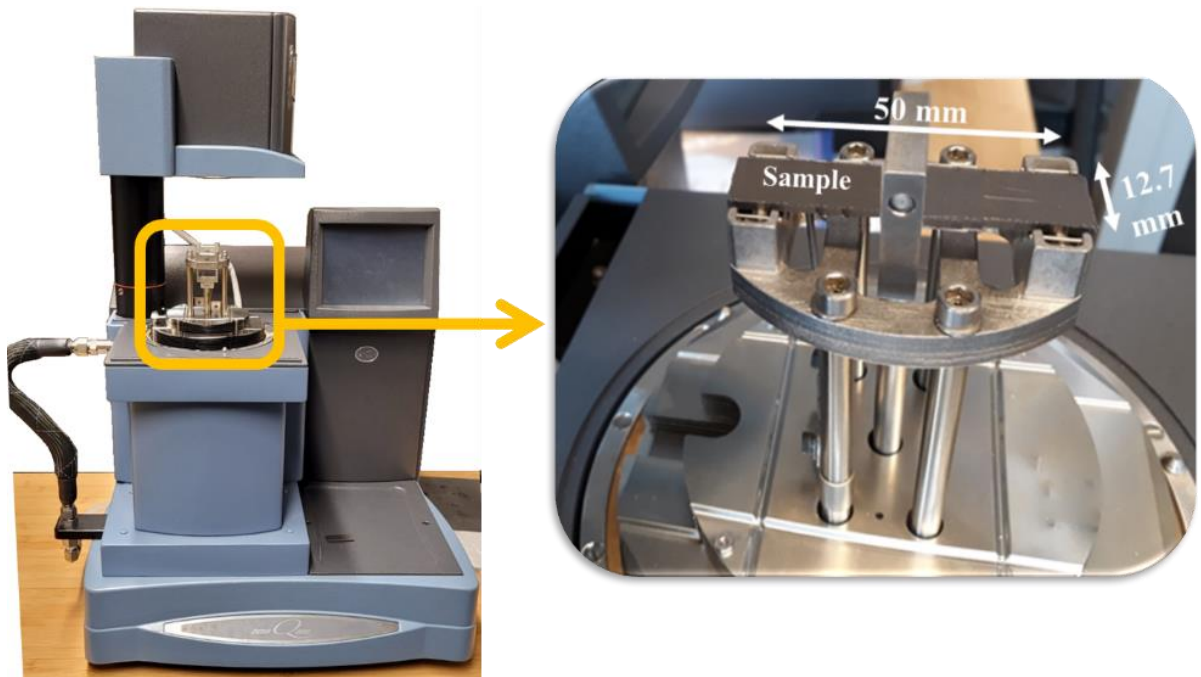
Figure 3.4: 3-point bending clamp of DMA Q800.

3.3.6   Scanning Electron Microscopy (SEM)

A scanning electron microscope was used to investigate the morphological characteristics of the composite samples. In SEM analysis, an electron microscope is used to produce images by scanning the surface of the specimen with the help of an electron beam. The SEM images of the composite material were produced using a Hitachi FlexSEM

1000, which was available at Ontario Tech University. However, some samples were sent to the University of Toronto for SEM analysis during the COVID-19 pandemic lockdown. The samples were gold coated and placed on conductive copper tape for better image processing. The operating voltage was 20 kV. The magnification of the microscope was adjusted according to the types of composites.

Chapter 4: Results and Discussion

This chapter discusses the results obtained through the analyses of experimental data. This experimental study is mainly divided into three sections. The first section investigates the effects of filler composition on the electrical and mechanical properties of the composites in which the thermoplastic composites were developed at different loading. The second of this chapter examines the effects of polymer matrix on the properties of electrically conductive thermoplastic composites. PP, nylon, and TPU were used to develop thermoplastic composites. The composites were prepared with the same filler formulations and their properties were compared to investigate the effects of the bonding matrix. The last section of this chapter includes empirical modeling to determine a material formulation that provides the optimum values of electrical conductivity and flexural strength. A parametric evaluation of secondary filler compositions was carried out to determine the most appropriate value of electrical conductivity and flexural strength. The significance of each secondary filler was evaluated by ANOVA. The empirical model was developed by using RSM to predict the values of electrical conductivity and flexural strength of the composites.

4.1 Effect of Filler Content on the Properties of Composites

In this study, electrically conductive Polypropylene (PP) based composites were developed using the twin-screw extrusion technique with the objective of investigating the effects of primary and binary fillers on the overall electrical performance of the composites in relation to their mechanical properties. Thermoplastic composites can be used in a variety of applications and are suitable for a wide variety of applications due to their inherent characteristics, such as light weight, availability of manufacturing methods, and ability to recycle. The incorporation of conductive fillers in the polymer matrix provides the ability to conduct heat and electricity. Electrically conductive thermoplastic composites are an excellent candidate for the manufacturing of fuel cell bipolar plates. The first part of this research work consists of studying the effect of graphite content on the electrical and mechanical properties of PP composites, whereas the second part focuses on the analysis of the effects of a binary filler composite developed by adding MWCNT and CB to the graphite/PP composites. The experimental results revealed that the maximum electrical conductivity obtained from the binary filler composites is significantly higher compared to

the single filler graphite/PP composites. The addition of binary fillers also improved the flexural strength of the composites. This experimental study constitutes new prospects in the development of electrically conductive thermoplastic composites with sound mechanical properties for fuel cell bipolar plates.

4.1.1 Sample Formulations

The experimental study was carried out in two parts: single filler composites and binary filler composites. The first part includes an investigation of the effect of graphite content on the electrical and mechanical properties of PP/graphite composites, and the second stage involves the determination of the synergistic effects of binary filler on PP/graphite composites. In the first phase, graphite was the only filler added to two different grades of polypropylene at different compositions. The polypropylene was fed through the main feeder and graphite from the side feeder. The feed rates of both feeders were controlled in such a way that the PP/graphite composites were produced by changing the graphite. The binary fillers were added to the composites in the second phase. Two types of binary filler composites were produced: CB-based composites and MWCNT-based composites. The material compositions of CB and MWCNT composites are provided in Table 4.1. The content of CB was fixed at 2.5 wt.% in the CB-based composites, and MWCNT was fixed at 2 wt.% in the MWCNT-based composites. These are the commonly used values of CB and MWCNT found in the literature resulting in a significant improvement in the electrical conductivity [15,56,65]. For CB-based composites, graphite was dry-mixed with CB, and the mixture was fed through the side feeder. For MWCNT-based composites, PP-CNT-25 master-batch was diluted with polypropylene at different formations feeding through the main feeder, whereas graphite was supplied from the side feeder. The synergistic effects of binary fillers were investigated by comparing the properties against the single filler PP/graphite composites produced in Phase 1.

Table 4.1: Description of material formulations of binary filler composites.

Run	PP (wt. %)	Total Filler Content (wt. %)	Filler composition (wt. %)		
			Graphite	CB	MWCNT
1	30	70	67.5	2.5	0
2	25	75	72.5	2.5	0
3	20	80	77.5	2.5	0
4	15	85	82.5	2.5	0
5	30	70	68	0	2
6	25	75	73	0	2
7	20	80	78	0	2
8	15	85	83	0	2

4.1.2   Single Filler Composites

The first part of this experimental study examines the effect of graphite content on the properties of single filler PP/graphite composites. Two different grades of polypropylenes were used in the formation of single filler graphite composites: homopolymer PP and copolymer PP. Graphite was added to the PP to produce PP/graphite composites with varying graphite contents. The electrical and mechanical properties of homopolymer and copolymer PP graphite have been investigated and compared.

4.1.2.1 Homopolymer PP Composites

The graphite was added to the homopolymer PP matrix by varying the composition from 0 wt.% to 84 wt.% with a step of 4 wt.%. Adding more than 84 wt.% of graphite to the polymer was not possible due to the high die pressure and motor load. The composites were tested for electrical conductivity and flexural strength. The stress-strain curve data obtained from flexural strength testing was analyzed to calculate flexural modulus, fracture strain, and fracture toughness. The composites with the graphite content below 48 wt.% filler content did not fully break during the flexural strength testing. Therefore, the data of fracture strain and fracture toughness were not collected for composites below 48 wt.%. The values of electrical conductivity, flexural strength, flexural modulus, fracture strain, and fracture toughness for each composition are listed in Table 4.2.

.

Table 4.2: Electrical and Mechanical properties of homopolymer PP composites.

S.no	Graphite content (wt%)	TPEC (S/cm)	IPEC (S/cm)	Flexural Strength (Mpa)	Flexural Modulus (Gpa)	Fracture Strain (%)	Fracture Toughness (J/m3)
1	84	21.7 ± 1.0	45.5 ± 2.6	11.8 ± 0.8	20.9 ± 1.1	0.12 ± 0.02	5.1 ± 0.4
2	80	13.0 ± 0.4	28.1 ± 1.3	12.8 ± 1.6	19.8 ± 0.1	0.10 ± 0.01	6.5 ± 1.5
3	76	3.2 ± 0.2	7.1 ± 0.5	24.4 ± 2.8	18.7 ± 0.9	0.28 ± 0.03	32.8 ± 10.5
4	72	2.2 ± 0.03	4.1 ± 0.1	31.7 ± 2.0	17.1 ± 2.1	0.31 ± 0.03	64.9 ± 12.5
5	68	0.5 ± 3E-3	2.1 ± 0.1	34.8 ± 2.2	14.8 ± 1.7	0.38 ± 0.03	86.6 ± 9.6
6	64	0.2 ± 9E-4	0.6 ± 2E-2	34.6 ± 2.3	14.3 ± 0.9	0.52 ± 0.06	110 ± 17.4
7	60	0.1 ± 7E-4	0.3 ± 7E-3	35.1 ± 0.4	12.5 ± 1.3	0.69 ± 0.03	160.4 ± 14.8
8	56	3E-2 ± 2E-4	0.2 ± 2E-3	34.9 ± 1.0	9.9 ± 0.8	0.97 ± 0.06	238.6 ± 30.2
9	52	1E-2 ± 2E-4	0.1 ± 3E-3	35.7 ± 0.5	8.9 ± 0.4	1.06 ± 0.02	270.0 ± 8.0
10	48	5E-3 ± 9E-4	0.1 ± 6E-3	35.6 ± 0.7	6.2 ± 0.8	1.37 ± 0.08	360.0 ± 30.6
11	44	3E-3 ± 2E-4	-	37.0 ± 0.3	6.0 ± 0.1	-	-
12	40	5E-4 ± 1E-5	-	36.8 ± 0.7	5.2 ± 0.5	-	-
13	36	1E-4 ± 5E-6	-	37.7 ± 0.6	3.6 ± 0.3	-	-
14	32	2E-5 ± 1E-6	-	38.1 ± 0.7	3.4 ± 0.1	-	-
15	28	1E-6 ± 1E-7	-	37.3 ± 0.4	3.2 ± 0.1	-	-
16	24	2E-7 ± 2E-9	-	37.8 ± 0.7	2.7 ± 0.2	-	-
17	20	6E-11 ± 1E-11	-	38.2 ± 1.2	2.5 ± 0.1	-	-
18	16	-	-	38.0 ± 1.1	2.4 ± 0.1	-	-
19	12	-	-	38.4 ± 1.3	2.3 ± 0.1	-	-
20	8	-	-	39.3 ± 1.8	2.1 ± 0.1	-	-
21	4	-	-	38.3 ± 0.6	1.8 ± 0.1	-	-
22	0	-	-	35.7 ± 1.3	1.6 ± 0.1	-	-

a) TPEC of homopolymer PP composites

TPEC testing was performed on graphite composites ranging from 20% to 84 wt.%. Electrical conductivity testing of composites below 20 wt.% graphite content was not possible with the lab-scale electrical conductivity setup because of very high specimen resistivity. The electrical conductivity values are plotted against the filler weight fraction in Figure 4.1(a). The electrical conductivity of the composites increased with an increase in the graphite content. A drastic surge in the electrical conductivity with a slight increase in graphite content was observed in the high filler content region between 68 wt.% and 84 wt.%. However, no significant change in the electrical conductivity was observed between 20 wt.% to 68 wt.% graphite content. A log-log graph was plotted in Figure 4.1(b) to analyze the possible relationship between conductivity and filler composition. The logarithm of electrical conductivity against the logarithm of graphite content yields a straight line with the power of relationship of 16.1. The maximum value of electrical conductivity recorded in this section was 21.7 S/cm at 84 wt.% graphite content. With an

increase in the filler concentration, the interaction between the graphite microparticles has been increased, leaving behind a reduced polymer-filler interface resulting in a significant enhancement in the electrical conductivity[66].

Figure 4.1: TPEC vs. filler weight fraction graphs for homopolymer PP composites (a) linear scale (b) logarithmic scale.

b) Flexural strength of homopolymer PP composites

The flexural strength testing of PP/graphite composites was performed to analyze the mechanical performance of the composites and is presented as a function of graphite content in Figure 4.2. The composites with graphite content below 28 wt.% did not break during the testing, and the procedure was stopped as the specimen deformation reached 5%. No considerable change in the flexural strength of the composites was recorded in the low filler loading region. However, a significant reduction in the flexural strength was observed between 72 wt.% and 84 wt.% graphite content. The increase in the graphite content reduces the resin content of the composite. The low polymer content caused poor wetting of graphite with the resin, resulting in poor mechanical performance. The deterioration of filler particles during melt-compounding may also lead to poor mechanical performance. The high shear stresses generated during the melt-compounding of highly filled composites damage the filler particles. The degradation of filler particles in the case of highly filled composites was due to the high shear stresses generated during the melt-compounding process. Figure 4.3(a-d) shows the micrographs of PP/graphite composites at 68 wt.% and 84 wt.%. The damages caused to the surfaces and edges of the graphite particles during the melt-compounding of 84 wt.% filled composites can be seen in Figure 4.3(c) and Figure 4.3(d).

$$y = 37.9 + 0.007(1 - e^{9.87x})$$
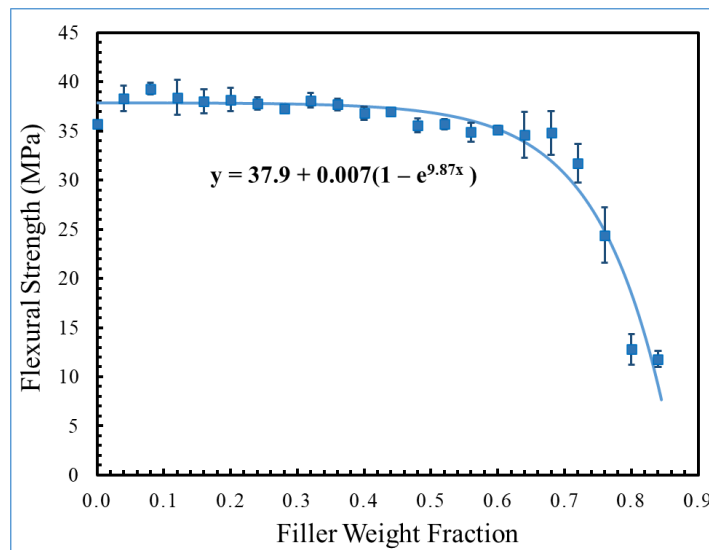
Figure 4.2: Flexural strength vs. filler weight fraction graph for homopolymer PP composites.
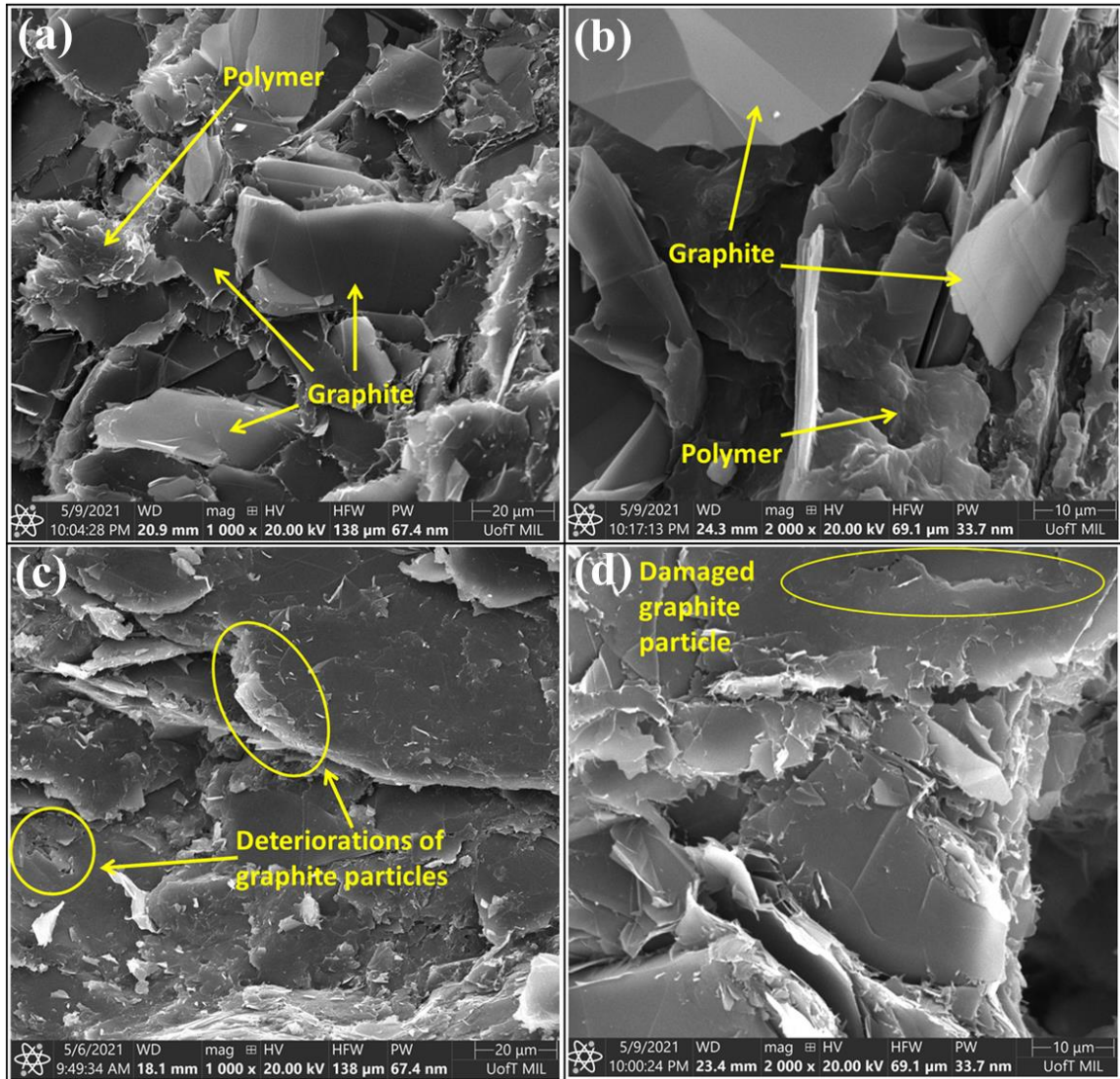
Figure 4.3: SEM micrographs of PP/graphite composites: (a) 68 wt.% graphite (b) magnified view of 68 wt.% graphite (c) 84 wt.% graphite (d) magnified view of 84 wt.% graphite.

4.1.2.2 Copolymer PP Composites

The graphite filler was added to the copolymer PP matrix to produce single filler copolymer PP composites. Based on the analysis of homopolymer PP composites, the filler content did not have a significant influence on the electrical and mechanical properties of the composites at a filler content of less than 48 wt.%. Moreover, like homopolymer PP composites, adding more than 84 wt.% of graphite to the polymer was not possible due to the very high viscosity of the composite and high pressure on the die. Therefore, the copolymer PP composites were produced by varying the graphite composition from 48

wt.% to 84 wt.% with a step of 4 wt.%. For each graphite composition, there were five samples tested for flexural strength and through-plane electrical conductivity, and their mean values and standard deviations were recorded. The mechanical and electrical properties of each filler composition are listed in Table 4.3.

Table 4.3: Measured Properties of copolymer PP-Graphite composites.

S.no	Graphite content (wt.%)	TPEC (S/cm)	IPEC (S/cm)	Flexural Strength (MPa)	Flexural Modulus (GPa)	Fracture Strain (%)	Fracture Toughness (J/m^3)
1	84	10.72 ± 0.16	25.4 ± 1.4	15.2 ± 1.5	13.8 ± 1.4	0.24 ± 0.02	21.0 ± 6.3
2	80	8.33 ± 0.23	17.2 ± 0.9	15.7 ± 1.4	10.6 ± 0.5	0.40 ± 0.06	38.6 ± 4.4
3	76	1.84 ± 0.01	3.7 ± 0.4	15.8 ± 1.1	9.3 ± 0.5	0.51 ± 0.03	52.8 ± 5.7
4	72	0.38 ± 9E-4	1.0 ± 6E-2	18.8 ± 1.6	8.7 ± 1.0	0.88 ± 0.04	122.1 ± 9.1
5	68	0.21 ± 5E-4	0.8 ± 5E-2	22.3 ± 1.2	8.2 ± 0.5	1.02 ± 0.15	162.0 ± 31.0
6	64	0.17 ± 1E-3	0.6 ± 1E-2	23.5 ± 1.4	7.2 ± 0.5	1.20 ± 0.06	200.0 ± 17.4
7	60	0.08 ± 1E-3	0.2 ± 8E-3	24.2 ± 1.1	6.1 ± 0.2	1.56 ± 0.10	256.0 ± 22.9
8	56	0.05 ± 2E-3	0.2 ± 3E-3	24.0 ± 0.6	5.5 ± 0.4	1.52 ± 0.15	270.6 ± 31.2
9	52	0.01 ± 2E-4	0.1 ± 3E-3	24.4 ± 0.4	4.9 ± 0.1	1.70 ± 0.06	308.2 ± 16.3
10	48	4E-3 ± 2E-4	0.1 ± 6E-3	23.4 ± 1.9	4.1 ± 0.1	1.78 ± 0.18	282.5 ± 25.1

a) TPEC of copolymer PP composites

The TPEC values of copolymer PP composites against the graphite weight fraction is plotted in Figure 4.4(a). As expected, the electrical conductivity increased with the increase in filler concentration. However, a significant increase was observed between 76 wt.% and 80 wt.% of graphite content. The composite at 84 wt.% concentration showed the highest conductivity of 10.7 S/cm. A log-log graph was plotted in Figure 4.4(b) to understand the relationship between electrical conductivity and filler composition at the low filler concentration region. It was observed from the logarithmic graph that the electrical conductivity of composites is increasing linearly on the log-log graph with a slope of 13.9.
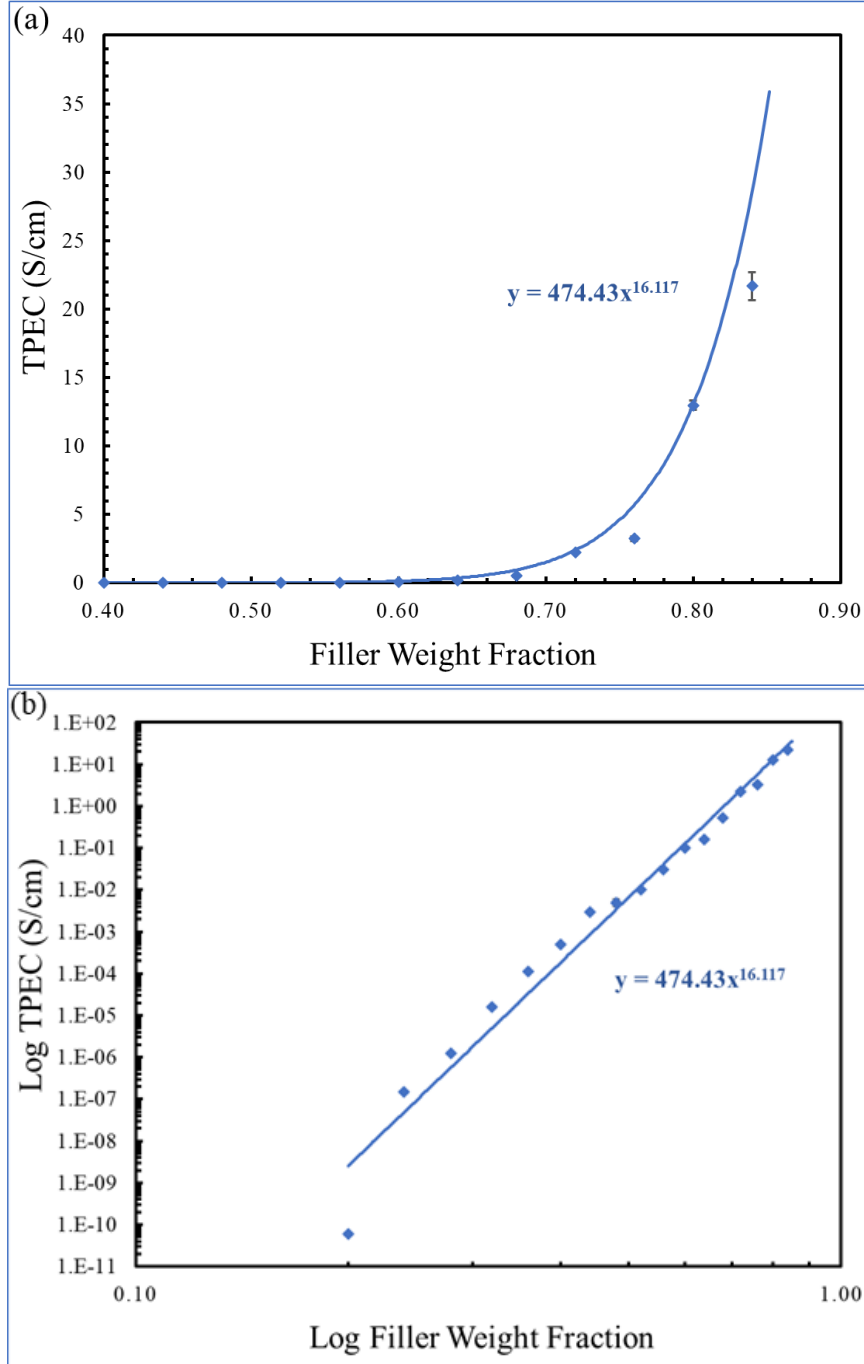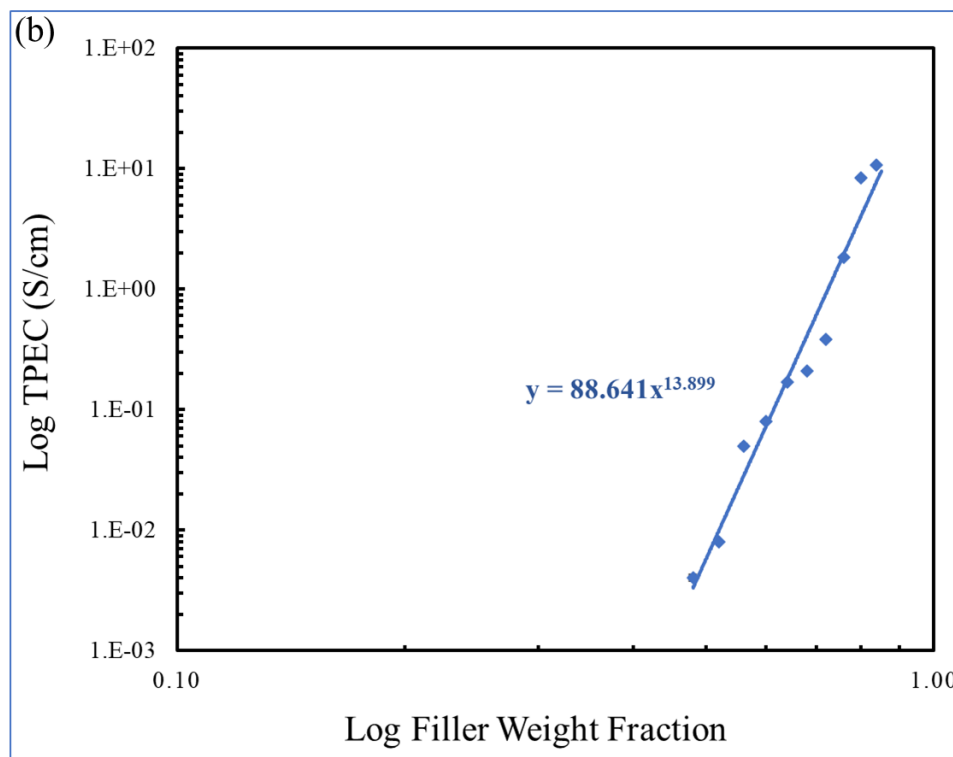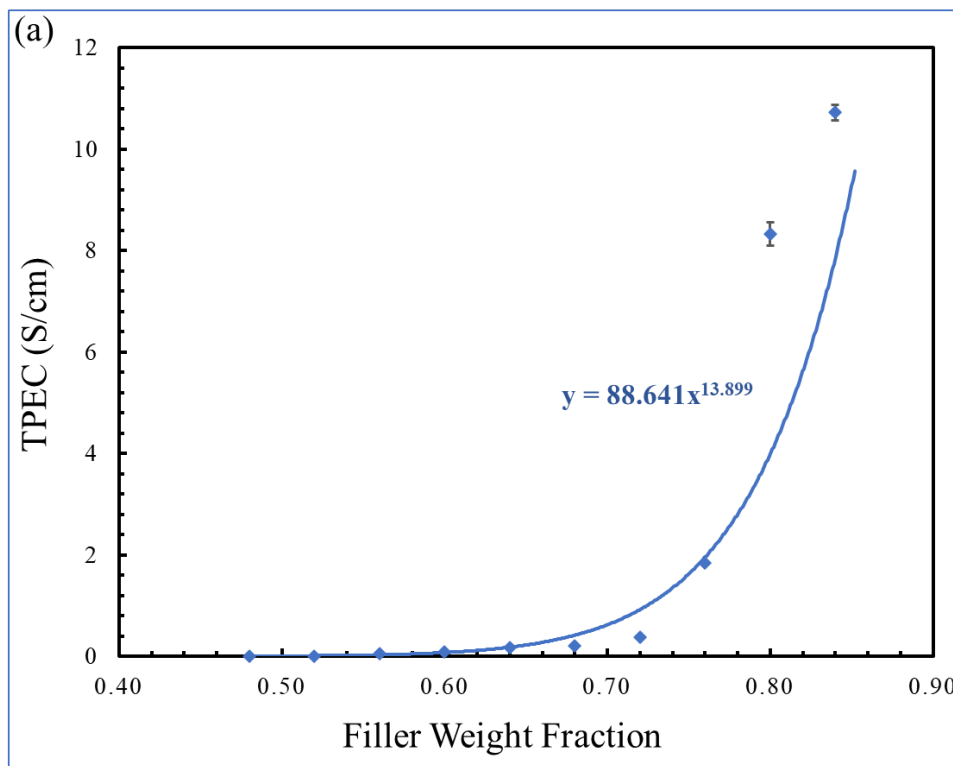
Figure 4.4: TPEC vs. filler weight fraction graphs for copolymer PP composites (a) linear scale (b) logarithmic scale.

b) Flexural strength of copolymer PP composites

The flexural strength of copolymer PP composites is plotted as a function filler weight fraction in Figure 4.5. Overall, flexural strength showed a decreasing trend with an increase in filler content. However, this decrement in the flexural strength is very prominent after 68 wt.% filler content. The maximum value of flexural strength recorded in this section was 24.4 MPa. The filler loading did not have any significant effect on the flexural strength when the filler content was less than 60 wt.%. The reduction in flexural strength occurred due to the poor wetting of graphite with the resin at high filler compositions.
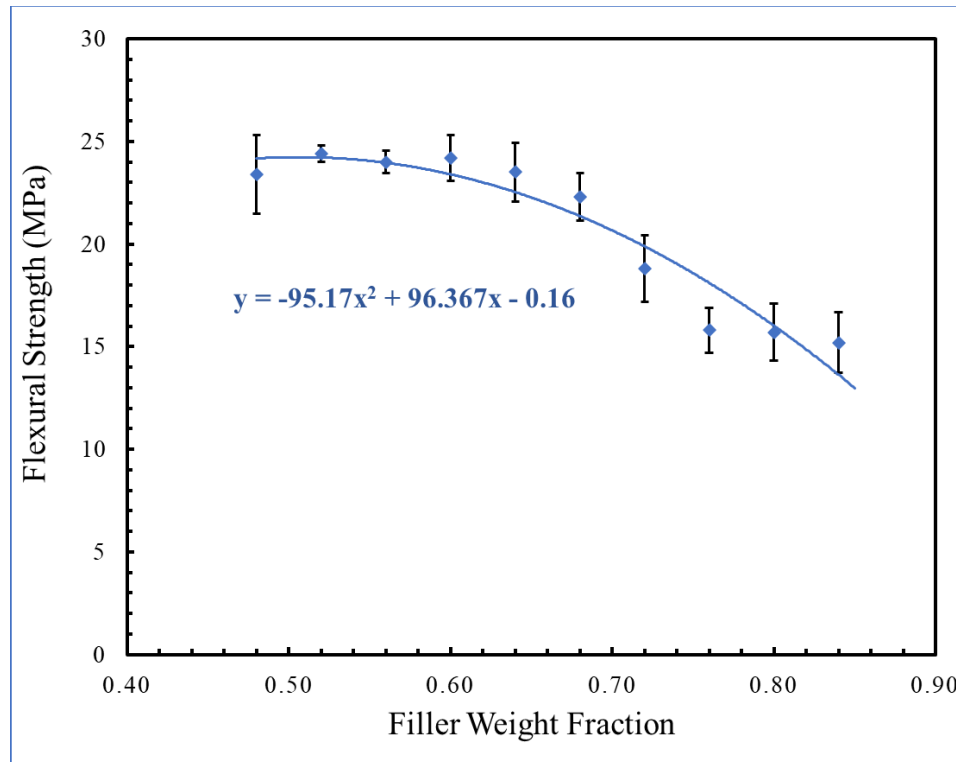
Figure 4.5: Flexural strength vs. filler weight fraction graph for copolymer PP composites.

4.1.2.3 Comparison of Homopolymer and Copolymer PP Composites

The electrical and mechanical properties of the homopolymer and copolymer PP composites are listed in Table 4.2 and Table 4.3, respectively. For the comparison of homopolymer and copolymer PP composites, the electrical conductivity, flexural strength, flexural modulus, fracture strain, and fracture toughness were plotted against the filler weight fraction and discussed in the following sections.

a) Comparison of TPEC

The TPEC values of homopolymer and copolymer PP composites were plotted as a function of filler weight fraction and compared in Figure 4.6. In both types of composite materials, increasing graphite content resulted in an increase in electrical conductivity. However, the trendline for electrical conductivity of homopolymer and copolymer composites is slightly different from each other. The electrical conductivity values of homopolymer PP composites are higher than the copolymer PP. The composites with graphite loading below 60 wt.% did not demonstrate any significant changes in electrical conductivity on varying graphite content. Noticeable variations in the electrical conductivity were observed when the graphite content increased 68 wt.%. The electrical conductivity of both composites was increased significantly when the graphite content was between 72 to 84 wt.%. In contrast, the conductivity of the homopolymer PP composites was almost twice that of the copolymer PP composites when the graphite content was 84 wt.%. The difference in the electrical conductivity values of both composites at low filler loading can be examined from the log-log graph in Figure 4.6(b). The electrical conductivity values of both composites yield a straight line in the logarithmic graph, corresponding to a logarithmic increase in the electrical conductivity as graphite content increases. However, the slope of the log-log graph for homopolymer PP composites is higher than the copolymer PP composites. An explanation for this could be due to improper mixing of graphite in the homopolymer PP composites. The melt flow rating of homopolymer PP resin was comparatively lower than the copolymer PP. At high filler content, the high viscosity of the polymer resin makes it difficult to mix the filler properly. The improper mixing of the conductive filler caused the electrical conductivity of the composites to increase rapidly, but the flexural strength of the composites drastically reduced at the same time. The flexural strength of the homopolymer and copolymer PP composites has been discussed in the following sections.
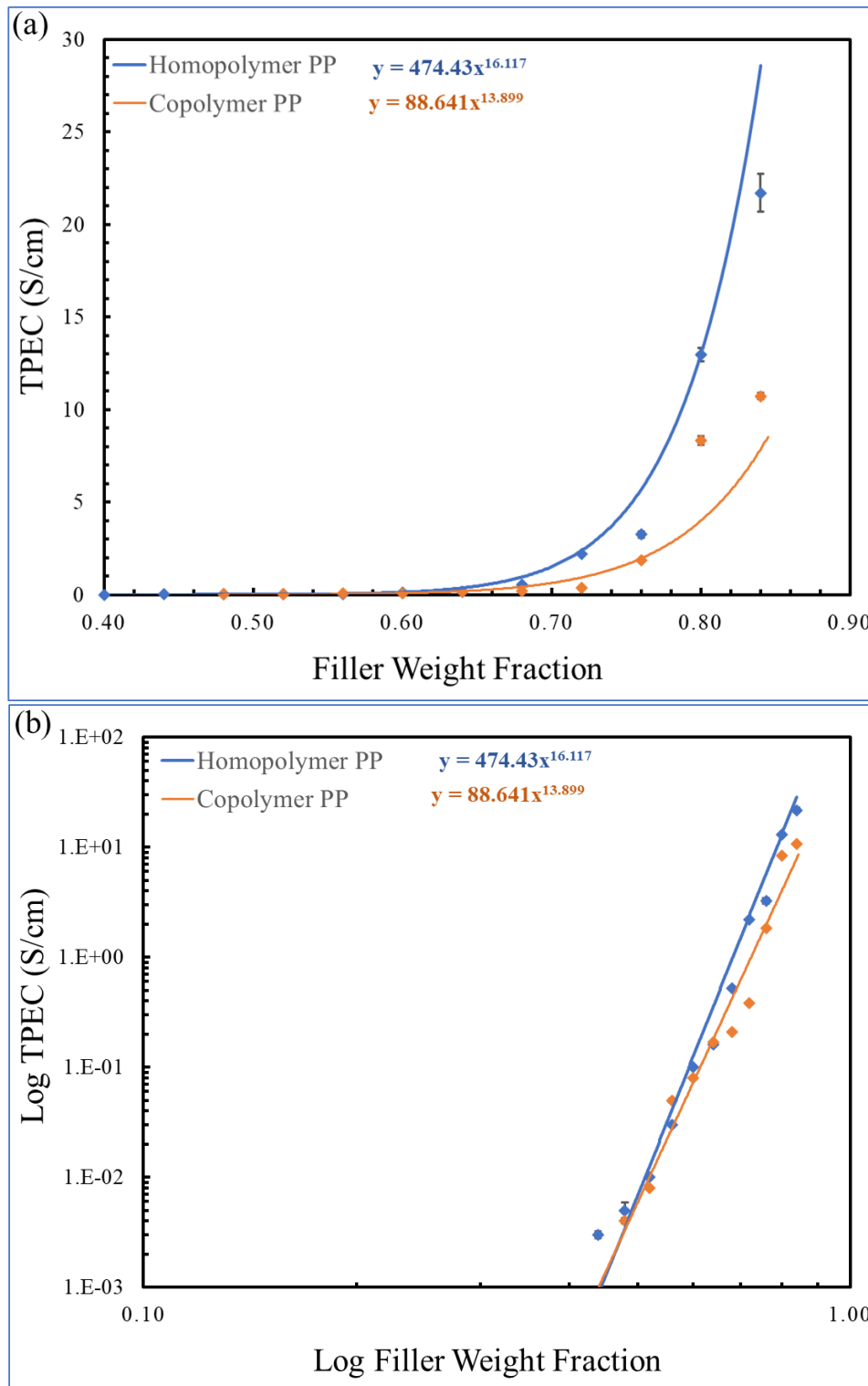
Figure 4.6: Comparison of TPEC values of the homopolymer and copolymer PP composites (a) linear graph (b) log-log graph.

b) Comparison of IPEC

Figure 4.7 shows the IPEC values of homopolymer and copolymer PP composites as a function of filler weight fraction. Similar to TPEC values, IPEC values demonstrated a similar trend. The electrical conductivity of homopolymer PP composites was comparatively higher than the copolymer PP composites. A drastic increase in the IPEC values was observed between 72 wt.% to 84 wt.% in both composites. The highest IPEC measurements recorded in the homopolymer PP and copolymer PP were 45.5 S/cm and 25.4 S/cm, respectively.
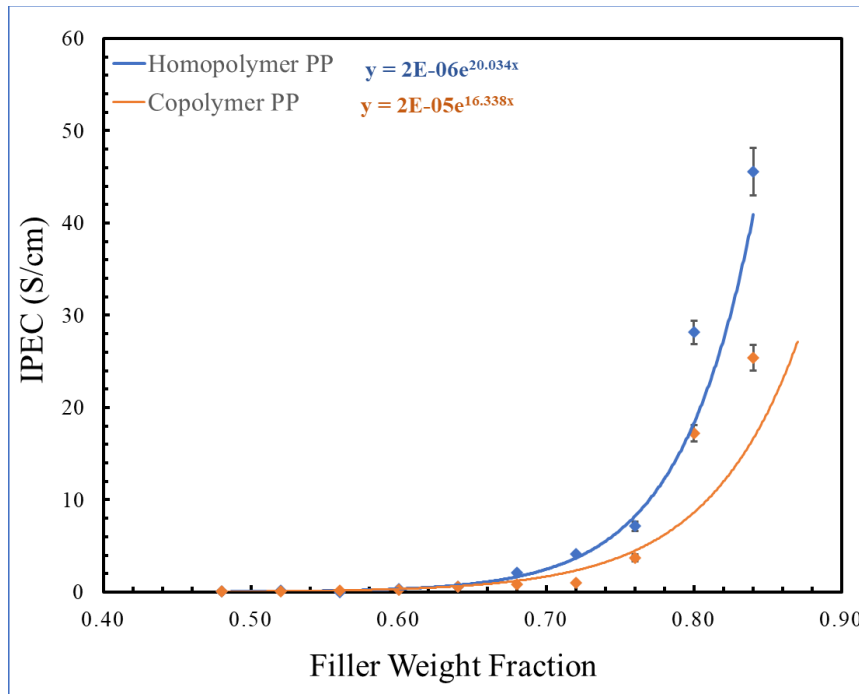
Figure 4.7: Comparison of IPEC of the homopolymer and copolymer PP composites.

c) Comparison of flexural strength

The flexural strength of homopolymer and copolymer PP is plotted against the filler weight fraction. Figure 4.8 shows the comparison of flexural strength of the homopolymer and copolymer PP composites. The homopolymer PP composites demonstrated higher flexural strength at low filler loading. The flexural strength of all the homopolymer composites below the 68 wt.% was more than 34 MPa, whereas the maximum flexural strength recorded in the case of copolymer composites was only 24.4 MPa. Both types of composites did not show any noticeable change in the flexural strength when the filler loading was less than 68 wt.%. The flexural strength started to decrease after 68 wt.% filler

content in both copolymer and homopolymer PP composites. This may be due to the weaker interfacial bonding of graphite with the resin at low polymer content. However, a significant reduction in the flexural strength of homopolymer PP composites was observed between 72 wt.% to 80 wt.%. The flexural strength of the homopolymer PP composites decreased exponentially at the high filler loading region. This may be due to the high viscosity of the homopolymer PP resin. As discussed in the previous section, the high viscosity of the resin makes it difficult to mix more filler in the matrix, and the improper mixing of the filler results in the poor mechanical strength of the composites. Another possible cause might be the degradation of filler particles during melt-compounding. As homopolymer has a higher viscosity than copolymer PP, the melt-compounding of highly loaded homopolymer PP composites generates relatively high shear stresses that can cause the deterioration of graphite particles. Figure 4.3(c) and (d) show the damage caused to the surfaces and edges of the graphite particles during melt-compounding of the 84 wt.% filled composites.

d) Comparison of flexural modulus

The flexural modulus of the composites was determined by calculating the slope of stress-strain curves of the 3-point bending test. According to the manufacturer's technical data sheet, the flexural modulus of homopolymer PP resins was 1585 MPa, and the flexural modulus was calculated from the stress-strain curve for homopolymer PP at 0 wt.% graphite content was 1551 MPa, confirming the validity of the test results. To compare the elasticity of the copolymer and homopolymer PP composites at different filler loading, the flexural modulus values of both composites are presented as a function of filler weight fraction in Figure 4.9. A linear relationship was observed between flexural modulus and filler weight fraction with the correlation coefficient (R^2) of 0.99 and 0.93 for homopolymer and copolymer composites, respectively. However, the flexural modulus of the homopolymer PP composites was higher than the copolymer PP composites. Moreover, the slope of the curve fit equation for the homopolymer PP composites is steeper than the copolymer PP composites, showing that the flexural modulus of homopolymer composites increases at a relatively higher rate. The slopes of the flexural modulus for the homopolymer and copolymer composite graphs are 0.40 GPa/wt.% and 0.23 GPa/wt.%,

respectively. For homopolymer PP composites, the highest flexural modulus was 20.9 GPa, while the highest value for copolymer PP composites was 13.8 GPa.
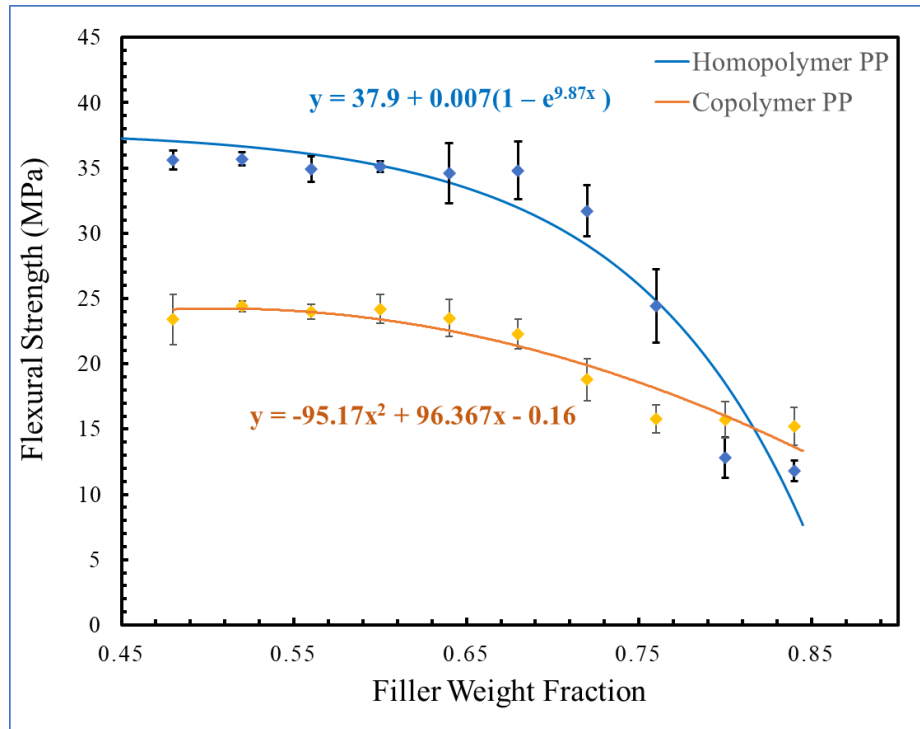
Figure 4.8: Comparison of flexural strength of the homopolymer and copolymer PP composites.

e) Comparison of fracture strain

The elongation at break values of the homopolymer and copolymer PP composites were measured from the stress-strain curves obtained from the 3-point bending test. Figure 4.10 shows the fracture strain of the composites plotted against the filler weight fraction. As expected, the fracture strain of the composites decreased with increasing the filler content. For all graphite compositions, copolymer PP composites exhibited higher fracture strains than homopolymer PP composites. Composites manufactured from homopolymer PP matrix were brittle and got fractured at a lower elongation than those of copolymer PP. Copolymer PP composites showed linearly decreasing fracture strain values with increasing filler loading. With a filler loading of 80 wt.% or higher, homopolymer PP composites fractured within 0.1% of elongation. A significant drop in the flexural strength of homopolymer PP composites was observed when the graphite content was more than 76 wt.%. Low polymer content and high melt viscosity may lead to improper mixing and poor interfacial bonding of graphite with resin.
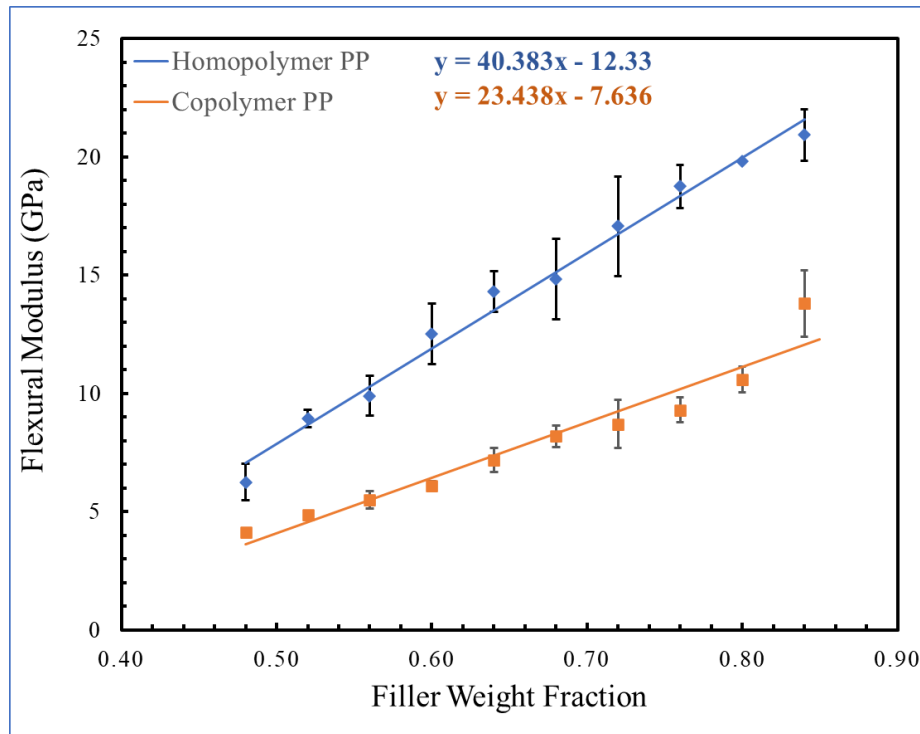
Figure 4.9: Flexural modulus of homopolymer and copolymer PP composites vs. filler content.
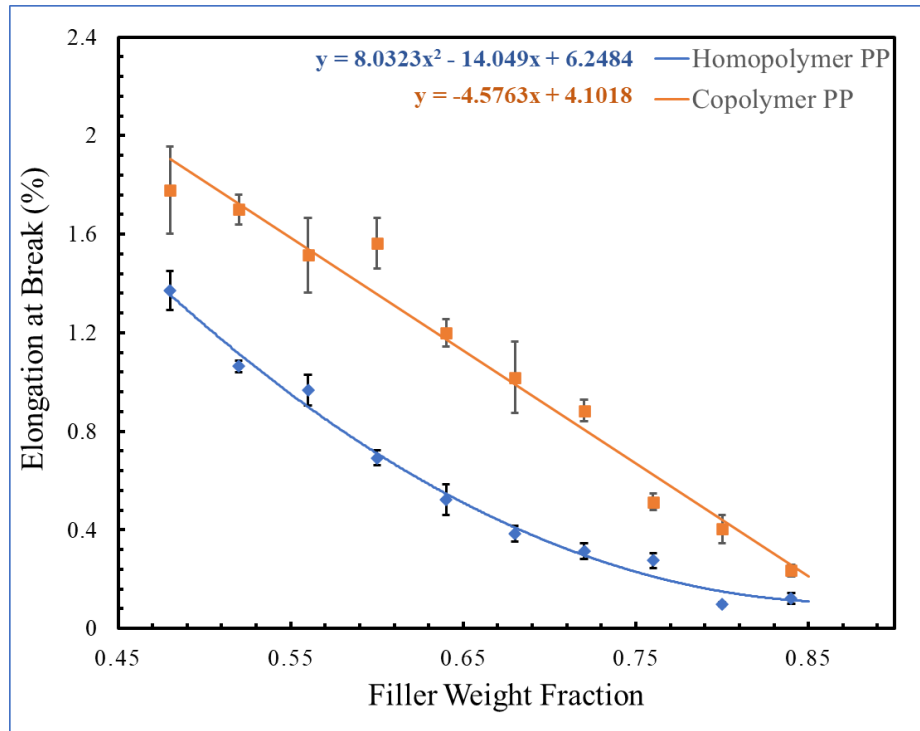
Figure 4.10: Comparison of fracture strain of the homopolymer and copolymer PP composites.

f) Comparison of fracture toughness

The fracture toughness of the composites was calculated from the area under the curve of the stress-strain graph generated during the flexural strength test. To compare the toughness of the copolymer and homopolymer PP composites, the flexural toughness of both composites is plotted as a function of filler weight fraction in Figure 4.11. The fracture toughness of both PP composites decreased with an increase in the filler content, but the reduction in toughness was significantly greater in homopolymer PP composites than in copolymer PP composites. The homopolymer PP composites exhibited relatively higher toughness at low filler loading. However, the toughness of homopolymer PP composites decreased more rapidly than that of copolymer PP. The fracture toughness data of the copolymer PP yields a straight line on the fracture toughness versus filler weight fraction graph, whereas the curve fit for the homopolymer PP composites shows a second-order polynomial relationship. The toughness data was calculated from the stress-strain values, and the flexural strength and fracture strain values for the homopolymer PP composites dropped significantly at higher filler loading. On the other hand, the elongation and flexural strength of copolymer composites decreased at a slower rate than those of homopolymer composites.
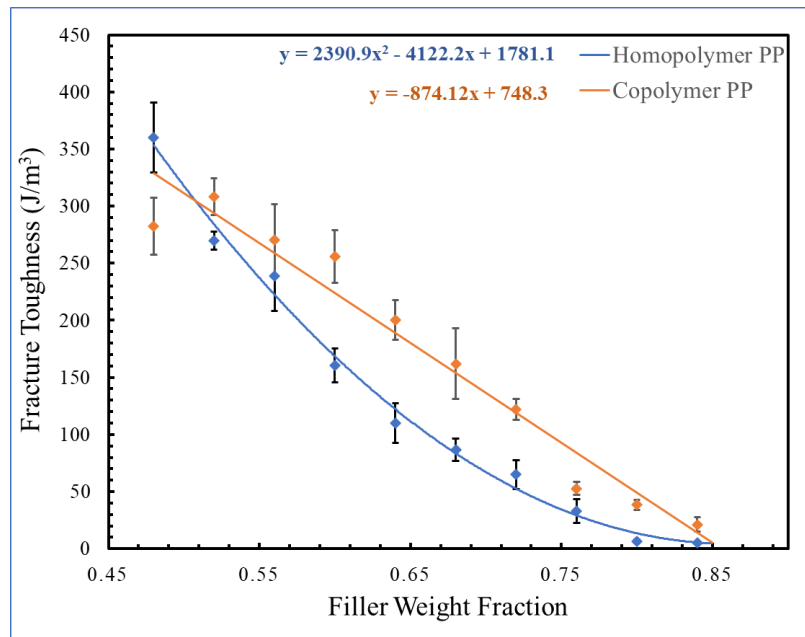
Figure 4.11: Fracture toughness of homopolymer and copolymer PP composites.

4.1.3 Binary Filler Composites

The properties of single filler homopolymer PP and copolymer PP composites were investigated and compared in the previous sections. The homopolymer PP composites demonstrated significantly higher electrical conductivity than the copolymer PP composites. The copolymer PP composites exhibited better strength and toughness at high filler loading. However, the maximum flexural strength of the copolymer PP composites was only 24.4 MPa, whereas the flexural strength of homopolymer PP composites was more than 30 MPa even at 72 wt.% graphite loading. Therefore, the homopolymer PP matrix was used to investigate the effects of binary fillers on the electrical and mechanical properties of the composites. The electrical conductivity of homopolymer PP/graphite composites was significantly increased with the filler loading between 72 wt.% to 84 wt.%. The same range of filler compositions of homopolymer PP composites was further selected to introduce binary fillers to the PP/graphite composites to improve electrical conductivity and flexural strength. CB and MWCNT were added to the PP/composites as binary fillers. The amount of MWCNT was 2 wt.% in each MWCNT-based composite, whereas the amount of CB was 2.5 wt.% in CB-based composites. The properties of binary filler composites are mentioned in Table 4.4.

Table 4.4: Properties of binary filler PP/graphite composites.

Run	PP Content (wt. %)	Total Filler Content (wt. %)	Filler composition (wt. %)			TPEC (S/cm)	Flexural Strength (MPa)
			Graphite	CB	MWCNT		
1	30	70	67.5	2.5	0	25.7 ± 0.8	33.7 ± 3.9
2	25	75	72.5	2.5	0	21.3 ± 2.0	28.4 ± 1.8
3	20	80	77.5	2.5	0	9.7 ± 0.4	36.9 ± 1.2
4	15	85	82.5	2.5	0	3.2 ± 0.3	35.6 ± 2.7
5	30	70	68	0	2	49.3 ± 2.4	21.0 ± 2.2
6	25	75	73	0	2	21.3 ± 2.0	22.5 ± 1.2
7	20	80	78	0	2	8.9 ± 0.2	28.5 ± 2.1
8	15	85	83	0	2	5.8 ± 0.2	27.2 ± 4.4

a) Effect of binary fillers on the electrical conductivity

The TPEC values of binary filler composites are plotted as a function of total filler content and compared with the single filler PP/graphite composites in Figure 4.12. The electrical conductivity of PP/graphite composites was significantly improved with the addition of binary fillers. It can be observed that the trendline of electrical conductivity is

different for each type of composite. The MWCNT-based composites exhibited the highest electrical conductivity of 49.2 S/cm at 85 wt.% filler content. Compared to the single filler graphite composites in the previous part, the addition of only 2 wt.% of MWCNT increased the electrical conductivity of the composites from 21.5 S/cm to 49.2 S/cm. The relationship between the TPEC values and filler content for the single filler, MWCNT-based composites, and CB-based composites can be defined by equations (4.1), (4.2), and (4.3), respectively.

$$y = 474.43x^{16.117} \qquad (4.1)$$
$$y = 274.7x^{11.225} \qquad (4.2)$$
$$y = 129.9 In(x) + 48.87 \qquad (4.3)$$

The single filler PP/graphite composites and MWCNT-based composites yield a linear relationship in the log-log graph. However, the slope of MWCNT-based composites on the logarithmic graph is lower than the PP/graphite composites. The difference in the slope of the log-log graph indicates that the synergistic effects of MWCNT on the PP/graphite composites are more significant at low filler loading than at high filler loading. The addition of CB also improved the electrical conductivity of the composites. The highest electrical conductivity observed in CB-based composites was 25.7 S/cm at 85 wt.% filler content. However, the electrical conductivity trend of CB-based composites is not similar to the MWCNT-based composites. A log-log is also plotted in Figure 4.12(b) to examine the Synergistics effects of binary fillers on a logarithmic scale. The slope of CB-based composites in the logarithmic graph is steeper than the MWCNT composites in the beginning, but it started to decrease noticeably after 75 wt.% filler content. This indicates that the addition of CB is not effective in highly filled composites. The rapid decline in the slope of CB-based composites is similar to the end of the percolation region described in the percolation theory of carbon-based composites [7,67]. According to the percolation theory, electrical conductivity increases sharply when the filler content is within a certain range. The increase in filler content after crossing the end of percolation region does not significantly increase the electrical conductivity. A similar phenomenon was also observed in a study in which graphite was added to the HDPE matrix, and after a certain amount, the slope of electrical conductivity vs. filler content graph started to decrease [68].
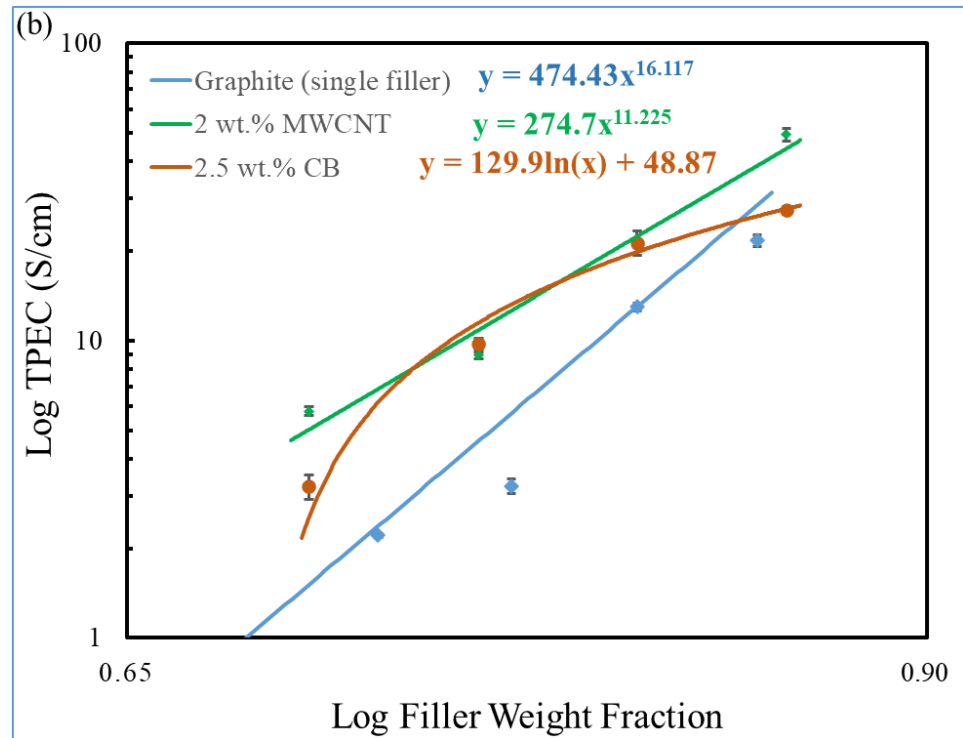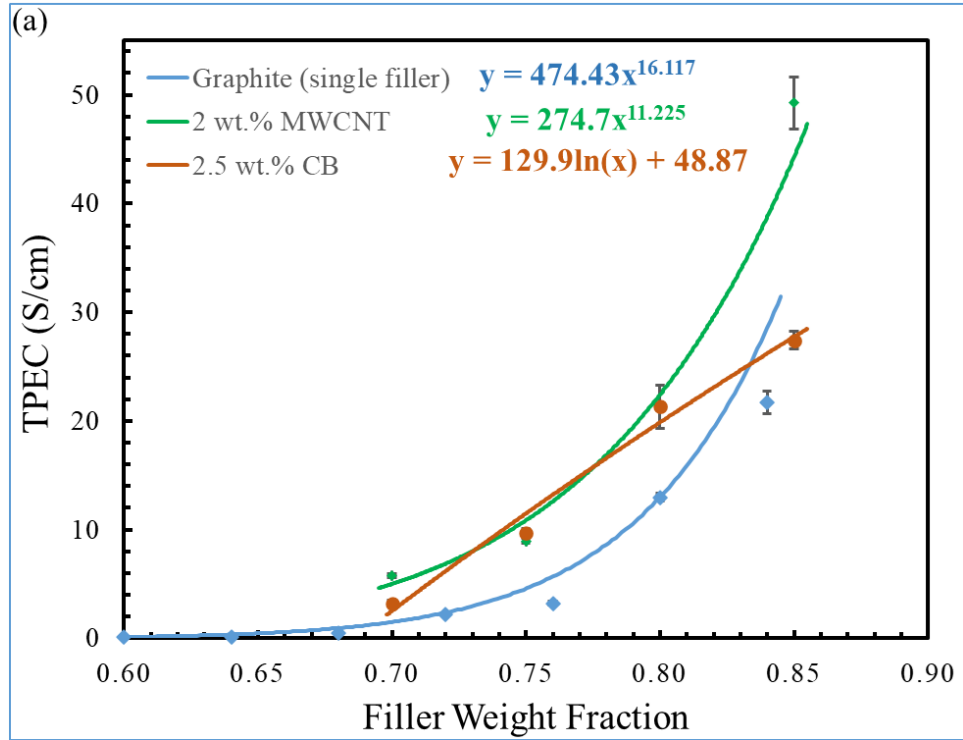
Figure 4.12: Comparison of electrical conductivity of single filler and binary filler composites (a) linear graph (b) log-log graph.

The synergistic enhancement of electrical conductivity with the addition of binary fillers can be proposed using the schematics illustrations in Figure 4.13 alongside the SEM micrographs (a-f).   The SEM images of single filler PP/graphite composites, MWCNT-based composites, and CB-based composites are presented in Figure 4.13(a), Figure 4.13(c), and Figure 4.13(e), respectively. The large aspect ratio of MWCNT particles helps in linking one graphite particle with another, resulting in the formation of a conductive network that increases the electrical conductivity of the composite material. The conductive path generated by the MWCNT can be seen in Figure 4.13(c) and Figure 4.13 (d). However, a decrease in the polymer content of the composite results in the poor dispersion of MWCNT and affects the interfacial interaction with the polymer. Hence, the effectiveness of MWCNT on the PP/graphite composites reduces with an increase in the total filler content. A very high surface area and small particle size of CB help fill the gaps between graphite particles and form additional conductive paths, enhancing the electrical conductivity of the composites. The linkages of CB generated between graphite particles can be seen in Figure 4.13(e) and Figure 4.13(f). However, an increase in the total filler loading decreases the polymer content of the composite, resulting in poor wetting of CB particles with the resin. The electrical conductivity of CB-based composites was 244% higher than single filler PP/graphite composites at 75 wt.% of total filler content. In contrast, the addition of CB to the PP/graphite increased the electrical conductivity by only 26.4% when the total filler content was 85 wt.%. Therefore, adding CB to the highly filler-loaded composites will not significantly improve the electrical conductivity of the composites.
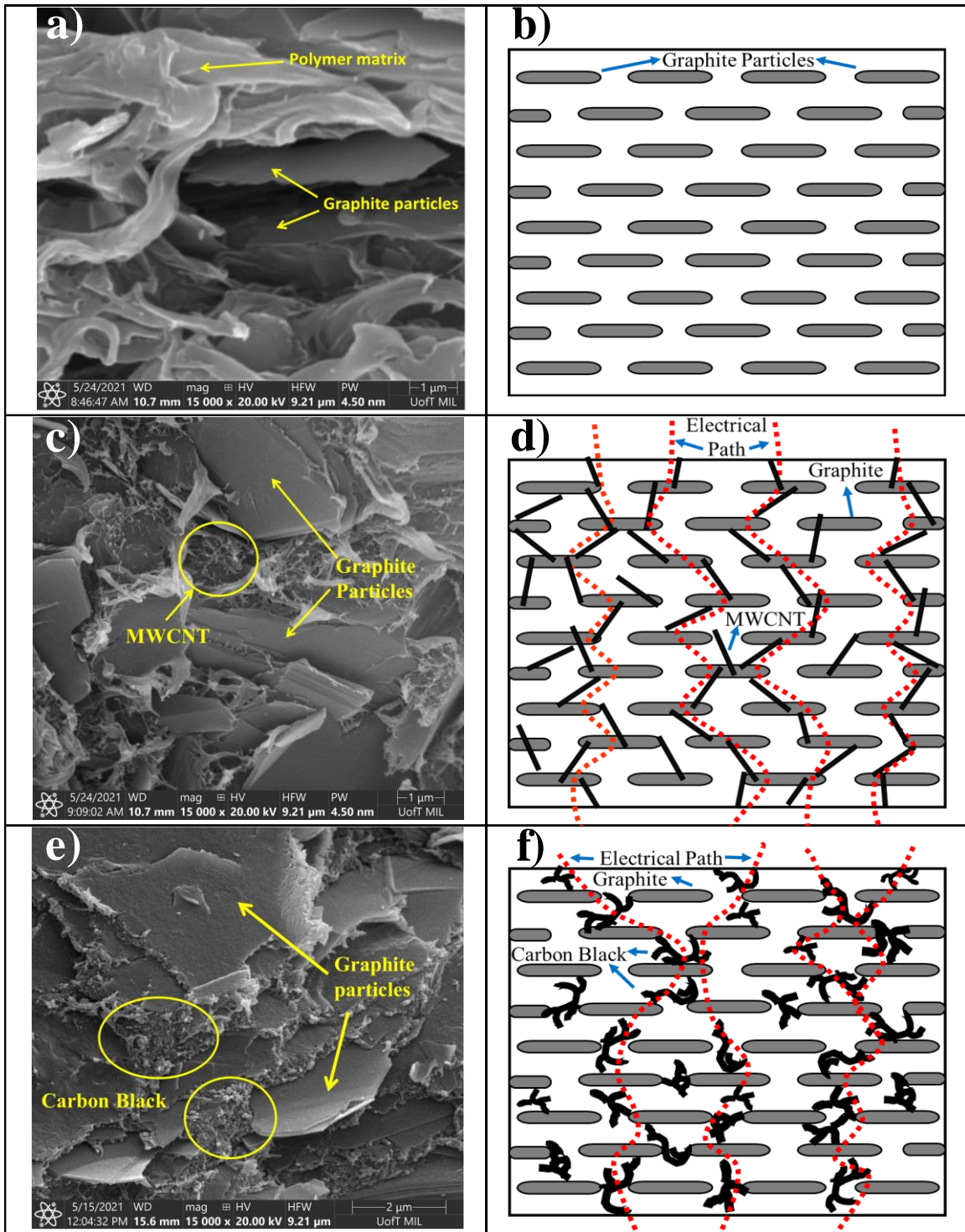
Figure 4.13: SEM micrograph and schematic illustration of PP composites; Graphite (a-b), MWCNT - Graphite (c-d), and (e-f) Carbon Black – Graphite.

b) Effect of binary filler on the flexural strength

The flexural strength of all three types of composites as a function of total filler content is depicted in Figure 4.14. The flexural strength of all composites decreased with an increase in the total filler content. The curve fit for single filler composite shows that the flexural strength is decreasing exponentially, whereas the reduction of flexural strength in the case of binary filler composites is linear with the slope of -0.283 MPa/wt.% for CB-based composites and -0.497 MPa/wt.% for MWCNT-based composites.

At a low filler content, the load of the polymer matrix was carried by graphite particles. The addition of MWCNT decreased the flexural strength of the composite, possibly due to the agglomeration of MWCNT, which can be seen in Figure 4.13(c). A similar phenomenon was found by Dhakate et al. who report that the addition of 2 vol.% of MWCNT decreased the overall bending strength of the composite [25]. At a higher filler content, the decrease in the polymer content causes poor wetting of graphite by the resin, resulting in an exponential reduction in the flexural strength of the PP/graphite composites. In contrast, the reduction in the flexural strength of MWCNT-based composites on increasing filler content is not as rapid as in single filler PP/graphite composites. The MWCNT particles in highly-filled composites may act as stress concentrators due to their rigidity and high aspect ratio [69]. The MWCNT particles support the load of the matrix when the graphite particles are unable to contribute to the bending strength due to the poor interfacial bonding with the resin. The high aspect ratio of MWCNT particles enables better interfacial bonding with the resin despite agglomeration and low polymer content. Liao et al. [69] also found that the addition of MWCNT improved the flexural strength of the composite when the total filler content was 80 wt.%. Thus, the addition of MWCNT as a binary filler in highly filled PP/graphite composites improves the bending strength of the composite. In the case of CB-based composites, the binary filler has a very high surface area compared to the primary graphite filler. The high surface area improved the interfacial interaction of the CB particle with the polymer, thereby enhancing the overall mechanical performance compared to the single filler PP/graphite composites.
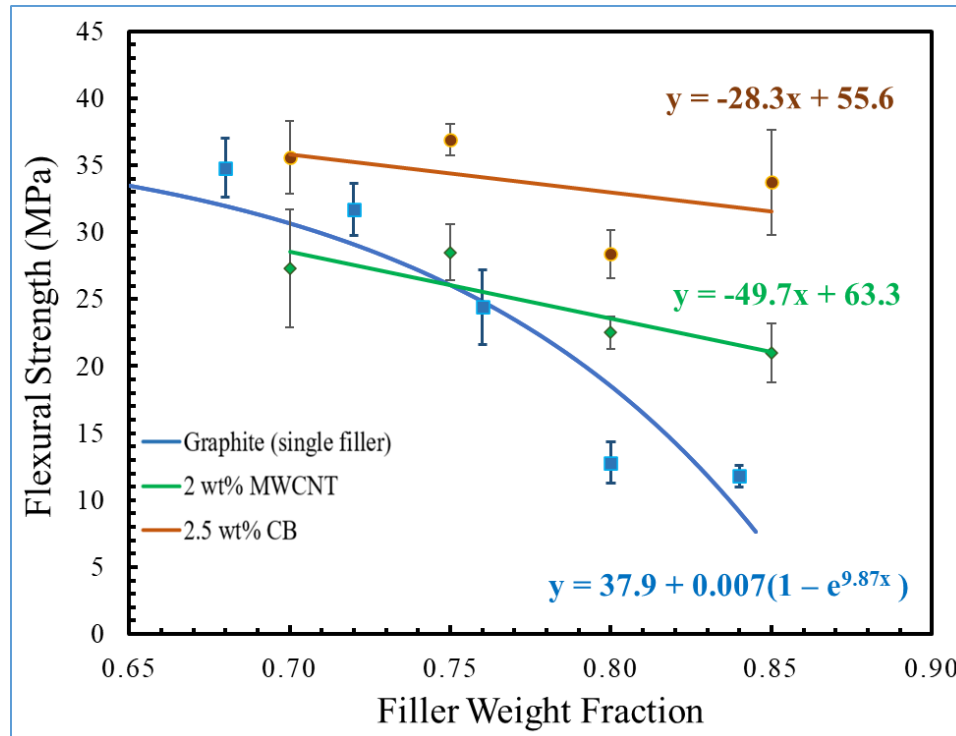
Figure 4.14: Flexural strength comparison of single filler and binary filler composites.

4.2 Effects of Thermoplastic Resins on the Properties of Composites

This study investigates how the properties of electrically conductive thermoplastic composites are affected by the inherent properties of polymer matrices. Thermoplastic resins are lightweight, recyclable, and easy to process into any shape. Carbon-based conductive fillers were added to the different polymer matrices to create electrically conductive paths inside the matrix and enhance their conductivity. Electrically conductive thermoplastic composites were produced by using a twin-screw extruder to study the effect of the bonding matrix on the electrical and mechanical properties of the composites. Graphite and CB were used as conductive fillers and incorporated into PP, nylon, and TPU at different compositions. This study has been categorized into two parts. This first section focuses on single filler polymer-graphite composites containing graphite as a single filler at different filler loadings. The second part examines the synergistic effects of binary fillers in different polymer matrices, where CB was added as a binary filler to polymer graphite. The composites were tested for through-plane electrical conductivity and flexural strength. The other mechanical properties such as flexural modulus, fracture strain, and fracture

56

toughness were also calculated from the stress-strain curves. The properties of PP, nylon, and TPU composites were plotted as a function of filler content and compared.

4.2.1   Filler Formulations

The investigation of thermoplastic resins was carried out in two parts. The first part of this study examines how the inherent properties of polymer matrix affect the electrical and mechanical properties of single filler composites. The polymer composites were manufactured by adding graphite to the PP, nylon, and TPU. The polymer material was fed through the main feeder of the twin-screw extruder, and graphite was introduced from the side feeder. By controlling the feed rates of both feeders, the composites were produced by varying the graphite compositions from 68 wt.% to 84 wt.%. The second part of the study is to investigate the interaction of the binary filler with the graphite in each polymer matrix and the synergistic effects of binary filler on the properties of the composites. The CB was added as a binary filler to the polymer/graphite composites. CB was dry-mixed with graphite at different ratios so that the binary filler composites could be produced by varying the CB content from 0 wt.% to 6 wt.%. The total filler content for all the binary filler composites was fixed at 75 wt.%, and the composition of graphite was configured accordingly. PP, nylon, and TPU composites were compared at different filler configurations to determine the influence of polymer matrices on composite properties.

4.2.2   Single Filler Composites

The single filler polymer/graphite composite pellets were processed through the compression molding technique. The samples for electrical conductivity and flexural strength testing were made from compression-molded discs. The values of electrical conductivity, flexural strength, elongation at break, fracture toughness, and flexural modulus for each composite are presented in Table 4.5.

Table 4.5: Electrical and mechanical properties of single filler PP, TPU, and Nylon composites.

S.no	Polymer matrix	Graphite content (wt.%)	TPEC (S/cm)	IPEC (S/cm)	Flexural Strength (MPa)	Flexural Modulus (GPa)	Fracture Strain (%)	Fracture Toughness (J/m³)
1		84	21.69 ± 1.02	45.5 ± 2.6	11.8 ± 0.8	20.9 ± 1.1	0.12 ± 0.02	5.1 ± 0.4
2		80	12.97 ± 0.35	28.1 ± 1.3	12.8 ± 1.6	19.8 ± 0.1	0.10 ± 0.01	6.5 ± 1.5
3	PP	76	3.24 ± 0.18	7.1 ± 0.5	24.4 ± 2.8	18.7 ± 0.9	0.28 ± 0.03	32.8 ± 10.5
4		72	2.21 ± 0.03	4.1 ± 0.1	31.7 ± 2.0	17.1 ± 2.1	0.31 ± 0.03	64.9 ± 12.5
5		68	0.52 ± 0.01	2.1 ± 0.1	34.8 ± 2.2	14.8 ± 1.7	0.38 ± 0.03	86.6 ± 9.6
6		84	26.29 ± 1.25	58.6 ± 4.5	14.1 ± 2.4	13.6 ± 3.7	0.23 ± 0.05	18.6 ± 6.5
7		80	4.37 ± 0.18	13.0 ± 1.5	17.7 ± 2.2	9.3 ± 0.4	0.65 ± 0.09	66.3 ± 10.3
8	TPU	76	2.54 ± 0.03	8.6 ± 0.6	17.8 ± 0.9	8.0 ± 1.5	0.81 ± 0.03	90.1 ± 6.0
9		72	1.43 ± 0.05	4.9 ± 0.1	18.1 ± 1.0	7.0 ± 0.1	0.92 ± 0.05	118.5 ± 9.2
10		68	0.92 ± 0.01	3.9 ± 0.1	18.4 ± 0.9	6.5 ± 0.2	1.10 ± 0.08	139.6 ± 17.3
11		84	3.65 ± 0.44	12.1 ± 0.9	38.7 ± 4.3	31.4 ± 0.9	0.31 ± 0.02	73.6 ± 5.8
12		80	2.67 ± 0.03	8.7 ± 1.2	49.7 ± 4.1	31.4 ± 2.1	0.35 ± 0.05	93.1 ± 25.9
13	Nylon	76	1.22 ± 0.04	3.3 ± 0.4	47.5 ± 5.8	24.5 ± 1.1	0.42 ± 0.05	125.4 ± 31.3
14		72	0.76 ± 0.03	2.3 ± 0.2	44.7 ± 1.1	17.5 ± 1.7	0.51 ± 0.07	114.0 ± 19.9
15		68	0.61 ± 0.02	2.1 ± 0.1	37.0 ± 2.2	15.8 ± 2.0	0.57 ± 0.05	156.5 ± 14.1

a) TPEC of single filler composites

The composites were tested for through-plane electrical conductivity on the lab-scale electrical conductivity set-up. The TPEC values are plotted as a function of filler weight fraction in Figure 4.15. Increasing graphite content led to an increase in the electrical conductivity of all types of composites. However, different composites have different trendlines for electrical conductivity. Among the composites tested, the TPU composite with 84 wt.% filler content had the highest electrical conductivity of 26.3 S/cm. Compared to PP and TPU composites, nylon composites had a lower electrical conductivity for all filler compositions. In the case of TPU composites, electrical conductivity increased substantially when filler content was increased from 80 wt.% to 84 wt.%. To determine the trend of electrical conductivity more precisely, a log-log graph of electrical conductivity values against filler weight fraction was plotted in Figure 4.15(b). The log-log graph

indicates that the electrical conductivity of all types of composites increases logarithmically as the filler content increases. The slope of PP composites on the logarithmic graph in Figure 4.15(b) is 16.12, while the slope of TPU and nylon composites are 14.66 and 9.11, respectively.

The polymer matrices used in this study have different densities. The comparison of PP, nylon, and TPU matrices was carried out by comparing the values of electrical conductivity on the same weight fraction of graphite. While filler weight fractions are the same for all matrices, filler volume fractions are different due to the difference in their densities. The conductivity network created by the filler particles inside the polymer matrix mainly depends on the ratio of the volume of filler to the volume of the polymer. For a better understanding of the values of electrical conductivity in different matrices, the electrical conductivity of the composites was plotted as a function of filler volume fraction in Figure 4.16. It can be observed in Figure 4.16(a) that the TPU composites have the highest filler volume fraction at 84 wt.% of filler composition. The sudden jump in the electrical conductivity of TPU composites can be attributed to the increase in filler volume fraction. Increasing filler weight composition from 80 wt.% to 84 wt.% in TPU composites increased the filler volume composition from 73 vol.% to 78 vol.%, which reduced the polymer content of the composites and increased the electrical connections between the graphite particles. In contrast, the filler volume fraction of nylon composites is higher than the PP composites, but the electrical conductivity of nylon composites is lower. This may be due to the degradation of filler particles during the melt-compounding, as the melt pressure and temperature were higher during the processing of nylon composites.
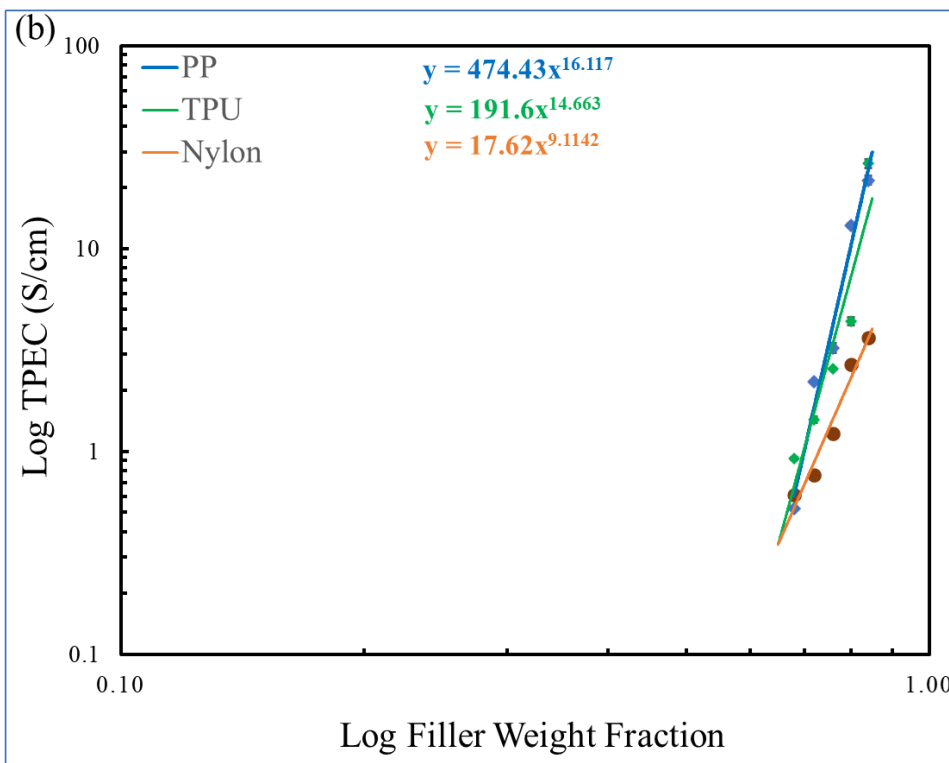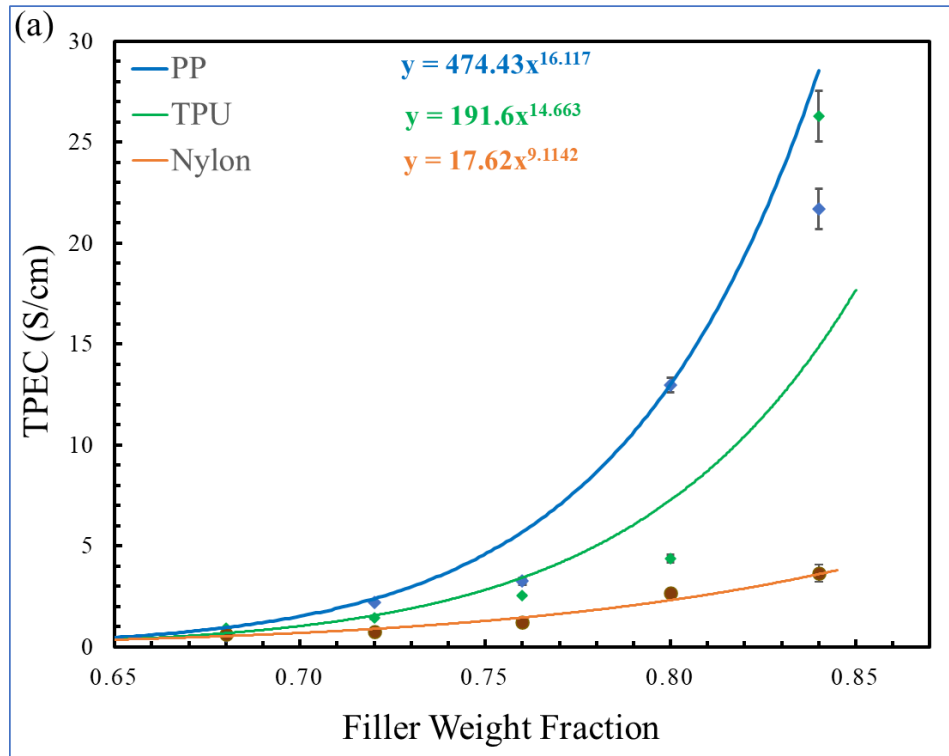
Figure 4.15: TPEC vs. filler weight fraction graph (a) linear scale (b) logarithmic scale.
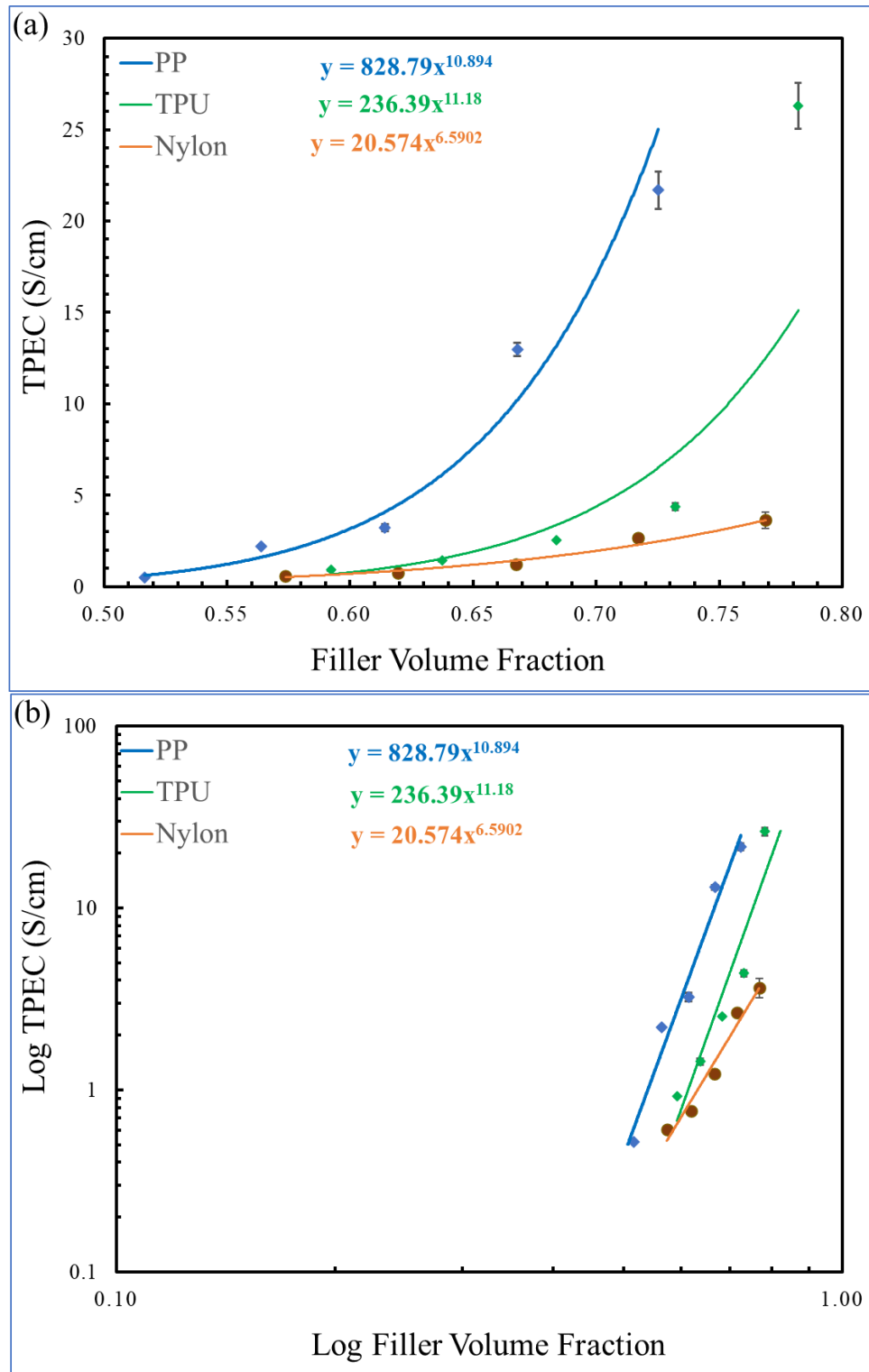
Figure 4.16: TPEC vs. filler volume fraction graph (a) linear scale (b) logarithmic scale

b) IPEC of single filler composites

The composites were tested for in-plane electrical conductivity, and IPEC values are plotted as a function of filler weight fraction and filler volume fraction in Figure 4.17(a) and Figure 4.17(b), respectively. In general, increasing graphite content increased IPEC for all composites. A sudden increase in the IPEC values was recorded in PP and TPU composites when the filler content increased from 76 wt.% to 84 wt.%. The IPEC of PP composites increased from 7.1 to 45.5 S/cm, while the IPEC of TPU composites increased from 8.6 to 58.6 S/cm in this region. This may be due to the low polymer content between the graphite particles. TPU composites have a sharper increase in IPEC than PP composites because TPU composites have the highest filler volume fraction, as shown in Figure 4.17(b). Similar to TPEC values, IPEC values of nylon composites were lower than TPU and PP composites. It may be related to the degradation of filler particles during melt-compounding since nylon composites had higher melt pressure and temperature than TPU and PP composites.

(a)

PP $y = 651.41x^{15.231}$
TPU $y = 290.27x^{11.984}$
Nylon $y = 54.022x^{9.0172}$

IPEC (S/cm)

Filler Weight Fraction
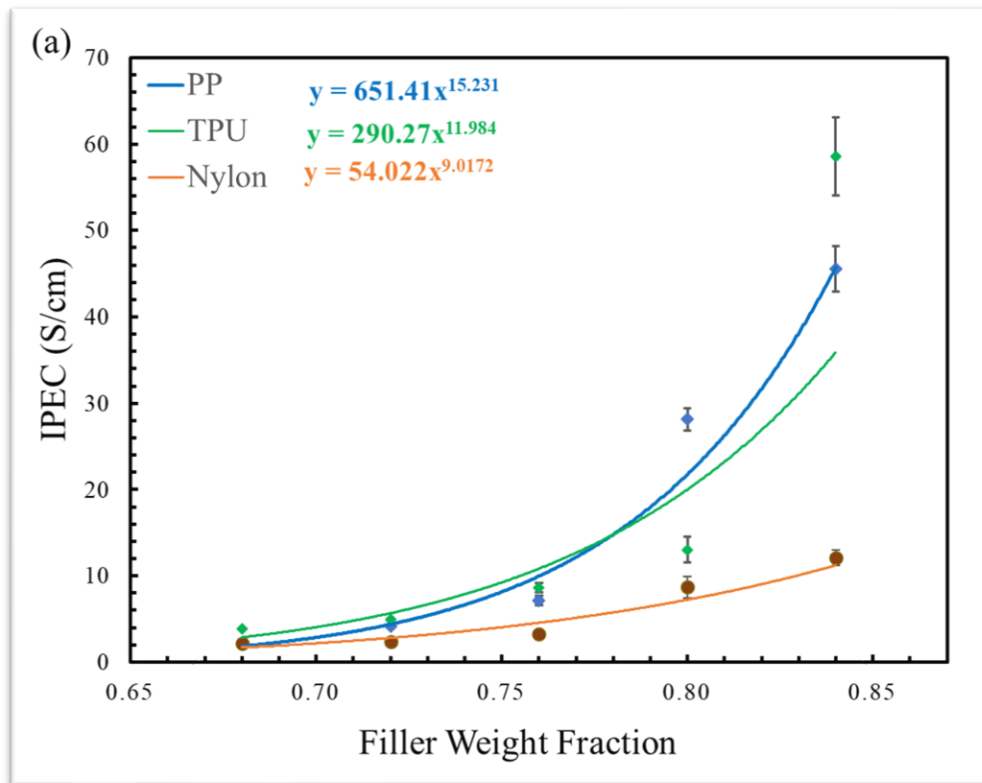
Figure 4.17: IPEC of single filler PP, TPU, and nylon composites plotted against (a) filler weight fraction and (b) filler volume fraction.

c) Flexural strength of single filler composites

The flexural strength testing of all the composites was performed by a 3-point bending test. The value of flexural strength is plotted as a function of filler weight fraction and filler volume fraction in Figure 4.18(a) and Figure 4.18(b), respectively. The highest value of flexural strength recorded in this section was 49.7 MPa with 80 wt.% filler loading in the nylon matrix. At different filler loadings, the composites have different values for flexural strength. Each composite has a different trend in flexural strength with an increasing filler loading. The flexural strength of PP and TPU composites was decreased with increasing filler loading. However, the flexural strength of TPU composites decreased linearly with increasing the filler content, while an exponential reduction in the flexural strength of PP composites was observed. This is a possibility due to the low polymer content in the composites, which caused poor wetting of graphite with the resins. As compared to PP, the flexural strength of TPU composites reduced linearly, which represents better interfacial bonding of the filler with graphite even at low polymer volume. Increasing the filler loading

increased the flexural strength of nylon composites, but it began to reduce after a specific filler loading. This may be attributed to the strong bonding of nylon with the graphite particles, and after a certain filler loading, the reduction in polymer content led to the poor wetting of graphite.
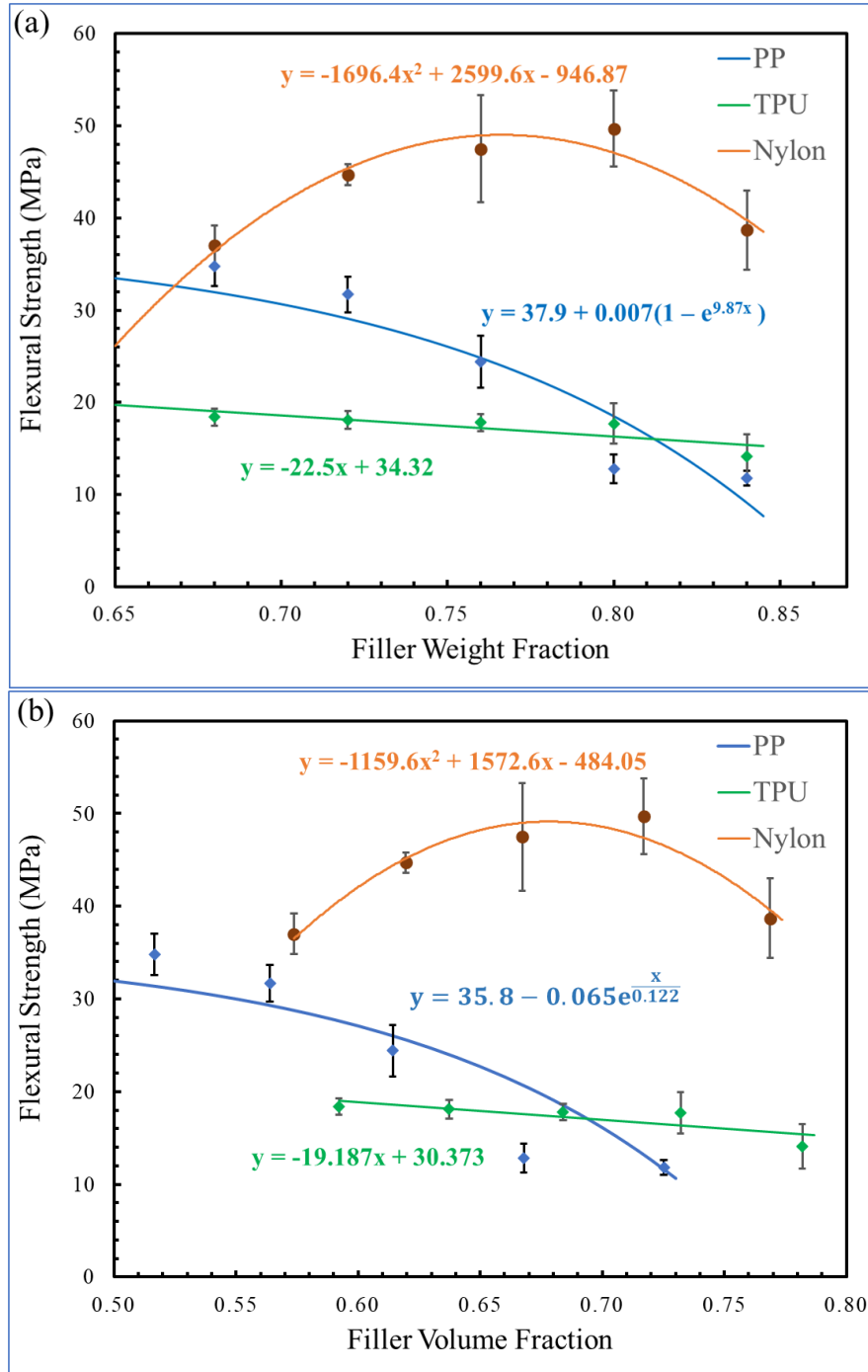
Figure 4.18: Flexural strength of single filler PP, TPU, and nylon composites plotted against (a) filler weight fraction and (b) filler volume fraction.

d) Fracture strain of single filler composites

The fracture strain of the composites was measured from the stress-strain curves data obtained from the flexural strength testing. The average elongation at break values of five composites for each composition, along with the standard deviation, is presented in Table 4.5. The fracture strain values of all the composites are presented as a function of filler weight fraction and filler volume fraction in Figure 4.19(a) and Figure 4.19(b), respectively. The fracture strain of the composites decreased with increasing the filler content. The TPU composites demonstrated the highest values of fracture strain at low filler loading. However, the fracture strain of TPU composites decreased drastically with an increase in the filler content. This may be due to the low polymer content of the composites. As shown in Figure 4.19(b), the TPU composites had the lowest polymer volume fracture as compared with the PP and nylon composites. The fracture strain of nylon composites reduced linearly with an increase in the filler content. PP composites exhibited the lowest fracture strain of all graphite compositions.

(a)

PP $y = 8.0323x^2 - 14.049x + 6.2484$

TPU $y = -24.287x^2 + 31.867x - 9.3719$

Nylon $y = -1.677x + 1.7058$
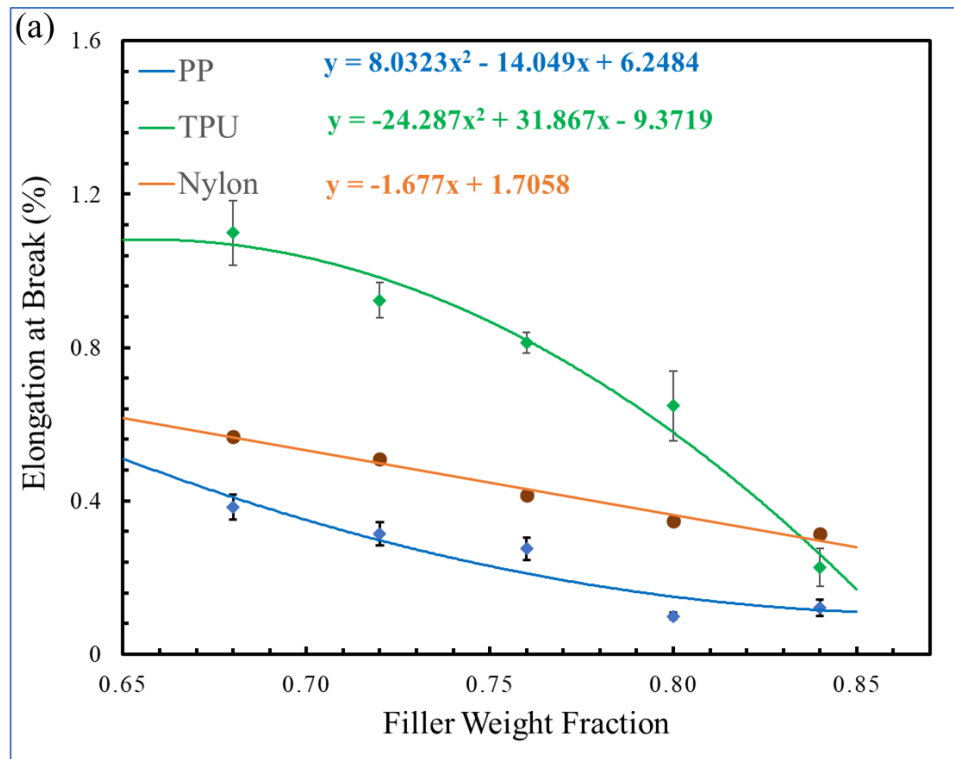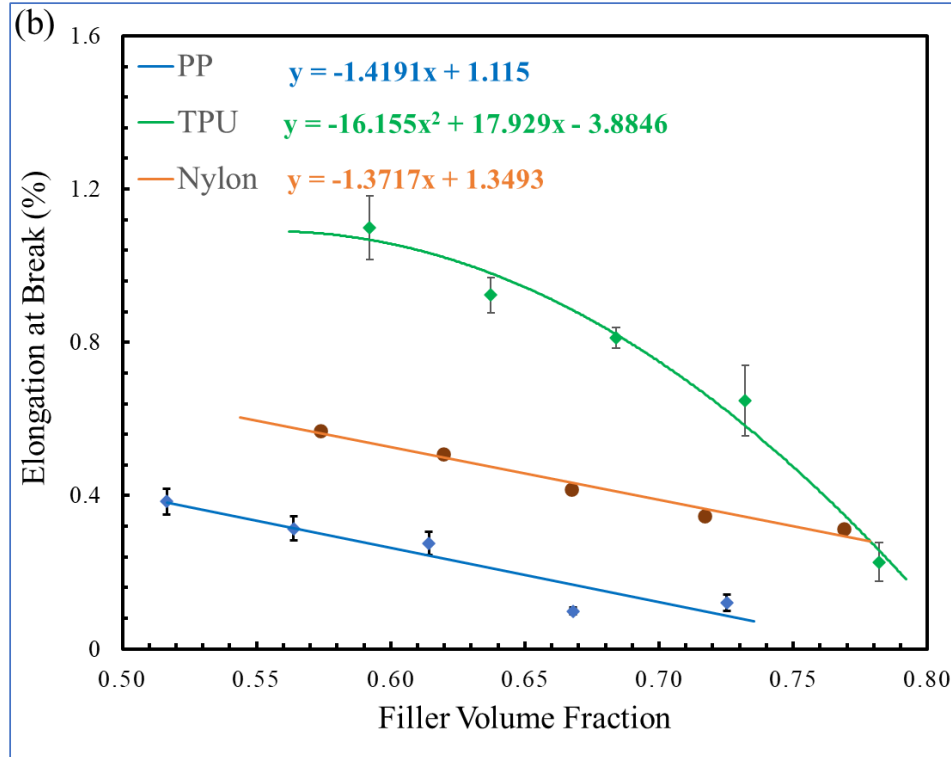
Figure 4.19: Fracture strain of single filler PP, TPU, and nylon composites plotted against (a) filler weight fraction and (b) filler volume fraction.

e) Fracture toughness of single filler composites

The fracture toughness of the composites was calculated by the area under the curve of stress-strain curves. The fracture toughness of the composites is plotted against the filler weight fraction and filler volume fraction in Figure 4.20(a) and Figure 4.20(b), respectively. Similar to elongation at the breaking point, the toughness of the composites decreased with increasing the filler loading. The nylon composites are comparatively tougher than the TPU and PP composites. The toughness of nylon reduced linearly with increasing the filler composition. Like elongation at break values, a significant reduction in the toughness of TPU composites was observed at higher filler loading, which may be due to the low polymer volume fraction. The PP composites demonstrated the lowest fracture toughness of all the compositions. Overall, the decreasing trend of the fracture toughness of the composites is similar to the fracture strain discussed in the previous section.
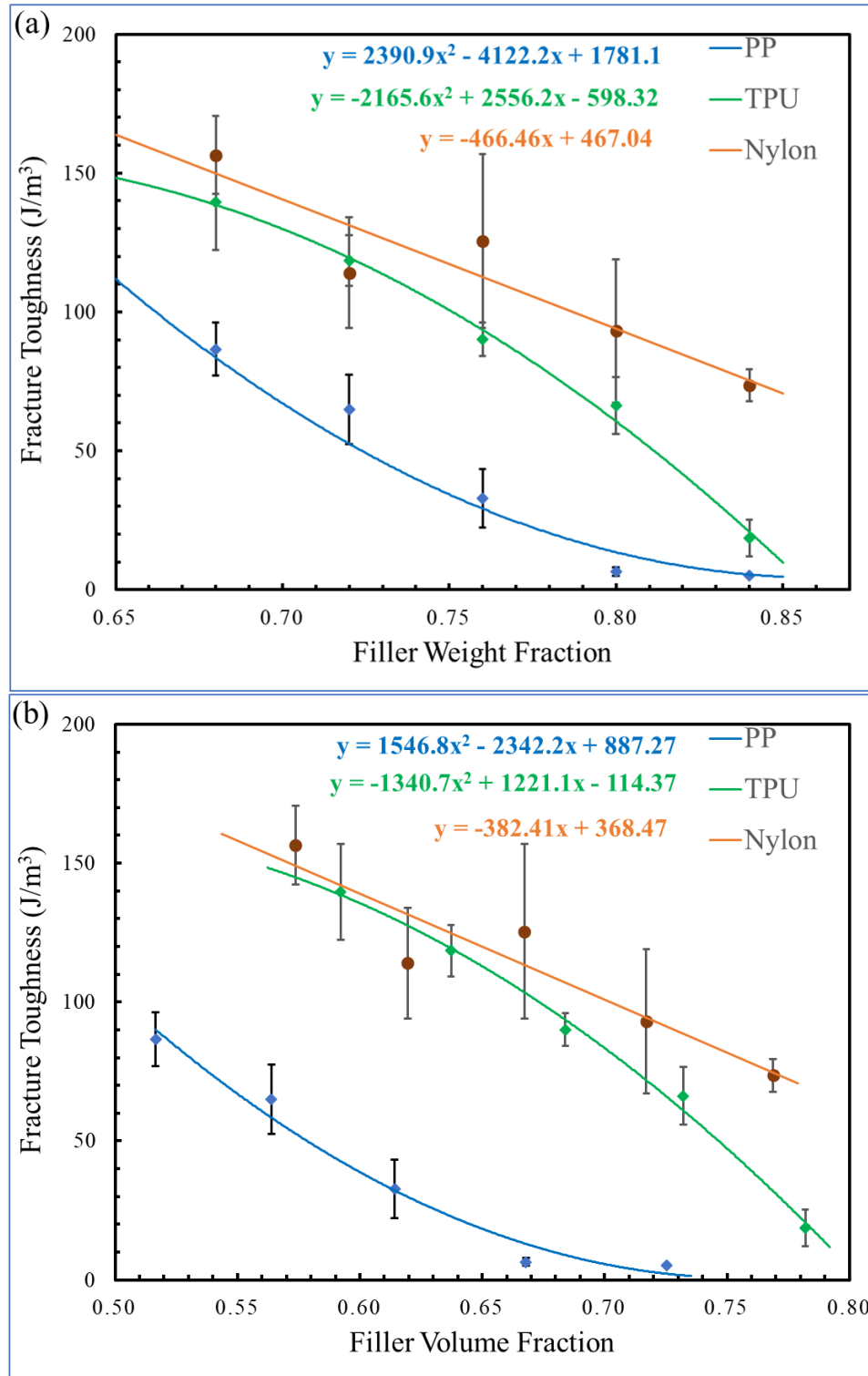
Figure 4.20: Fracture toughness of single filler PP, TPU, and nylon composites plotted against (a) filler weight fraction (b) filler volume fraction.

f) Flexural modulus of single filler composites

The flexural modulus of the composites was calculated from the slope of stress-strain curves obtained from the flexural strength testing of the composites. The average and standard deviation of five samples for each composition are listed in Table 4.5. Figure 4.21(a) and (b) presented the flexural modulus values of PP, nylon, and TPU composites as a function of filler weight fraction and filler volume fraction, respectively. The flexural modulus of the composites was highly influenced by the flexural modulus of the bonding matrix. Composites made of nylon had the highest values of flexural modulus, while composites made of TPU had the lowest values. The flexural modulus of all composites increases linearly with graphite content. However, the slope of the curve fit equation in the case of nylon composites is almost three times higher than the TPU and PP composites. In contrast, the trendlines of PP and TPU composites are almost parallel to each other.
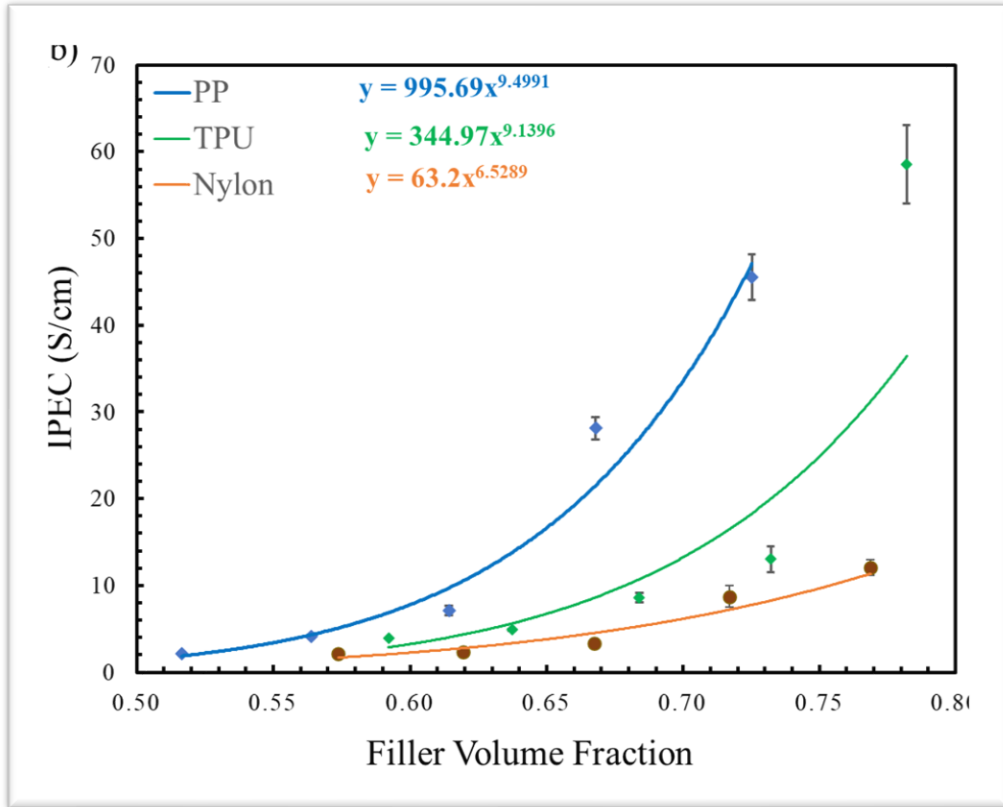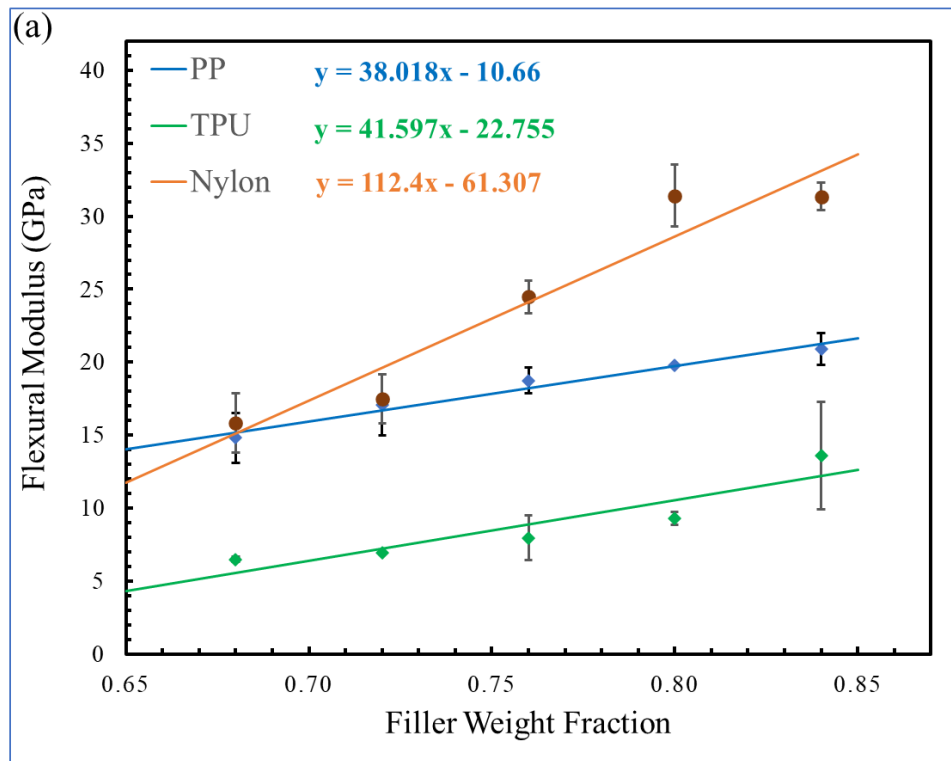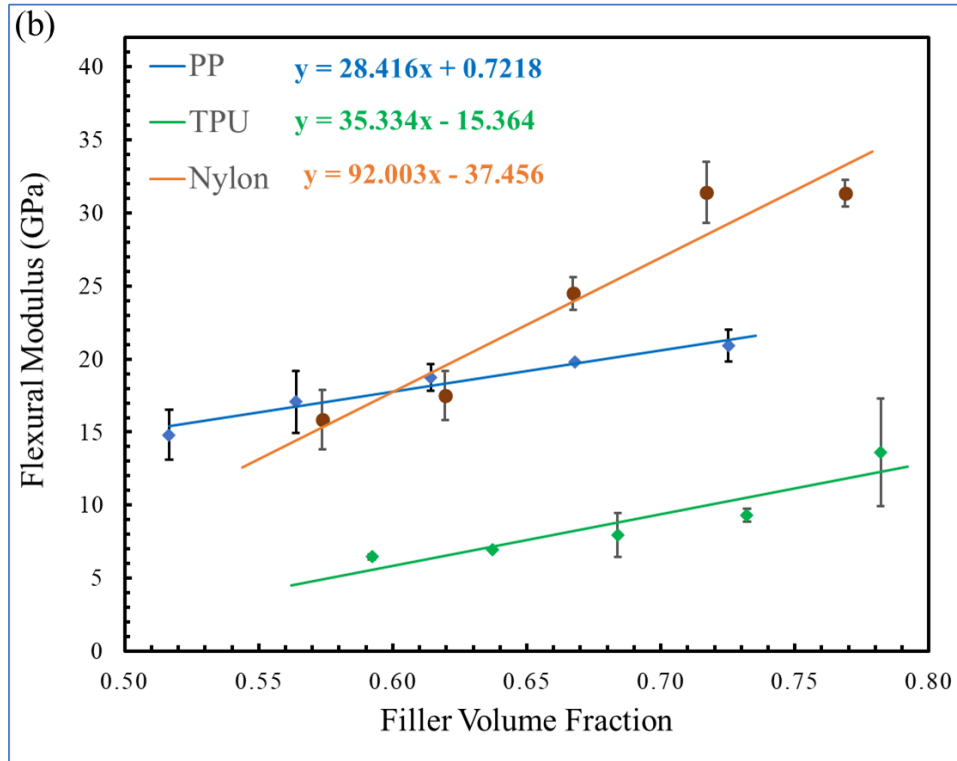
Figure 4.21: Flexural modulus of single filler PP, TPU, and nylon composites plotted against (a) filler weight fraction (b) filler volume fraction.

4.2.3 Binary Filler Composites

The binary filler composites were prepared by adding the CB as a binary filler to the single filler polymer/graphite composites on different compositions. The base filler was graphite, and the total filler content was fixed at 75 wt.%. The CB was added at different compositions ranging from 0 wt.% to 6 wt.%. The composition of graphite was adjusted according to the content of CB. Similar to the single filler composites, the characterization of electrical and mechanical properties of binary filler composites was also carried out. The properties of binary filler composites are listed in Table 4.6

.

Table 4.6: Electrical and mechanical properties of binary filler PP, TPU, and Nylon composites

S.no	Polymer matrix	CB Content (wt.%)	TPEC (S/cm)	Flexural Strength (MPa)	Flexural Modulus (GPa)	Fracture Strain (%)	Fracture Toughness (J/m^3)
1		0	2.8 ± 0.2	30.3 ± 1.3	18.8 ± 0.9	0.31 ± 0.03	55.7 ± 12.9
2	PP	2	8.7 ± 0.1	35.2 ± 0.8	19.7 ± 1.4	0.38 ± 0.04	85.8 ± 5.6
3		4	15.2 ± 0.1	35.9 ± 1.2	17.7 ± 1.1	0.35 ± 0.05	79.1 ± 6.3
4		6	21.2 ± 0.3	28.5 ± 1.3	15.1 ± 0.8	0.23 ± 0.05	35.4 ± 4.6
5		0	2.2 ± 0.2	17.9 ± 0.7	7.8 ± 0.3	0.84 ± 0.04	95.3 ± 7.3
6	TPU	2	6.8 ± 0.4	24.3 ± 1.7	11.5 ± 1.1	0.83 ± 0.10	125.5 ± 40.6
7		4	14.7 ± 0.4	38.3 ± 1.5	25.0 ± 3.0	0.33 ± 0.02	77.2 ± 4.9
8		6	46.2 ± 0.1	16.7 ± 0.6	11.0 ± 0.7	0.32 ± 0.02	34.3 ± 4.8
9		0	1.1 ± 0.1	46.9 ± 1.1	22.3 ± 1.4	0.44 ± 0.06	127.1 ± 16.2
10	Nylon	2	2.9 ± 0.1	56.0 ± 5.2	32.3 ± 4.0	0.45 ± 0.05	148.9 ± 34.6
11		4	7.6 ± 1.5	55.1 ± 4.8	33.1 ± 3.8	0.34 ± 0.05	104.8 ± 22.9
12		6	9.7 ± 2.0	42.6 ± 5.8	29.2 ± 1.5	0.25 ± 0.03	58.4 ± 6.9

a) TPEC of binary filler composites

Adding CB as a binary filler significantly improved the TPEC values of the composites. The TPEC of the binary filler composites is plotted as a function of CB content in Figure 4.22. The TPU composites with 6 wt.% CB demonstrated the highest electrical conductivity of 46.2 S/cm. The electrical conductivity value of single filler nylon/graphite composite was 1.1 S/cm. The incorporation of 6 wt.% of CB to nylon/graphite composite enhanced the electrical conductivity by nine times, reaching 9.7 S/cm. The electrical conductivity of PP/graphite composites increased to 21.2 S/cm after the addition of CB at 6 wt.%, almost 7.5 times the electrical conductivity of PP/graphite composites without CB. The synergistic effects of CB on the electrical conductivity are very evident in the case of TPU composites, where electrical conductivity increased by 21 times with 6 wt.% addition of CB. The polymer content between the graphite particles acts as an insulation layer and prevents electron hopping. The high surface area of CB connects graphite particles by forming additional conductive links between them, improving the electrical conductivity of the composite. Kang et al. [70] recorded a noticeable improvement in the electrical conductivity on 5 wt.% CB as a binary filler in the graphite-phenolic resin. King et al. [15]

added CB as a binary filler in PP/graphite composites and recorded a significant increase in the electrical conductivity, from 0.29 S/cm to 2.8 S/cm. Electrical conductivity of PP and nylon composites increased linearly on the addition of CB, with slopes of 3.1 and 1.5 S/cm for every wt.% of CB, respectively. In contrast, the electrical conductivity of TPU composites increased exponentially, and the electrical conductivity spiked between 2 and 4 wt.% of CB content. The exponential increase in the electrical conductivity of the TPU composites was possibly due to the low polymer content of the composites. The density of TPU is comparatively higher than the PP and nylon. Therefore, the polymer volume fraction of TPU composites at 75 wt.% filler loading was lower than the PP and nylon composites. The high content of CB in TPU composites consumed a considerable amount of polymer, reducing the amount of polymer content between the graphite particles. This low polymer content also led to improper filler mixing during melt compounding, which caused a surge in electrical conductivity.
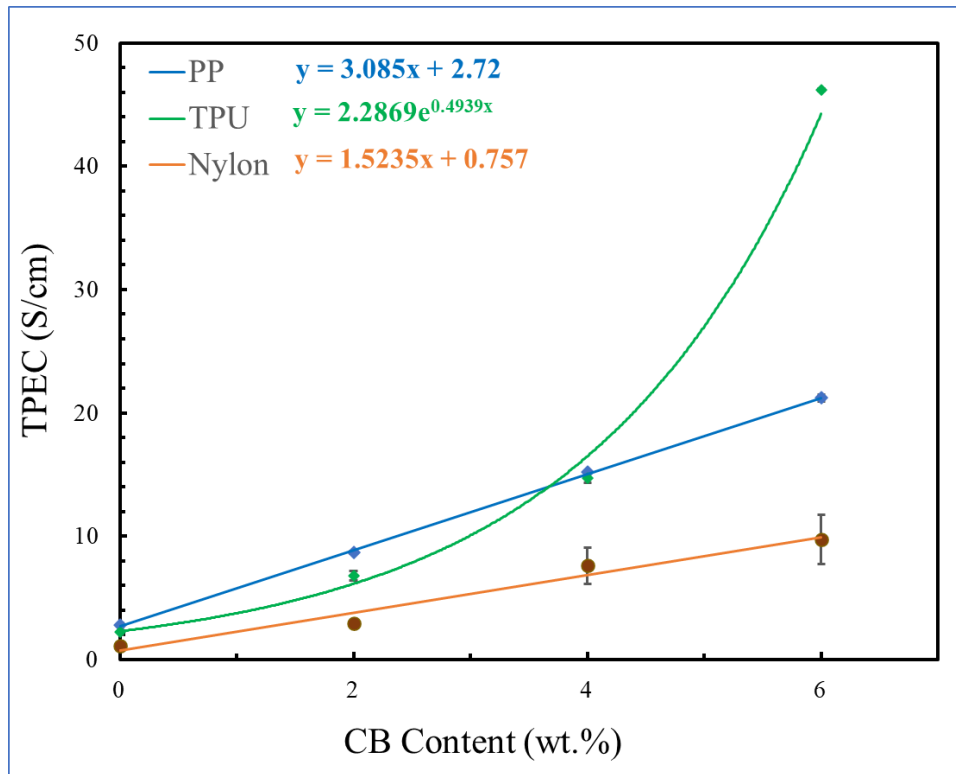
Figure 4.22: Electrical conductivity of PP, TPU, and nylon composites as a function of CB content.

b) Flexural strength of binary filler composites

The flexural strength of the binary filler composites was measured by a 3-point bending test. The flexural strength of the binary filler composites was plotted against the CB content in Figure 4.23. The mechanical properties of all types of composites were significantly improved by introducing a small amount of CB. In contrast, the high composition of CB had a negative impact on flexural strength. The highest flexural strength recorded in binary filler composites was 56 MPa with 2 wt.% CB in nylon composites. In PP/graphite composites, the flexural strength increased from 30.3 to 35.2 MPa when 2 wt.% CB was added to the composite but decreased from 35.9 to 28.5 MPa when CB content was between 4 and 6 wt.%. A similar trend was observed in the case of TPU and nylon composites. As mentioned in the previous section, the high surface area of CB improves interfacial bonding with the resin, thereby enhancing flexural strength. In contrast, the high CB content inside the composite caused it to absorb a large amount of resin, thus causing the graphite to have poor wetting and, in turn, reducing its flexural strength [70]. Similar results were observed when Kang et al. [70] incorporated CB as a binary filler at different compositions for manufacturing lightweight fuel cell stacks. The bending strength of the composites increased with an addition of 1 wt.% of CB but started to decrease after adding more than 3 wt.% CB.

The flexural strength values of all the binary filler nylon composites were higher than that of TPU and PP composites. TPU composites had comparatively low flexural strengths. The overall flexural strength of the composites was influenced by the flexural strength of the bonding matrix. The curve fit equations for flexural strength versus CB content graph show similar trends for all composites. The slopes of curve fit equations can be used to calculate the amount of CB that will give the maximum flexural strength. The slopes of PP, TPU, and nylon composites trendlines are zero at 2.85, 3.52, and 2.74 wt.% of CB, respectively.
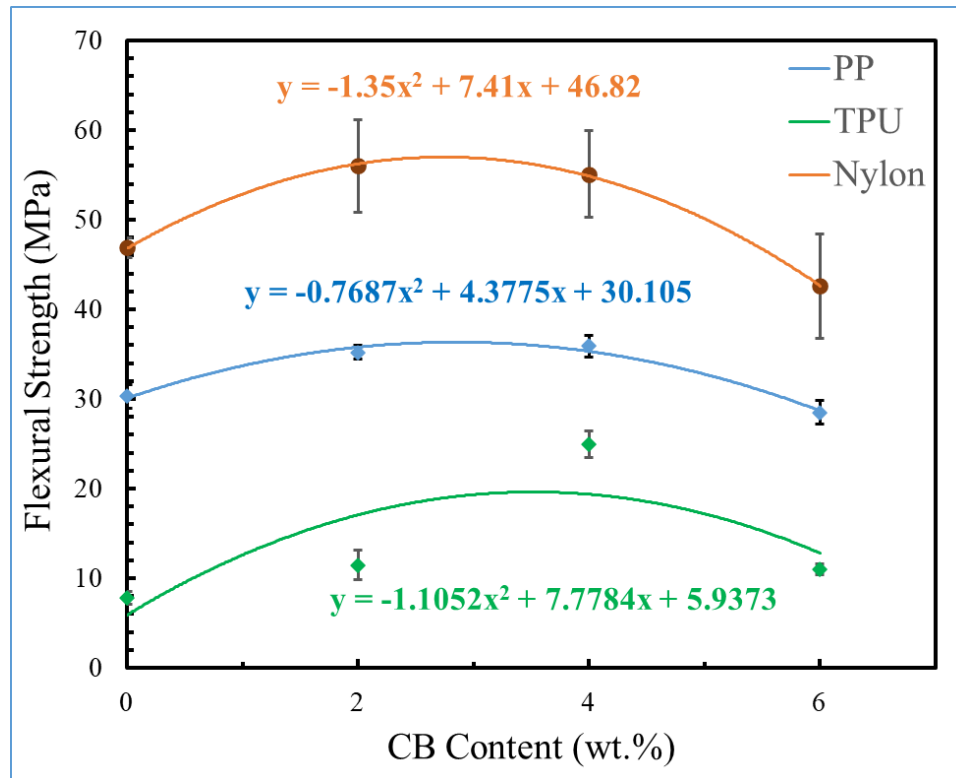
Figure 4.23: Flexural strength of PP, TPU, and nylon composites as a function of CB content.

c) Fracture strain of binary filler composites

The fracture strain values of the binary filler composites were analyzed from the stress-strain curves data of the 3-point bending test. The mean values of elongation at break and the standard deviation of five composites are given in Table 4.6. The fracture strain of all the binary composites is presented as a function of CB content in Figure 4.24 to investigate the effects of polymer matrices on the flexibility of the composites. A 2 wt.% addition of CB did not significantly affect the fracture strain of the composites. Fracture strain of the composites began to decrease when CB content exceeded 2 wt.%. This might be due to poor wetting of graphite since most of the resin volume was absorbed by CB particles. The fracture strain of TPU composites was significantly higher than the PP and nylon composites at low CB content. However, a sudden drop in the elongation at the breaking point was recorded in TPU composites when the CB content increased from 2 to 4 wt.%. This may be attributed to the low polymer content of composites. As discussed in the previous sections, the polymer content of the TPU composites is lower than the PP and nylon composites. Because a significant amount of the TPU resin was consumed by CB

particles, the graphite particles were not properly wetted and mixed, resulting in a considerable decline in fracture strain value.
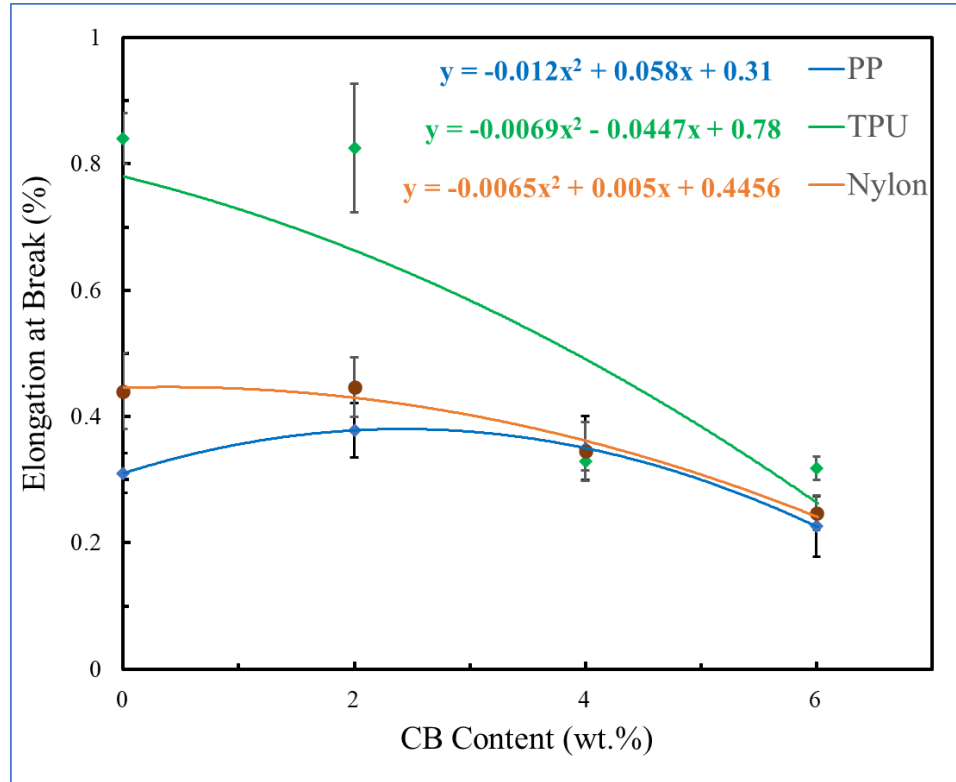
Figure 4.24: Fracture strain of PP, TPU, and nylon composites as a function of CB content

d) Fracture toughness of binary filler composites

The fracture toughness of the PP, nylon, and TPU-based binary filler composites was compared and presented as a function of CB content in Figure 4.25. The fracture toughness of all types of composites was improved by adding a small amount of CB. In contrast, increasing the CB content for more than 2 wt.% had a negative impact on the toughness. At low CB content, the polymer matrix had a significant impact on the fracture toughness of the composites. The nylon composites demonstrated the highest fracture toughness, whereas PP composites had the lowest values. However, toughness values of all the composites were close to each other when the CB content was 6 wt.%. The addition of CB content improves interfacial bonding of the filler with the resin due to the high surface area of the CB particle, making composites tougher and stronger. On the other hand, increasing the CB composition after a certain amount absorbed too much resin causes poor wetting of

graphite with the resin. Similar trends were observed in the case of fracture strength and fracture strain of the composites.
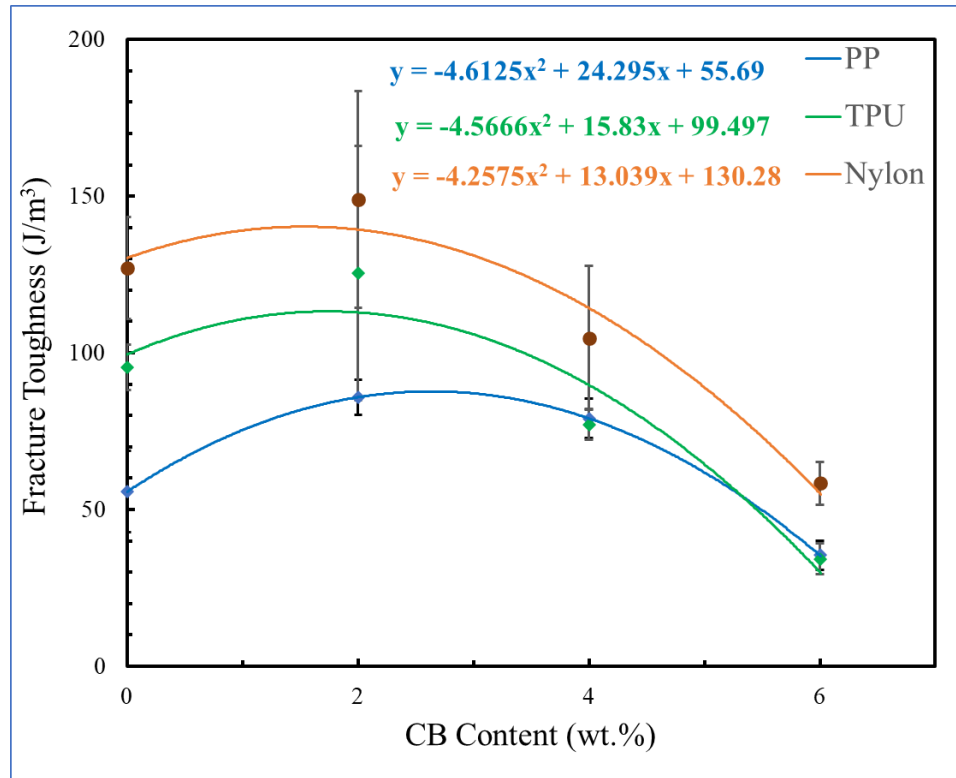
Figure 4.25: Fracture toughness of PP, TPU, and nylon composites as a function of CB content.

e) Fracture modulus of binary filler composites

The stress-strain curve data obtained from the flexural strength testing was used to calculate the modulus of elasticity of the binary filler composites. Figure 4.26 shows the flexural modulus of the binary filler composites as a function of CB content. The composition of CB affected the flexural modulus of PP, nylon, and TPU composites in different ways. In PP composites, the flexural modulus decreased as CB content increased. The reduction in flexural modulus of PP composites, however, wasn't significant. The TPU composites exhibited significant variation in flexural modulus. As the CB content was increased from 0 to 4 wt.%, the flexural modulus of TPU composites increased by almost three times, from 7.8 GPa to 24.9 GPa. However, the flexural modulus of TPU composites dropped to 10.9 GPa when the CB content was 6 wt.%. A similar trend was observed in nylon composites. When the CB content was increased from 0 to 2 wt.%, the modulus of

elasticity of nylon composites increased from 22.3 to 32.3 GPa, but when the CB content was increased from 4 to 6 wt.%, it reduced from 33.0 to 29.2 GPa.

.

The plotted equations shown in the figure are:

$$y = -0.2187x^2 + 0.6575x + 18.915$$

$$y = -1.1052x^2 + 7.7784x + 5.9373$$

$$y = -0.8637x^2 + 6.2584x + 22.53$$
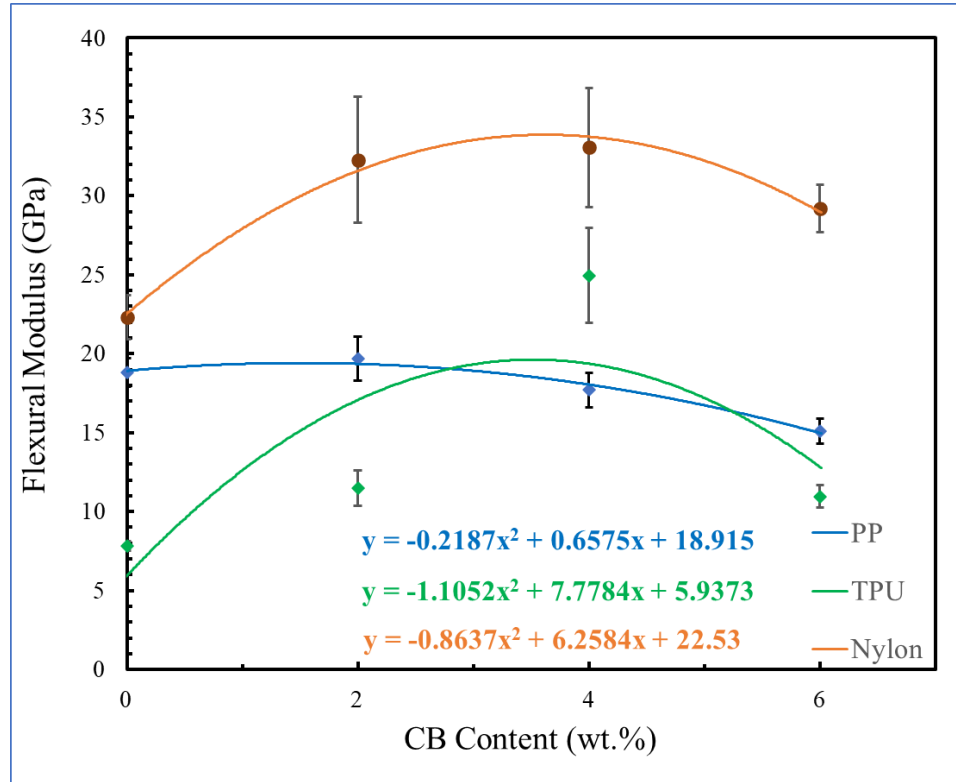
Figure 4.26: Flexural modulus of PP, TPU, and nylon composites as a function of CB content.

4.3 Optimization of Filler Compositions of Thermoplastic Composites

An optimization study has been carried out with the intention of achieving the optimum value of electrical conductivity and flexural strength. Secondary fillers were added to the polymer/graphite composites in binary, ternary, and quaternary formations. The processability of the composite, above 75 wt.% filler content was challenging due to very high viscosity. Increasing the filler loading above 75 wt.% had an adverse effect on the flexural strength. As an alternative, the electrical conductivity could be improved by adding secondary fillers. It was observed in section 4.1 that the electrical conductivity of the composites increased drastically in a high filler loading region. Replacement of graphite with other conductive fillers in this region could further increase the electrical conductivity. The effects of polymer matrix on properties of electrically conductive thermoplastic

composites have been evaluated in section 4.2. Nylon-based composites performed better mechanically but had poor electrical properties. On the other hand, highly loaded TPU composites offered good electrical conductivity but poor mechanical properties. A compromise was observed in nylon and TPU-based composites in terms of electrical and mechanical properties, respectively. In contrast, PP-based composites demonstrated the most balanced properties.

Based on these findings, the PP matrix was used in this study to produce electrically conductive thermoplastic composites. The graphite was used as a primary filler, and MWCNT, CB, CF, and EG were added to the PP-graphite composites as secondary fillers at different compositions. The total filler content was fixed at 75 wt.%, and the compositions of secondary filler were considered as the control input factors of the optimization study. The first step of this study was to investigate the feasibility of using MWCNT, CB, CF, and EG as secondary fillers, in which these fillers were added to the PP/graphite composites one by one at different compositions and the properties of the composites were analyzed. The feasibility study helped to determine the input factors and levels of the experimental design. A full factorial design of the L-27 Orthogonal Array (OA) was used as a Design of Experiment (DOE). The TPEC and flexural strength of the composites were considered as the output responses. The experimental data were interpreted by the Analysis of Variance (ANOVA) to evaluate the significance of each secondary filler. Furthermore, mathematical modeling was performed by Response Surface Methodology (RSM) to predict the properties of the composites as a function of filler composition.

4.3.1 Feasibility Study of Different Secondary Fillers

The feasibility of using CF, MWCNT, CG, and EG as secondary fillers was investigated in order to finalize the input factors and levels of the experimental design of the optimization study. The effects of adding these fillers as binary composites have been discussed in the following sections.

4.3.1.1 Feasibility of Using Carbon Fiber

The effect of adding graphite to the PP matrix was studied in Section 4.2. Due to the high die pressure generated during the melt compounding of homopolymer PP, the CF was

added to the copolymer PP composites. In continuation of this study, and with the main purpose of enhancing mechanical properties, carbon fiber (CF) was added as a binary filler. Different filler combinations were made by replacing the graphite content with CF at 5 wt.%, 10 wt.%, 15 wt.% while maintaining the total filler content constant at 80 wt.% and 85 wt.%. The carbon fibers were dry-mixed with copolymer PP pellets and fed through the main feeder, and the side feeder was used to supply graphite.

The electrical conductivity, flexural strength, flexural modulus, and fracture toughness were evaluated for each composition as listed in Table 4.7. Figure 4.27 shows the graph of electrical conductivity vs. the CF content. It shows that the addition of CF in the composites is not beneficial for electrical conductivity. The conductivity of the composites decreased with an increase in CF content. However, the conductivity decreased gradually for the 85 wt.% filler content, but for 80 wt.% filler content, the conductivity suddenly reduced on adding 5 wt.% CF content and then started to increase slightly on further addition of CF.

Table 4.7: Properties of CF-PP composites.

Total filler (wt.%)	CF content (wt.%)	Electrical Conductivity (S/cm)		Flexural Strength (MPa)		Flexural Modulus (GPa)		Fracture Toughness (J/m^3)	
85 wt.%	0%	10.72	± 0.16	15.2	± 1.5	13.8	± 1.4	20.9	± 6.3
	5%	9.81	± 0.73	18.9	± 1.7	11.3	± 1.4	24.3	± 6.1
	10%	9.62	± 0.31	19.7	± 1.8	10.7	± 0.3	26.1	± 7.4
	15%	7.82	± 0.28	21.6	± 1.2	14.2	± 1.6	48.2	± 4.6
80 wt.%	0%	8.33	± 0.23	15.7	± 1.4	9.2	± 0.4	41.2	± 7.2
	5%	6.52	± 0.05	18.2	± 1.2	6.8	± 0.7	50.6	± 7.9
	10%	2.92	± 0.11	20.0	± 1.1	8.5	± 0.2	60.8	± 12.0
	15%	4.89	± 0.07	21.3	± 0.9	10.9	± 1.4	66.5	± 15.6
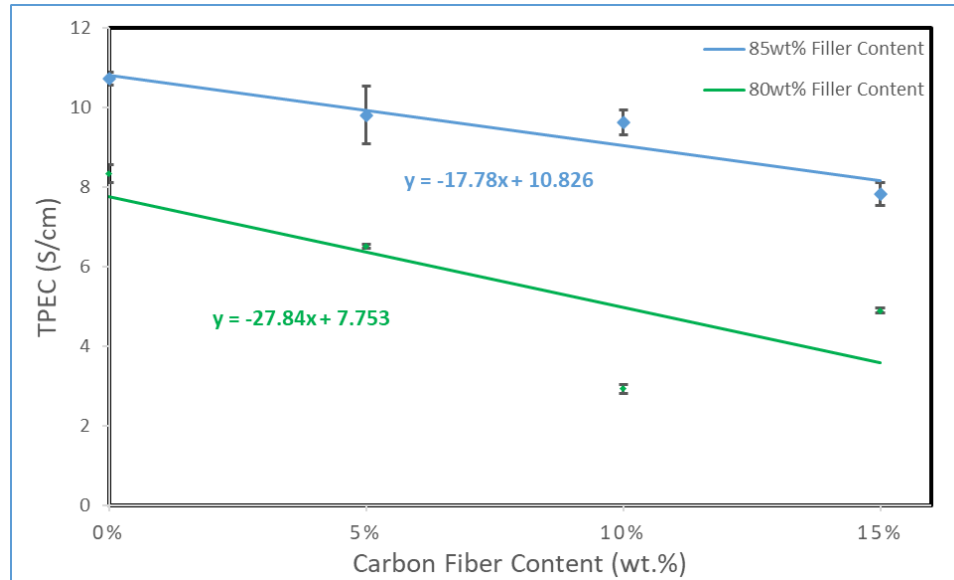
Figure 4.27: Electrical conductivity of CF composites vs. CF content.

Figure 4.28 and Figure 4.29 show the effects of CF content on flexural strength and flexural modulus, respectively. No significant difference was observed in the flexural strength of 80 wt.% and 85 wt.% filler content. The flexural strength linearly increased with an increase in CF content for both 80 wt.% and 85 wt.% total filler compositions. That indicated the reinforcing role of the CF. However, the flexural modulus decreased on replacing 5 wt.% graphite with CF and then gradually started to increase on further addition of CF content. Figure 4.30 represents the relationship of fracture toughness of the CF composites with the amount of CF inside the composites. The fracture toughness was obtained by calculating the area under the curve of the stress-strain graph. The stress-strain graphs obtained from the flexural strength testing were utilized for the fracture toughness calculations. Similar to the flexural strength and flexural modulus, the fracture toughness of five samples was calculated for each composite. The fracture toughness of 80 wt.% filled composites is around 15 J/m^3 higher than the 85 wt.% filled composites. However, the fracture toughness linear increased with an increase in CF content, and the gradients of the fracture toughness vs. CF content curve for 80 wt.% and 85 wt.% filled composites are almost similar. The fracture toughness of the composites linearly increased with an increase in the CF content.
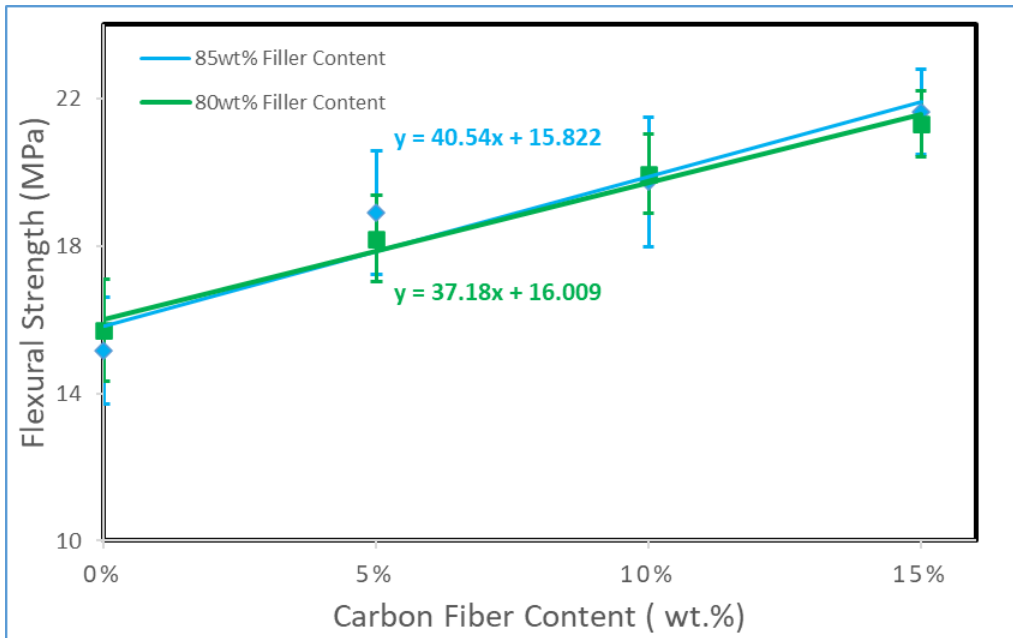
Figure 4.28: Flexural strength of CF composites vs. CF content.
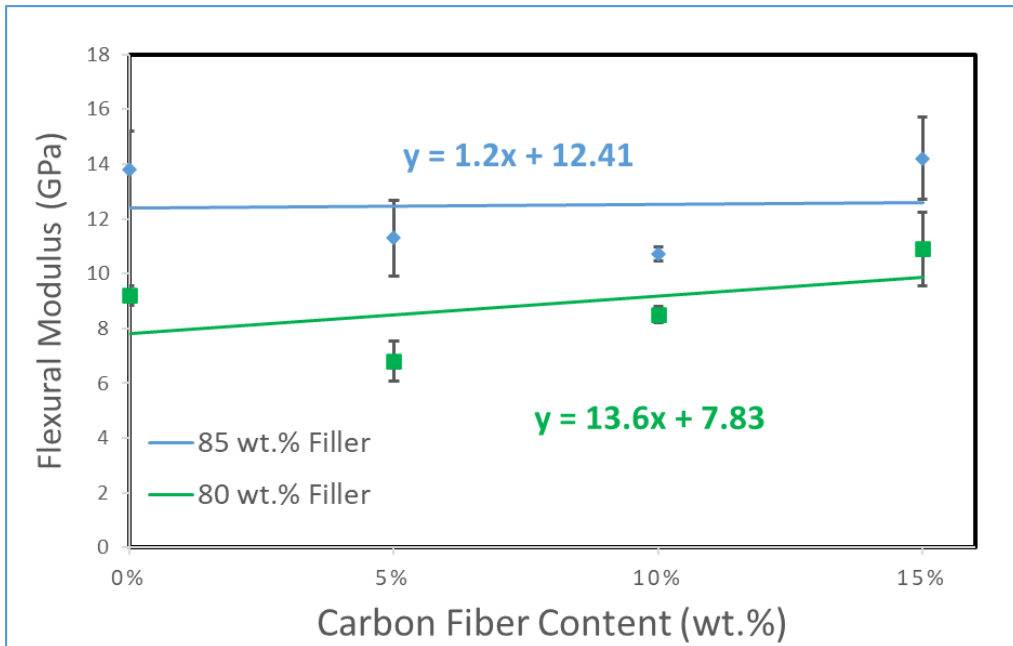
Figure 4.29: Flexural modulus of CF composites vs. CF content.
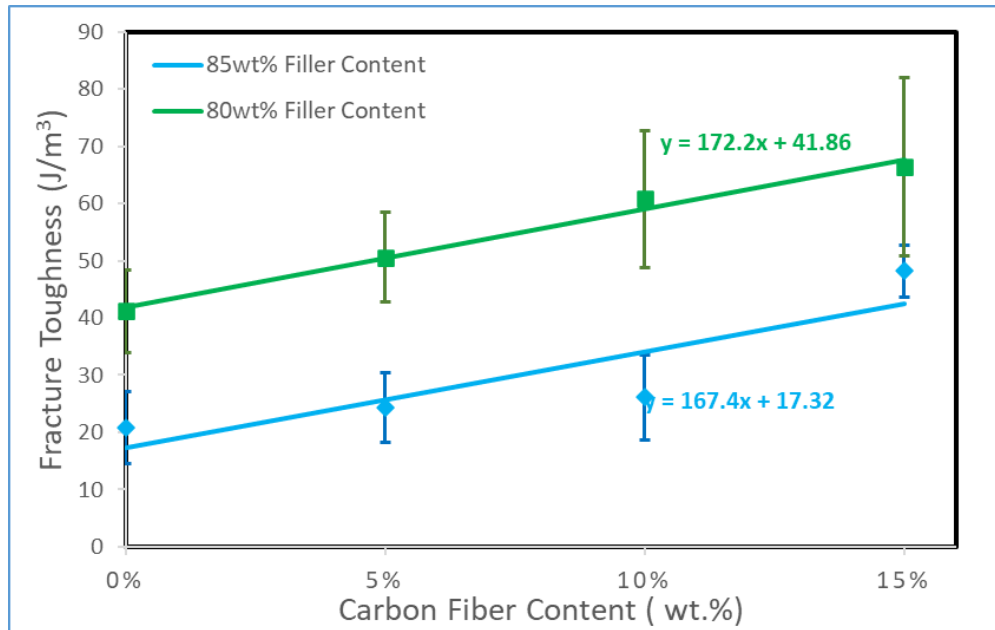
Figure 4.30: Fracture toughness of CF composites vs. CF content.

Adding CF to the composites improves the mechanical properties. However, the increase in the flexural strength on the addition of CF is meager as compared to the values found in the literature [50]. The bonding between the fibers and the polymer matrix and the length of fibers are the two main factors that can affect the mechanical properties of composite material. The fracture morphology of the composites was analyzed with the help of scanning electron microscopy (SEM) and can be seen in Figure 4.31. The interfacial bonding between the fibers and the resin is good enough to improve the mechanical properties. The length of fibers inside the composites was also investigated with the help of a digital microscope. A pellet of composite material was first heated at 600 C in the nitrogen environment until all the polymer content was degraded and removed. After this, the sample was squeezed between two microscope slides, and the particles of CF and graphite were carefully spread on the slide. Figure 4.32 shows the microscopic view of the CF and graphite particles. It was found that the length of the fibers was reduced from 3 mm to 200 microns during the melt-compounding process, due to which the CF did not have a significant contribution to the flexural strength of the composites. Also, it has adverse effects on electrical conductivity. Therefore, CF is not a suitable filler material for making electrically conductive composites.
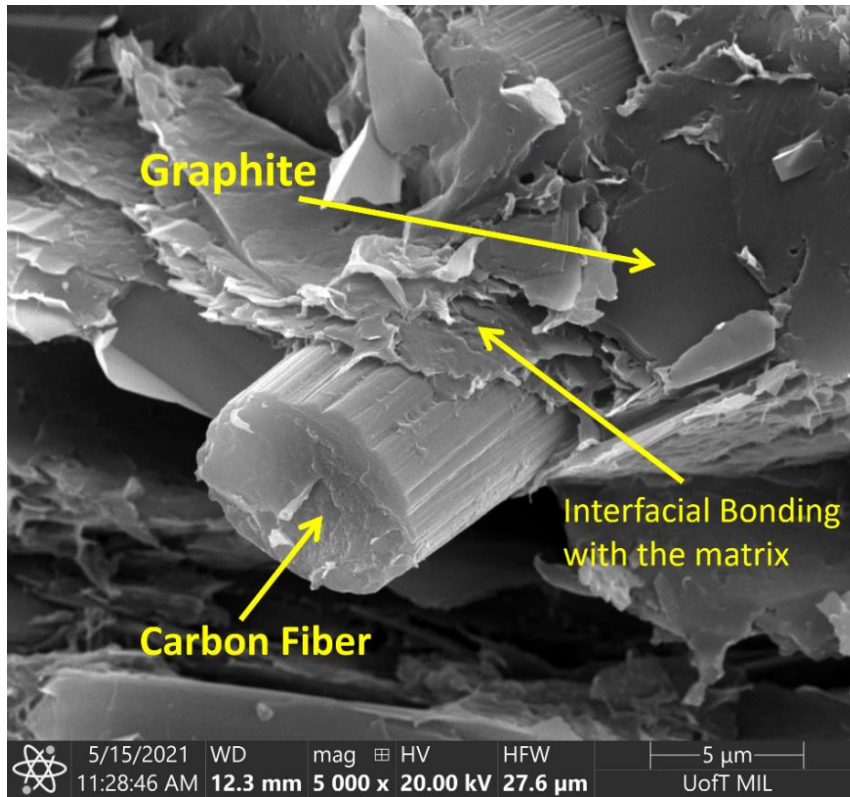
Figure 4.31: SEM micrograph of carbon fiber reinforced composite.
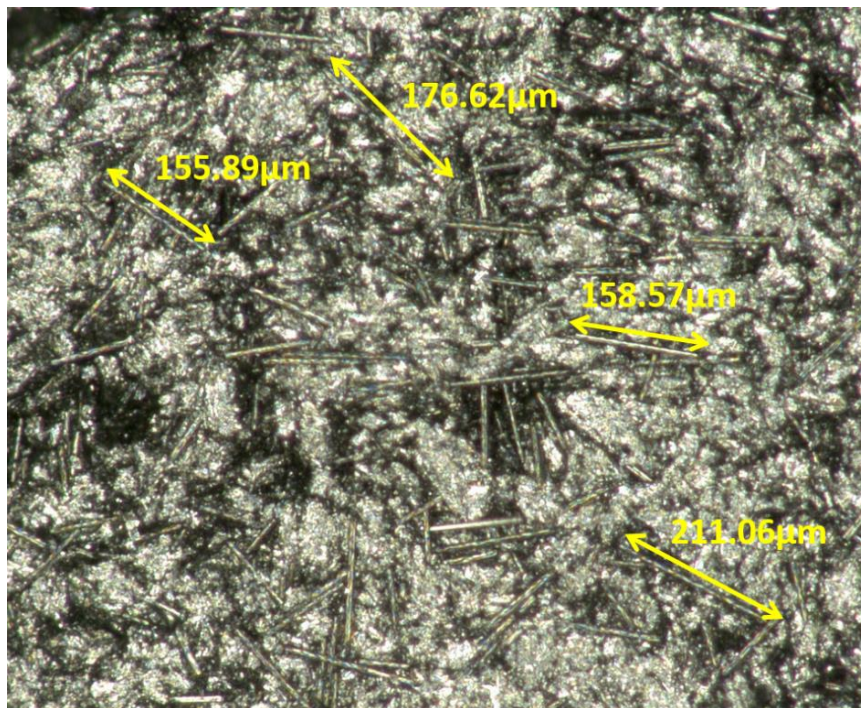
Figure 4.32: Length of carbon fibers after the melt-compounding.

4.3.1.2 Feasibility of Using Expanded Graphite

EG is a comparatively new material used as a conductive filler for developing electrically conductive composites. The EG was received in the form of expandable graphite, and it was expanded in a lab furnace, Vulcan 3-550 [Figure 4.33]. The expandable graphite material was placed inside the furnace for 15 minutes at 700 C. Figure 4.34(a) and Figure 4.34(b) show the particle size of EG before and after the expansion, respectively. The particle size was increased from 600 microns to 1 cm during the expansion process. The homopolymer grade of PP was used as a polymer matrix in this study. This study was completed in two stages. In the first stage, the EG was used as a single filler, and the composites were made by varying the EG content at three different compositions. In the second stage, the EG was used as a binary filler, and four different filler combinations were made by maintaining the total filler content constant at 75 wt.% and replacing the graphite content with EG at 0 wt.%, 10 wt.%, 20 wt.%, and 30 wt.%.

Figure 4.33: Vulcan 3-550 lab furnace.
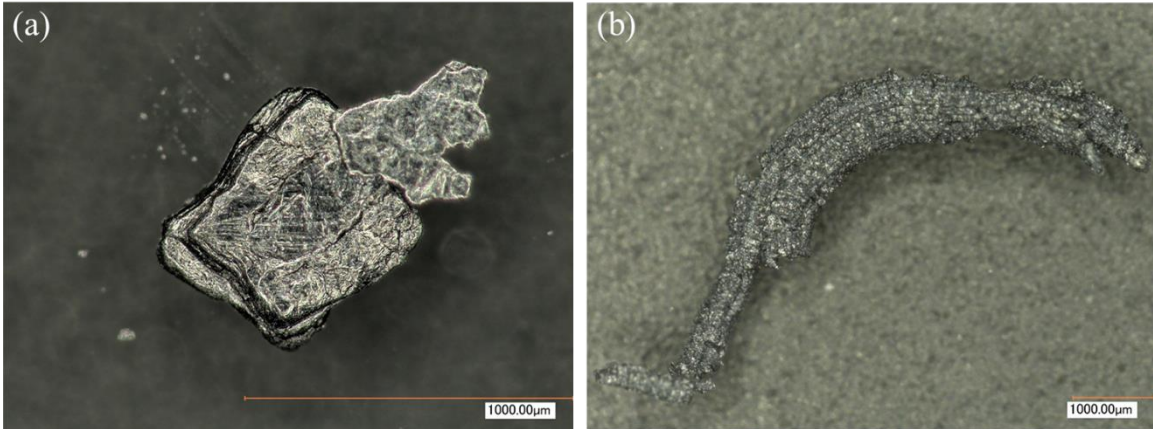
Figure 4.34: Particle size of EG particles: (a) before expansion (b) after expansion.

The electrical conductivity of EG-filled composites as a single filler and its comparison with those of graphite-filled is shown in Figure 4.35. The electrical conductivity values of EG/PP composites between 35 wt.% to 45 wt.% filler loading are very much close to the electrical conductivity values of PP/graphite composites between 60 wt.% to 65 wt.% filler loading. Similarly, the electrical conductivity of EG composites at 53.5 wt.% filler content is greater than that of the graphite composites at 68 wt.% filler content. It is mainly due to the larger particle size of EG, which makes better conductive paths inside the composites. Hence, EG has better effects on the electrical properties than the regular graphite filler.
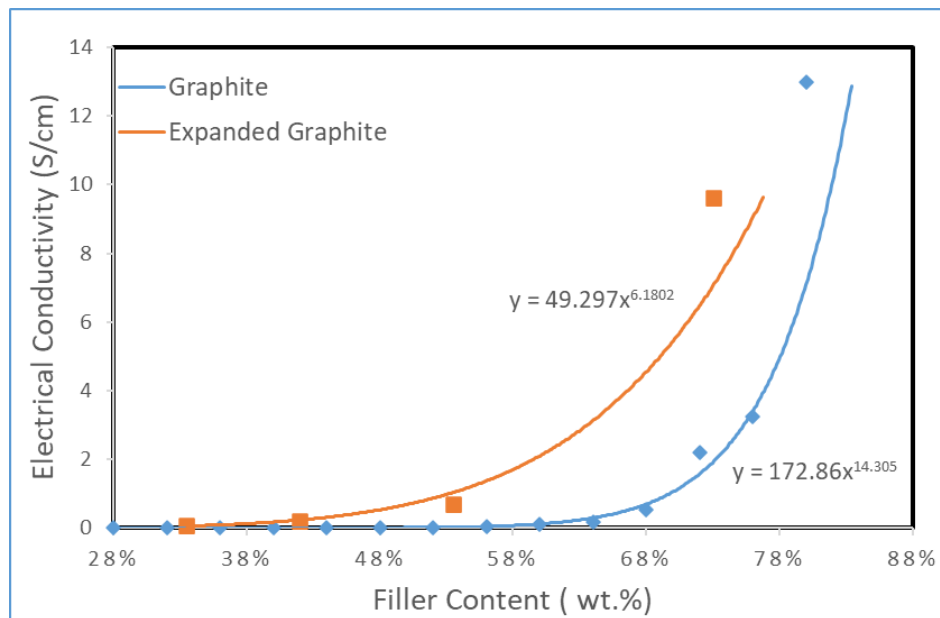
Figure 4.35: TPEC comparison of EG and graphite composites.

The EG was added as a binary filler in the second stage. The effects of adding EG in the graphite on the electrical and mechanical properties are listed in Table 4.8. The effects of EG content on the electrical conductivity and flexural strength are represented in Figure 4.36 and Figure 4.37, respectively. The electrical conductivity linearly increased with increasing EG content. Similarly, a linear reduction in the flexural strength was observed on the addition of EG into the composites. However, the change in the electrical conductivity and flexural strength is not very significant as compared to other binary fillers. Figure 4.38 shows the graph of flexural modulus and fracture toughness of composites against the EG content. The flexural modulus decreased with increasing the EG content. In contrast, the fracture toughness increased with an increase in the EG content. In conclusion, the addition of EG as a binary filler can improve the electrical properties with a tiny reduction in mechanical strength.

Table 4.8: Electrical and Mechanical properties of expanded graphite composites.

Total filler content (wt.%)	EG content (wt.%)	Electrical Conductivity (S/cm)	Flexural Strength (MPa)	Flexural Modulus (GPa)	Fracture toughness (J/m^3)
75 wt.%	0	2.83 ± 0.19	30.3 ± 1.3	18.8 ± 0.9	55.7 ± 12.9
	10	4.86 ± 0.54	28.7 ± 1.6	17.1 ± 1.2	55.3 ± 17.2
	20	3.52 ± 0.08	28.8 ± 0.4	14.5 ± 2.0	56.9 ± 8.8
	30	4.60 ± 0.06	28.7 ± 1.4	11.4 ± 0.9	66.0 ± 12.6
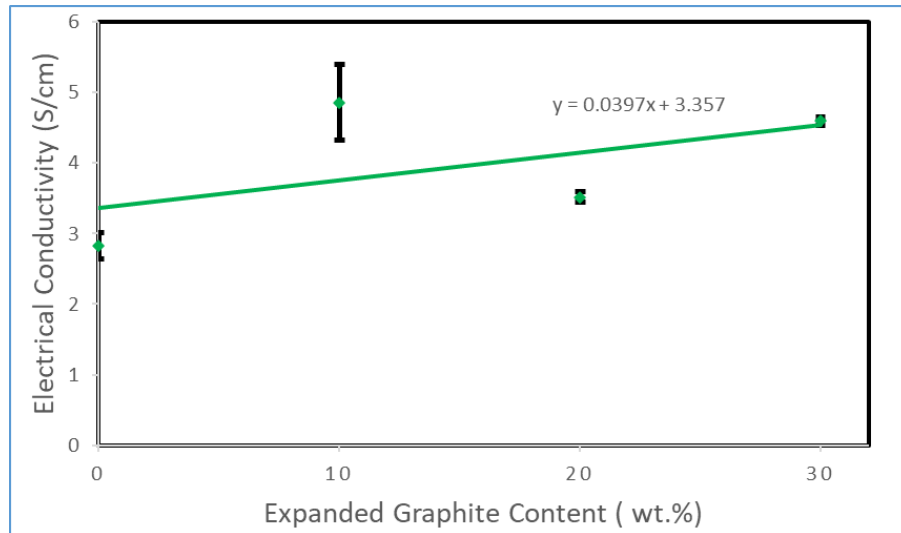
Figure 4.36: Electrical conductivity of the composites vs. EG content.

85
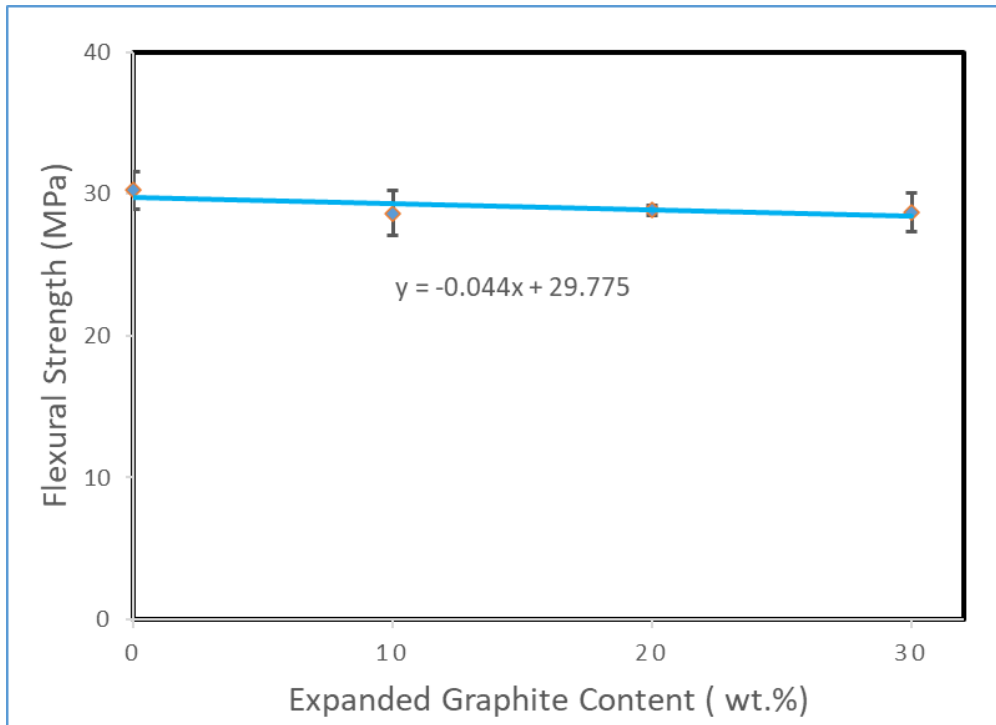
Figure 4.37: Flexural strength of the composites vs. EG content.
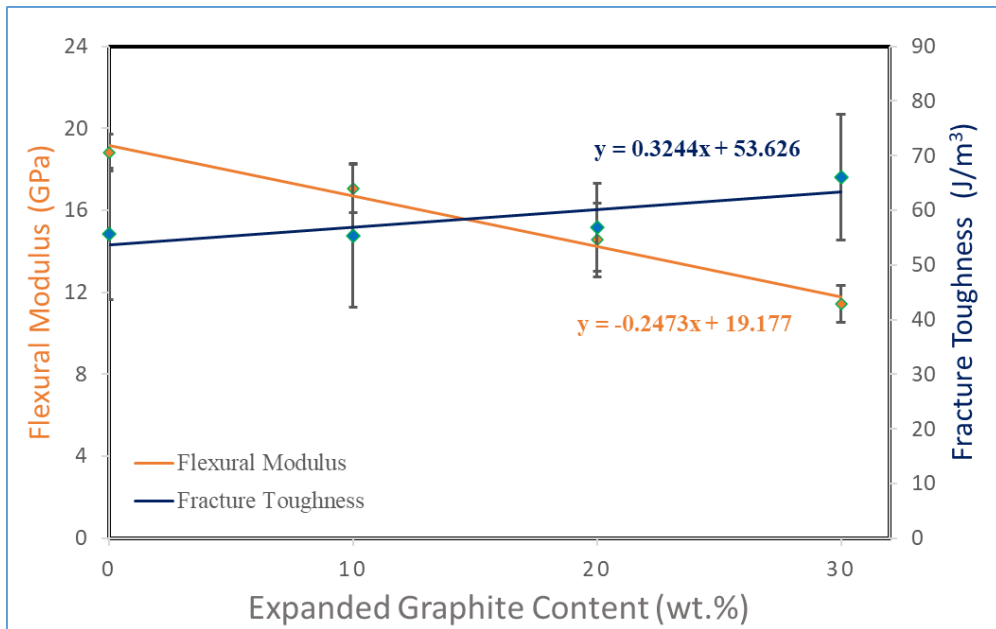
Figure 4.38: Flexural modulus and fracture toughness of the composites vs. EG content.

4.3.1.3 Feasibility of Using Carbon Black

After testing EG as a binary filler in the previous section, the purpose of this study is to see the feasibility of CB being used as a binary filler. The total filler content of the composite was fixed at 75 wt.%, and CB was added to the PP/graphite composite at different compositions ranging from 0 wt.% to 6 wt.%, and the composition of graphite was adjusted accordingly. The CB was dry-mixed with the graphite filler and fed into the side feeder. The homopolymer PP was fed through the main feeder. The effects of adding CB on the mechanical and electrical properties are listed in Table 4.9.

Table 4.9: Electrical and Mechanical properties of CB composites

Total filler content (wt.%)	CB Content (wt.%)	TPEC (S/cm)	Flexural Strength (MPa)	Flexural Modulus (GPa)	Fracture Toughness (J/m3)
75	0	2.8 ± 0.2	30.3 ± 1.3	18.8 ± 0.9	55.7 ± 12.9
	2	8.7 ± 0.1	35.2 ± 0.8	19.7 ± 1.4	85.8 ± 5.6
	4	15.2 ± 0.1	35.9 ± 1.2	17.7 ± 1.1	79.1 ± 6.3
	6	21.2 ± 0.3	28.5 ± 1.3	15.1 ± 0.8	35.4 ± 4.6

The addition of CB as a binary filler showed a promising effect on the electrical conductivity of the composites. Figure 4.42 shows how the tiny particles of CB fill the void between the graphite particles and help in making new conductive paths, increasing conductivity. As shown in Figure 4.39, the value of electrical conductivity with 2 wt.% of CB is almost three-fold greater than the electrical conductivity without CB. Adding 2 wt.% CB to the composites also increased the flexural strength. However, as shown in Figure 4.40, the flexural strength started to decrease with the further addition of CB in the composites. Similarly, the fracture toughness also increased on adding 2 wt.% of CB and then started to decrease at larger CB content, as shown in Figure 4.41. Reduction in flexural modulus at 4 wt.% of CB content was also recorded. However, the reduction in the flexural strength, fracture toughness, and flexural modulus with 4 wt.% of CB was not significant as compared to the enhancement in the electrical conductivity. In conclusion, CB is a promising filler material for electrically conductive composites.
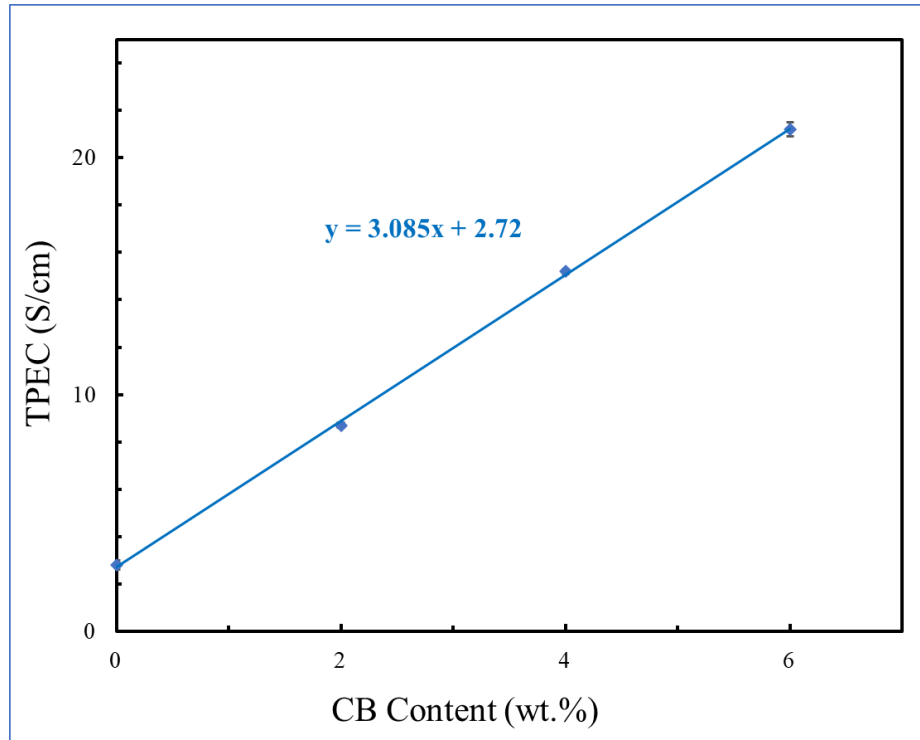
Figure 4.39: Electrical conductivity of CB composites vs. CB content.
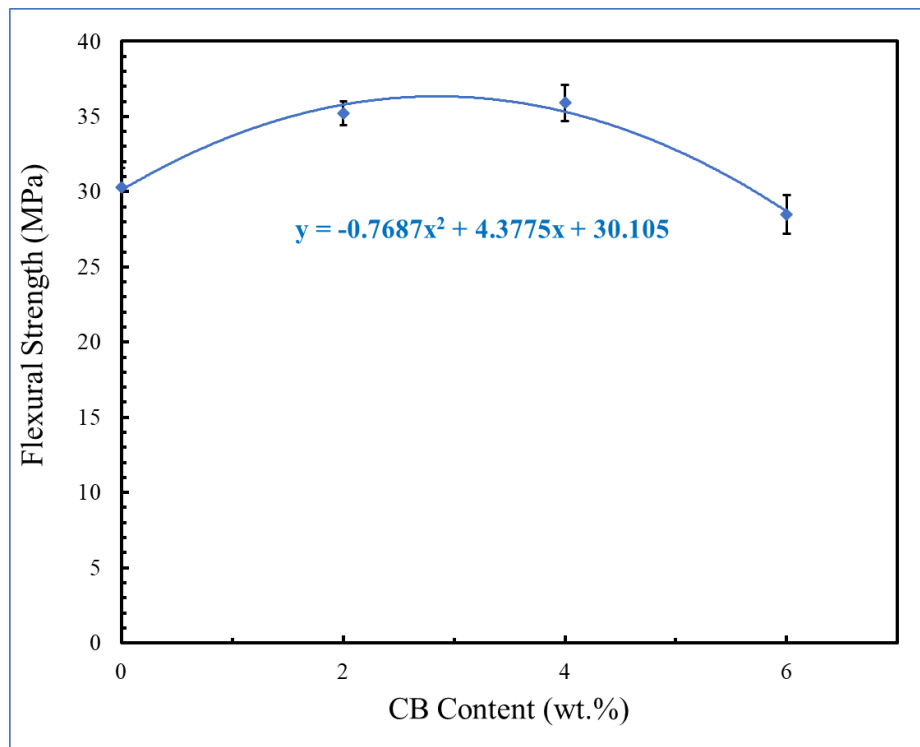
Figure 4.40: Flexural strength of CB composites vs. CB content.
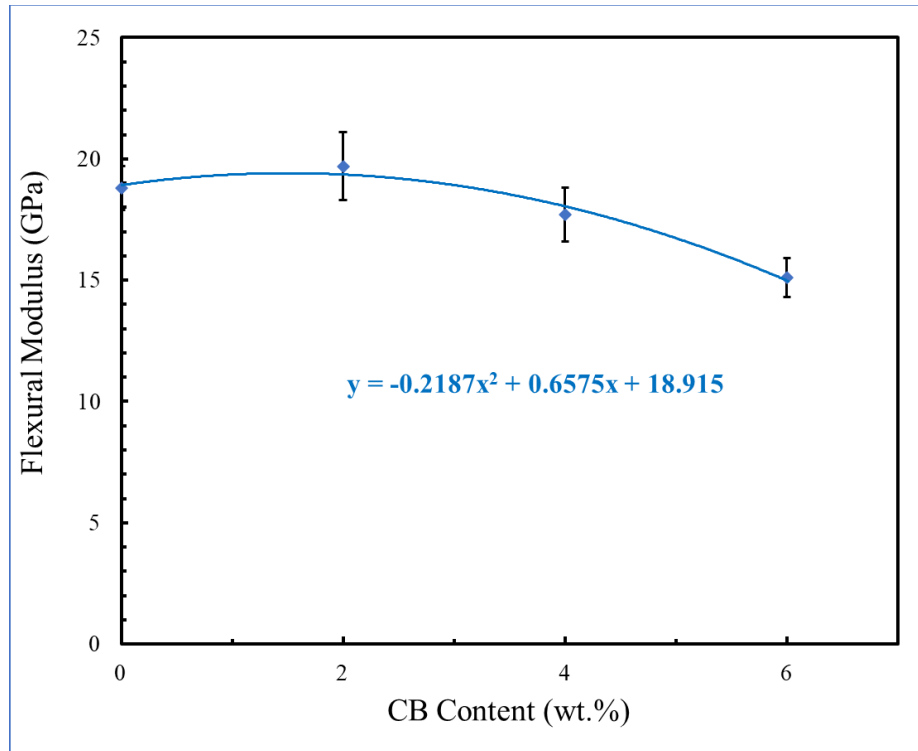
Figure 4.41: Flexural modulus of CB composites vs. CB content.
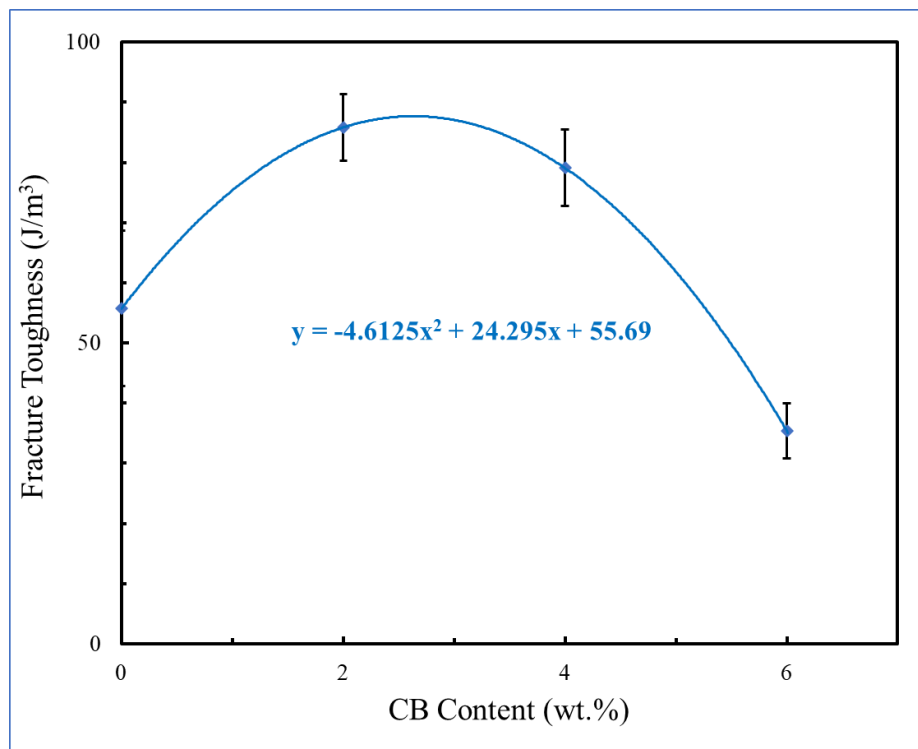
Figure 4.42: Fracture toughness of CB composites vs. CB content.

4.3.1.4 Feasibility of Using MWCNT

This study aims to investigate the feasibility of MWCNT as a binary filler for electrically conductive thermoplastic composites. Similar to the previous studies, the total filler content was fixed at 75 wt.%, and three different combinations of MWCNT composites were made by replacing 2 wt.%, 4 wt.%, and 6wt.% of graphite content with MWCNT. The effects of adding MWCNT on the electrical conductivity and flexural strength are listed in Table 4.10.

Table 4.10: Electrical conductivity of MWCNT composites.

Total filler content (wt.%)	CNT content (wt.%)	TPEC (S/cm)	Flexural Strength (MPa)
75	0	2.8 ± 0.2	30.3 ± 1.3
	2	8.9 ± 0.2	28.5 ± 2.1
	4	20.5 ± 1.3	23.3 ± 1.9
	6	21.5 ± 1.1	22.0 ± 1.5

The electrical conductivity of the composites was drastically increased with increasing MWCNT content in the composites up to 4 wt.%. However, as shown in Figure 4.43, the improvement in the electrical conductivity is not very significant with the further addition of MWCNT. The sudden boost in the electrical conductivity on the minor addition of MWCNT is due to the formation of new conductive paths inside the composites. The conductive network of MWCNT can be seen in Figure 4.45. The higher aspect ratio of MWCNT particles helps them in generating multiple conductive paths by making links between the graphite particles. Once the graphite particles are linked with each other, the further addition of MWCNT will not significantly contribute to the enhancement of electrical properties. Figure 4.44 shows the flexural strength of the composites as a function of MWCNT content. The addition of MWCNT exhibits an adverse effect on the flexural strength of the composites. This may be attributed to the agglomeration caused by MWCNT.
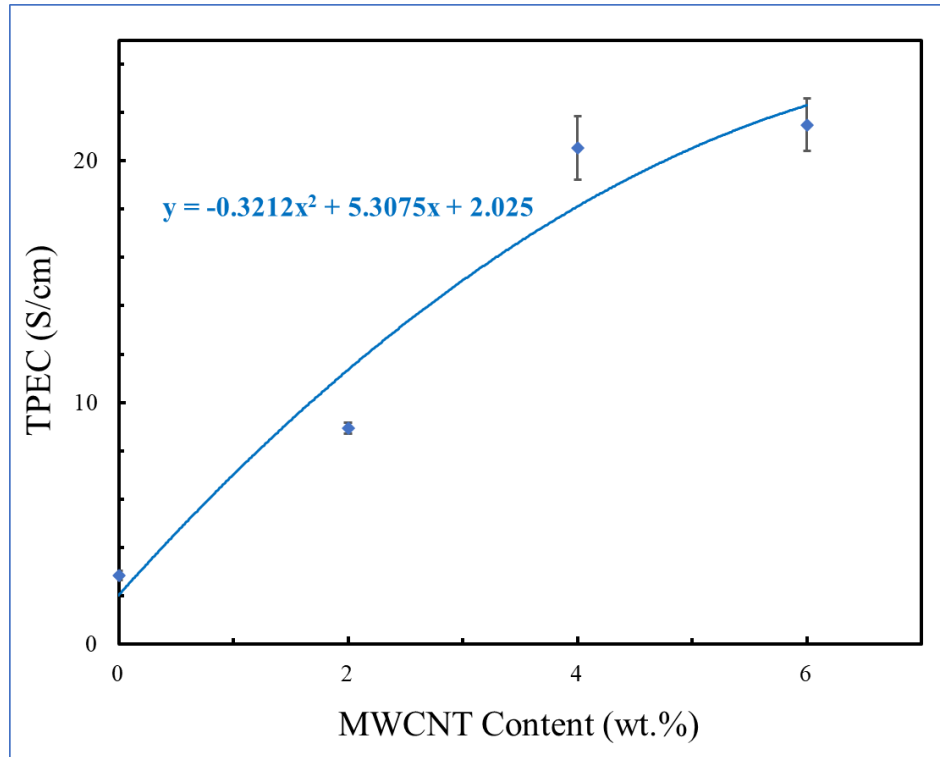
Figure 4.43: Electrical conductivity of composites as a function of MWCNT content.
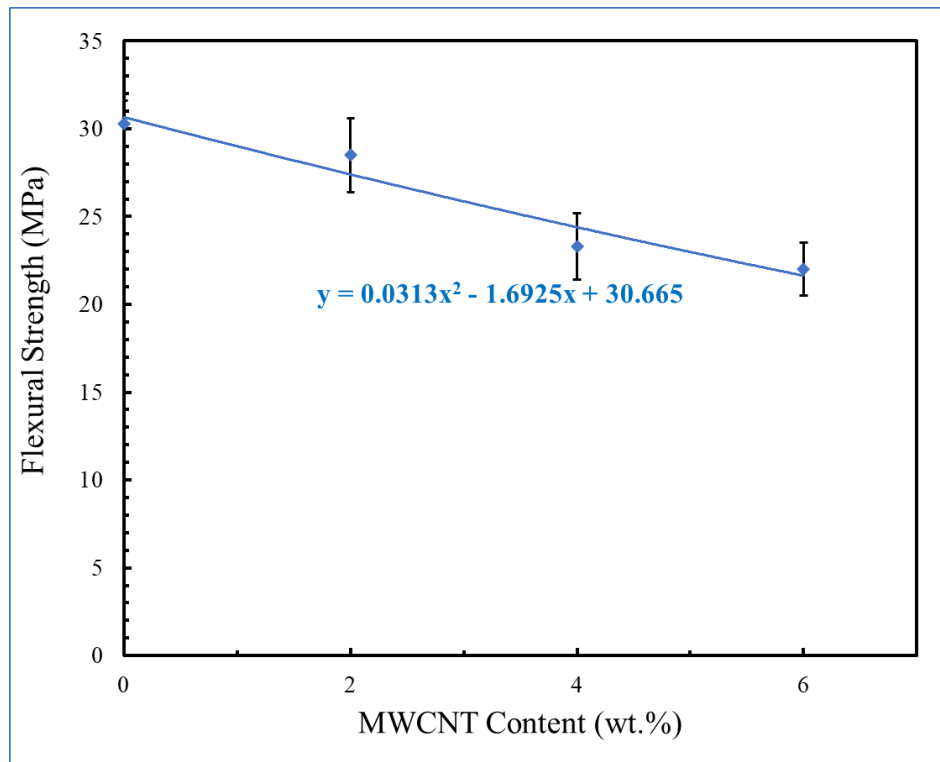
Figure 4.44: Flexural strength of composites as a function of MWCNT content.
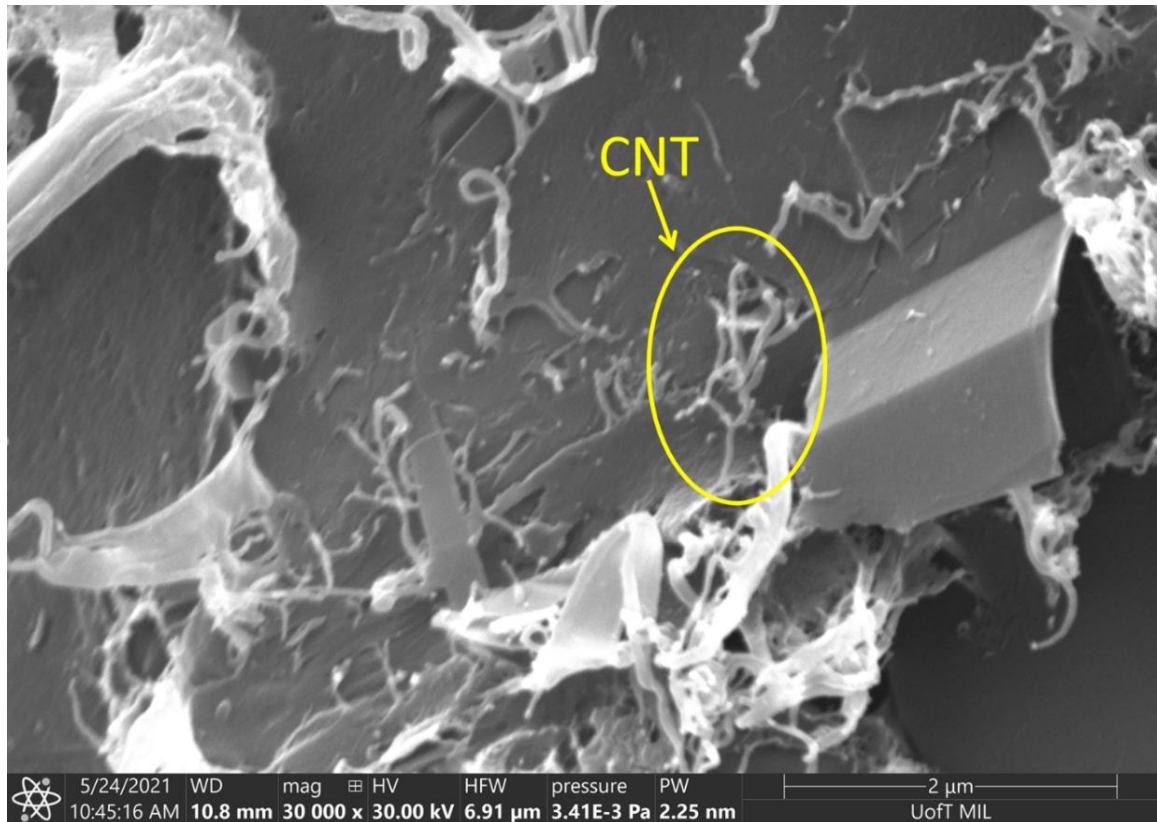
Figure 4.45: SEM micrograph of MWCNT reinforced PP/graphite composite.

4.3.2 Design of Experiments

The feasibility of adding MWCNT, EG, CB, and CF as secondary fillers has been evaluated in the previous section. It was observed that the addition of CF had a negative effect on the electrical conductivity of the composites. A slight improvement in flexural strength was observed with the addition of CF, but it was not significant. Therefore, CF was not used in the experimental design of the optimization study. It was observed in the open literature that the addition of a slight amount of carbon nanotubes substantially improves the electrical conductivity of the composites. The addition of carbon nanotubes above 4 wt.% does not affect the electrical conductivity significantly [65,71]. Similar results were observed in the feasibility study of MWCNT. Hence, 4 wt.% was set as the maximum level of MWCNT composition. The researchers observed a sudden jump in electrical conductivity of EG composites when the EG content was between 10 wt.% to 30 wt.% [27,72,73]. Based on the experimental results of EG composites and literature reviews, the upper limit for the EG content was set to 30 wt.% in the experimental design. According to the feasibility study of CB, the addition of 6 wt.% CB reduced the flexural

strength below 30 MPa. Thus, the maximum amount of CB used in this study was 5 wt.%. The same composition of CB as a secondary filler has been used in multiple research studies [42,56,70]. The input factors of the DOE and their levels are mentioned in Table 4.11. Each factor has three levels of variations. The total filler content was fixed at 75 wt.% for each run, wherein the composition of graphite was configured according to the compositions of the secondary fillers. A full-factorial design based on three control factors with three-level variation was designed to investigate the effect of each secondary filler and the possibility of any interactions between fillers. The design is based on 27 experimental runs with two output responses. ANOVA was used to study the significance of each input parameter. Table 4.12 represents the values of the process parameters as well as the output response for the DOE.

Table 4.11: Control factors and levels of the DOE.

Control Factors	Symbol	Level 1	Level 2	Level 3
MWCNT (wt.%)	A	0	2	4
EG (wt.%)	B	0	15	30
CB (wt.%)	C	0	2.5	5

4.3.1 Effects of Filler Interaction on the Electrical Conductivity

The PP/graphite composites prepared for the DOE were tested for the through-plane electrical conductivity measurements. Five specimens of each experimental trial were tested, and the average values of electrical conductivity, along with the standard deviation, are mentioned in Table 4.12. The high electrical conductivity values were observed at 15, 21, and 27 trials, wherein all of them contained a high level of CB and MWCNT. The highest electrical conductivity of 39.6 S/cm was investigated in this study at the 27th experimental trial with 4 wt.% MWCNT, 30 wt.% EG, and 5 wt.% CB.

The effects of binary fillers on the conductivity network inside the composite material can be seen in SEM micrographs shown in Figure 4.46. The electrical conductivity of single filler PP/graphite composite was observed to be 2.8 S/cm at trial 1. The presence of a polymer layer between the graphite particles can be seen in Figure 4.46(a). This layer acts as an insulation between graphite particles, preventing electron hopping, which results in low electrical conductivity.

Table 4.12: Output responses of DOE.

Run#	A (MWCNT)	B (EG)	C (CB)	Electrical Conductivity (S/cm) (Through-Plane)	Flexural Strength (MPa)
1	0	0	0	2.8 ± 0.2	30.3 ± 1.3
2	0	0	2.5	9.7 ± 0.4	36.9 ± 1.2
3	0	0	5	19.3 ± 1.2	34.2 ± 2.8
4	0	15	0	3.6 ± 0.1	28.8 ± 0.4
5	0	15	2.5	9.5 ± 0.2	31.7 ± 2.3
6	0	15	5	19.3 ± 1.1	34.1 ± 2.3
7	0	30	0	4.6 ± 0.1	28.7 ± 1.4
8	0	30	2.5	12.2 ± 0.5	35.0 ± 2.0
9	0	30	5	24.6 ± 1.5	32.2 ± 2.8
10	2	0	0	8.9 ± 0.2	28.5 ± 2.1
11	2	0	2.5	19.7 ± 0.5	26.1 ± 3.1
12	2	0	5	29.6 ± 0.7	25.1 ± 0.9
13	2	15	0	9.5 ± 0.2	27.4 ± 2.6
14	2	15	2.5	15.7 ± 0.4	34.2 ± 3.8
15	2	15	5	38.8 ± 0.9	29.4 ± 1.8
16	2	30	0	10.6 ± 0.3	26.9 ± 4.4
17	2	30	2.5	22.3 ± 1.1	34.2 ± 1.9
18	2	30	5	32.4 ± 0.3	27.4 ± 0.6
19	4	0	0	20.5 ± 1.3	23.2 ± 1.9
20	4	0	2.5	31.9 ± 0.8	26.5 ± 2.0
21	4	0	5	36.6 ± 0.6	28.6 ± 3.2
22	4	15	0	14.0 ± 0.2	23.6 ± 1.8
23	4	15	2.5	25.8 ± 0.6	26.4 ± 2.9
24	4	15	5	36.4 ± 0.2	26.2 ± 2.6
25	4	30	0	12.1 ± 0.6	29.1 ± 2.7
26	4	30	2.5	27.5 ± 0.4	32.0 ± 3.8
27	4	30	5	39.6 ± 1.1	29.4 ± 1.7

a. The total filler content of the composites for each trial is 75 wt.%.

b. Graphite was the base filler, and the composition of graphite for each trial was configured according to the compositions of control factors.

The introduction of MWCNT in PP/graphite composites demonstrated promising performance in terms of electrical conductivity. The addition of 4 wt.% MWCNT to PP/graphite composite at the 19th run resulted in an electrical conductivity increase by more than seven times, reaching 20.5 S/cm. The high aspect ratio of MWCNT allows the creation of connections between graphite particles, thus forming new conductive paths for the electrons, lowering the electrical resistivity. Figure 4.46(b) shows the conductive network formed by MWCNT. Similar effects on the electrical conductivity of composites using carbon nanotubes have been reported in previous studies. King et al. [15] reported that the electrical conductivity was increased from 0.29 S/cm to 17.9 S/cm on adding 6 wt.% of carbon nanotubes to the PP/graphite composites. Pötschke et al. [71] added MWCNT to polycarbonate and observed a tenfold decrease in electrical resistivity of the composites as the MWCNT load was increased from 1 wt.% to 1.5 wt.%.

A significant improvement in the electrical conductivity was observed on adding CB as a binary filler to the PP/graphite composites. The addition of 5 wt.% CB increased the electrical conductivity from 2.8 S/cm to 19.3 S/cm. The CB particles create links between the graphite particles due to their smaller particle size and high surface area, thereby forming additional electrical paths and improving electrical conductivity. Figure 4.46(d) illustrates the conductive network formed by CB particles. Numerous research studies have reported a significant enhancement in the electrical properties of using CB as a binary filler. Kang et al. [70] investigated the effects of CB as a binary filler in the graphite-phenolic resin composites for fuel cell application and observed a considerable increase in the electrical conductivity on adding 5 wt.% of CB. King et al. [15] observed the reduction in the electrical resistivity of PP/graphite composites from 3.43 to 0.36 Ω-cm with the addition of 2.5 wt.% CB. Heiser et al. [42] found that the electrical resistivity of nylon/graphite composites was greatly reduced by adding 5 wt.% CB.

The incorporation of EG in the PP/graphite composites demonstrated positive effects on electrical conductivity. The addition of 30 wt.% of EG to the PP/graphite composites increased the electrical conductivity from 2.8 S/cm to 4.6 S/cm. However, the increase in electrical conductivity observed in this study is not significant because the effectiveness of EG particles on the electrical conductivity mainly depends on the conductive linkages

formed inside the composites. The vermicular shape, porous structure, and high aspect ratio of EG particles help in forming continuous conductive paths inside the polymer matrix [74,75]. The mixing technique is crucial in preserving the particle structure from potential disintegration during the manufacturing of composites [76]. Similar to natural graphite particles, EG has a layered structure but with wider spacing between the layers [77]. The loose structure of EG makes it a soft and porous material [27]. The deterioration of EG particles during the processing might affect their ability to form electrical connections. The high shear force generated during the melt-compounding inside the twin-screw extruder could cause particles of EG to break apart. The fragmentation of EG particles can be seen in Figure 4.46(c). Similar studies on the manufacturing of EG composites at low rpm inside the internal mixture or by solution processing resulted in better electrical properties. Dhakate et al. [27] added EG to the phenolic resin and studied the effect of EG on the electrical conductivity (in-plane) of the composites. The EG particles were dry mixed with novolac phenolic resin powder and then processed in a compression mold. The electrical conductivity of 110 S/cm was achieved in the in-plane direction at 40 wt.% of EG content. Wu et al. [72] mixed the EG with PP in an internal mixer at 60 rpm for 10 minutes. They observed a sudden jump in the electrical conductivity when the EG content was between 10 to 15 wt.%. Sever et al. [73] added EG to the high-density polyethylene. The mixing took place in an internal mixture at the mixing speed of 35 rpm for 15 minutes, with 10 wt.% EG, the electrical conductivity increased dramatically.

The interactions between the secondary fillers in ternary and quaternary filler configuration can be seen in Figure 4.50(a-f). The CB was added as a ternary filler to the PP/graphite/MWCNT composites and demonstrated significant improvement in the electrical conductivity. The electrical conductivity of the PP/graphite/MWCNT/CB composites is plotted as a function of CB and MWCNT content in Figure 4.47(a) and Figure 4.47(b), respectively. The electrical conductivity value of PP/graphite/MWCNT/CB composite in experimental run 21 is almost equal to the sum of the electrical conductivity of PP/graphite/CB and PP/graphite/MWCNT composites in experimental runs 3 and 19, respectively. The addition of 5 wt.% CB in PP/graphite/MWCNT composites in experimental run 10 increased the electrical conductivity from 8.9 S/cm to 29.6 S/cm (trail#12). Similar results were recorded on adding MWCNT in the PP/graphite/CB

composites. The incorporation of 4 wt.% of MWCNT in PP/graphite/CB composites in experimental run 2 increased the electrical conductivity from 9.7 S/cm to 31.9 S/cm (trial#20). The addition of CB in PP/graphite/MWCNT composites substantially enhanced the conductivity network formed by MWCNT particles. The conductive linkages made by the combination of CB and MWCNT can be seen in Figure 4.50(a-b). King et al. [15] used 2.5 wt.% of CB as a ternary filler in PP/graphite/MWCNT composites and observed an increase in electrical conductivity from 17.9 to 37.3 S/cm.
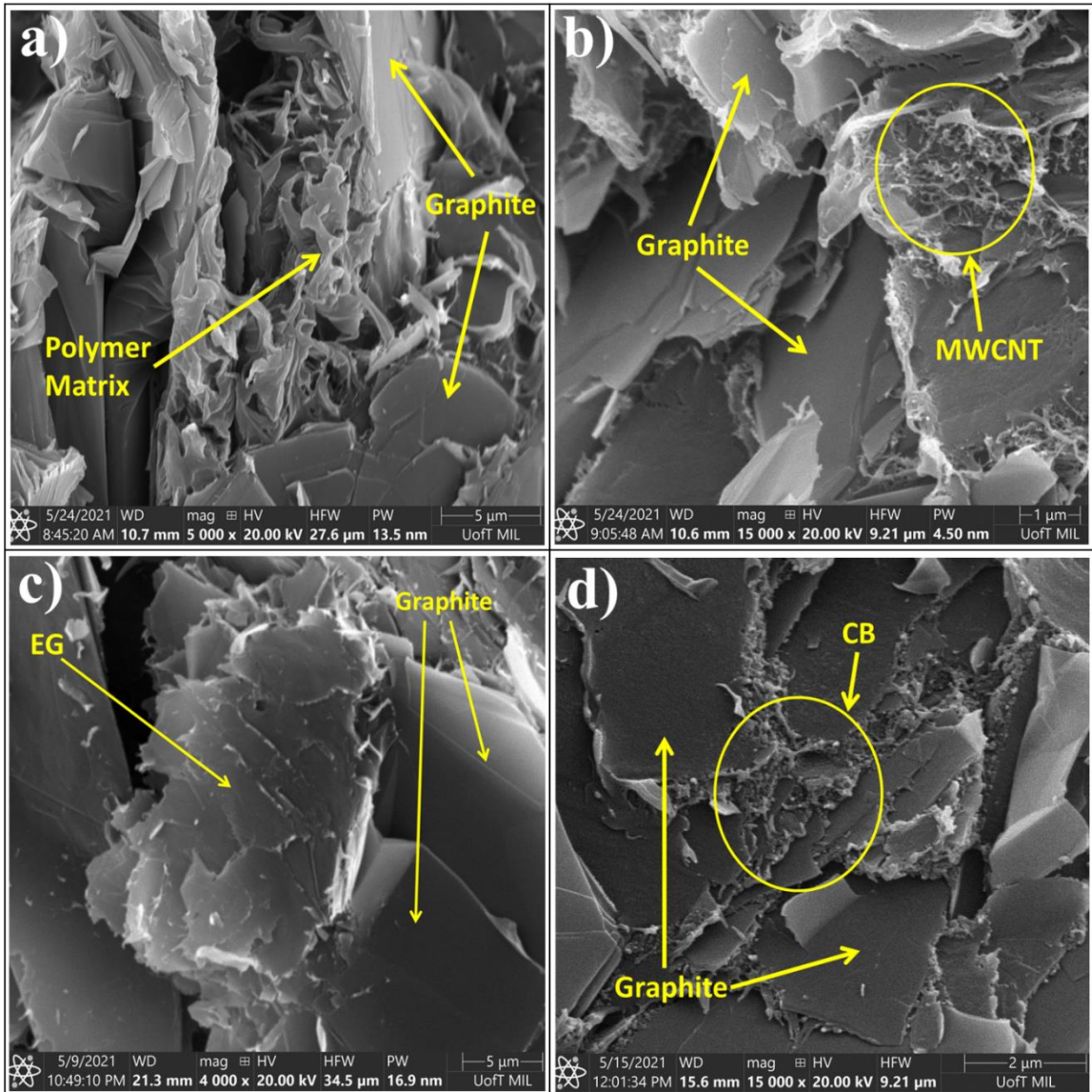
Figure 4.46:SEM micrograph of PP composites: (a) PP/graphite, (b) PP/graphite/MWCNT, (c) PP/graphite/EG, (d) PP/graphite/CB.

As a ternary filler, CB also demonstrated promising results when added to the PP/graphite/EG composites. The fragments of EG particles, when combined with the CB, formed electrical paths between graphite particles, which can be seen in Figure 4.50(c-d). The electrical conductivity of the PP/graphite/MWCNT/EG composites is presented as a function of EG and MWCNT content in Figure 4.48(a) and Figure 4.48(b), respectively. It can be observed from the graphs that the electrical conductivity of the composites significantly increased on increasing the CB content. The electrical conductivity of PP/graphite/MWCNT/EG composites with 30 wt.% EG is slightly higher than the electrical conductivity of the composites with 0 wt.% EG and 15 wt.% EG composites. However, no significant difference was observed between the electrical conductivity values of 0 wt.% EG and 15 wt.% EG filled composites. The maximum value of electrical conductivity observed in PP/graphite/EG/CB composites was 24.6 S/cm. The conductivity values of PP/graphite/EG/CB composites were observed to be significantly higher than those of PP/graphite/EG composites, but no significant difference was found when compared with PP/graphite/CB composites, indicating triviality of EG.

The addition of EG as a ternary filler to the PP/graphite/MWCNT composites exhibited adverse effects on the electrical conductivity. The electrical conductivity of the PP/graphite/MWCNT/EG composites is presented as a function of EG and MWCNT content in Figure 4.49(a) and Figure 4.49(b), respectively. Figure 4.49(b) shows that the MWCNT had promising effects on the electrical conductivity when the EG content was 0 wt.%. The addition of MWCNT did not demonstrate significant effects when the composites were loaded with 30 wt.% of EG. It can be seen from Figure 4.49(a) that the addition of EG in PP/graphite/MWCNT reduced the electrical conductivity of the composites when the MWCNT content was 4 wt.%. The conductivity of PP/graphite/MWCNT composites reduced from 20.5 S/cm to 12.1 S/cm with the addition of 30 wt.% of EG. This could be attributed due to the deformation of EG particles during the melt mixing process. The high shear stress generated during the melt-compounding process caused the rigid particles of MWCNT to penetrate through the soft and porous EG particles. The penetration of MWCNT inside the EG can be seen in Figure 4.50(e-f). Therefore, the EG particles break the conductive links established by MWCNT rather than creating additional electrical paths.
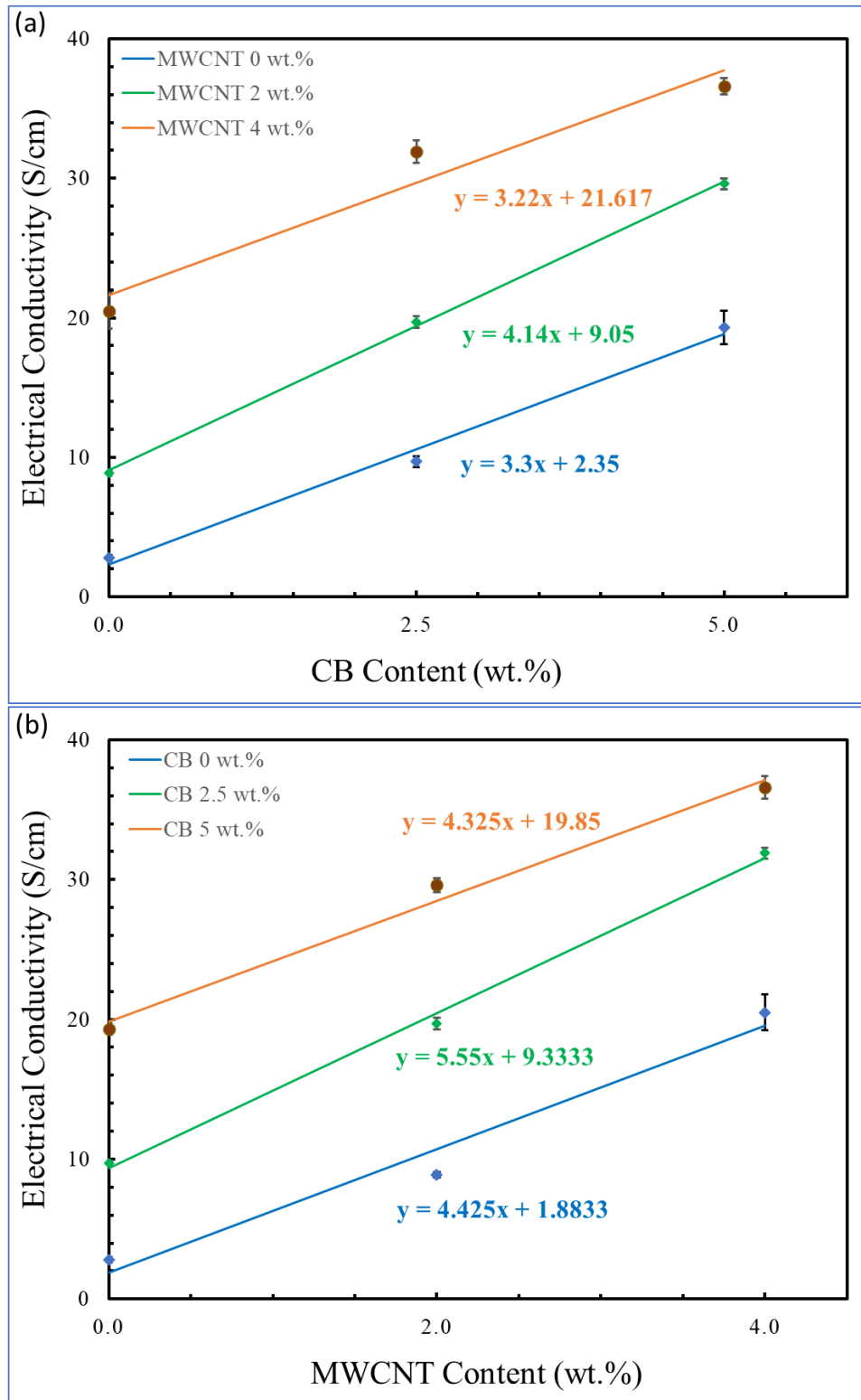
Figure 4.47: Electrical conductivity of PP/graphite/MWCNT/CB composites (a) as a function of CB content (b) as a function of MWCNT content.
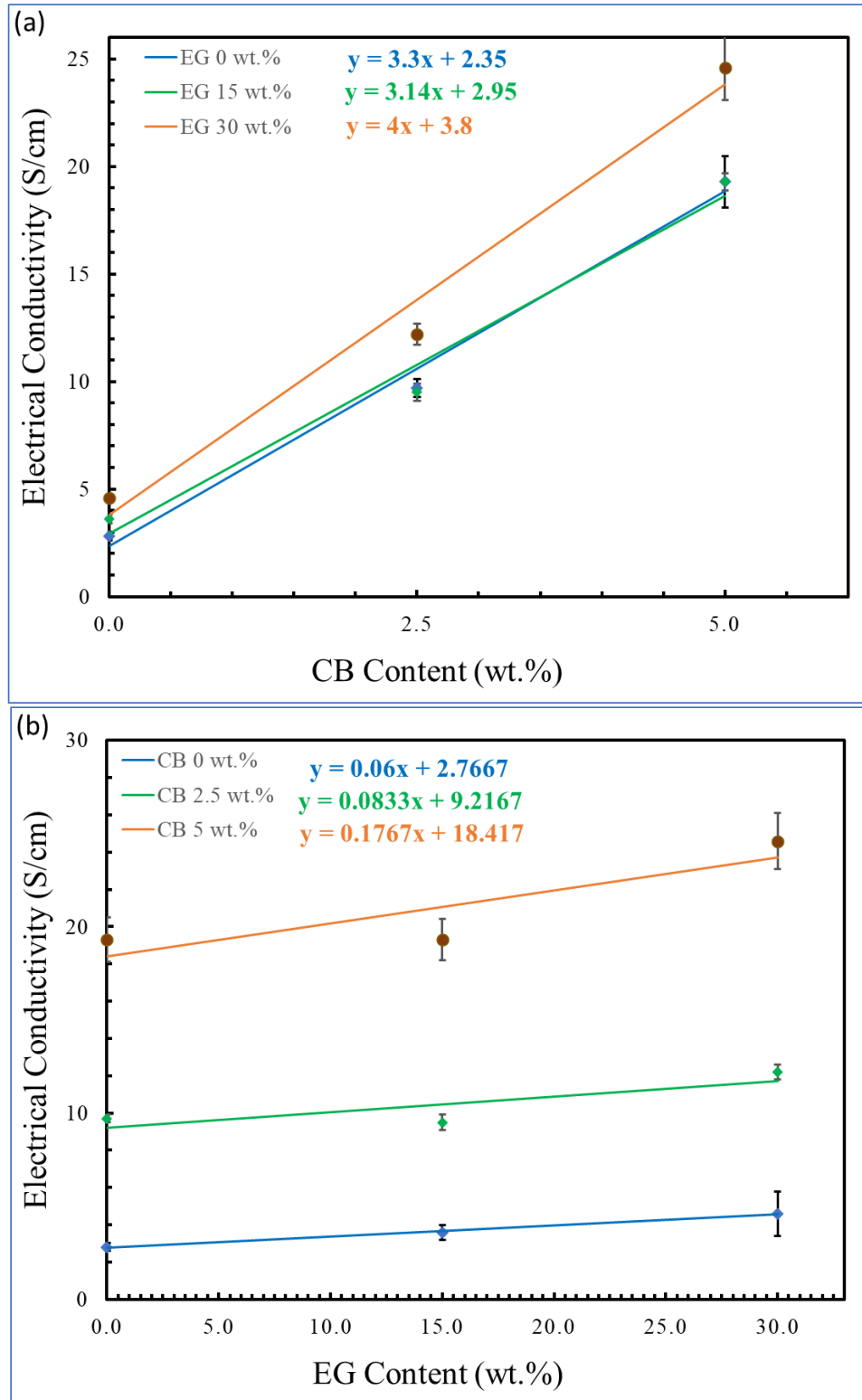
Figure 4.48: Electrical conductivity of PP/graphite/EG/CB composites (a) as a function of CB content (b) as a function of EG content.
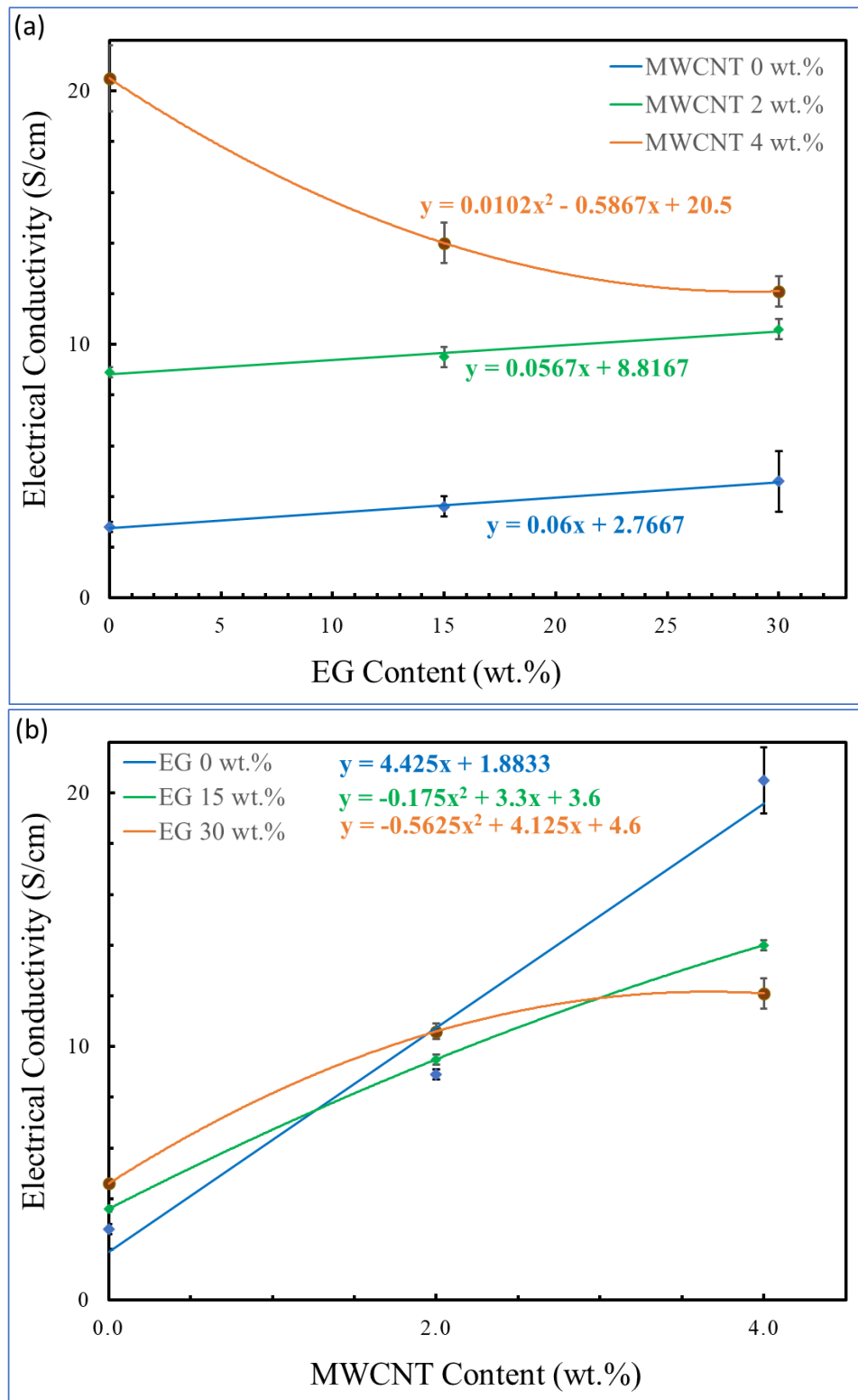
Figure 4.49: Electrical conductivity of PP/graphite/MWCNT/EG composites (a) as a function of EG content (b) as a function of MWCNT content.
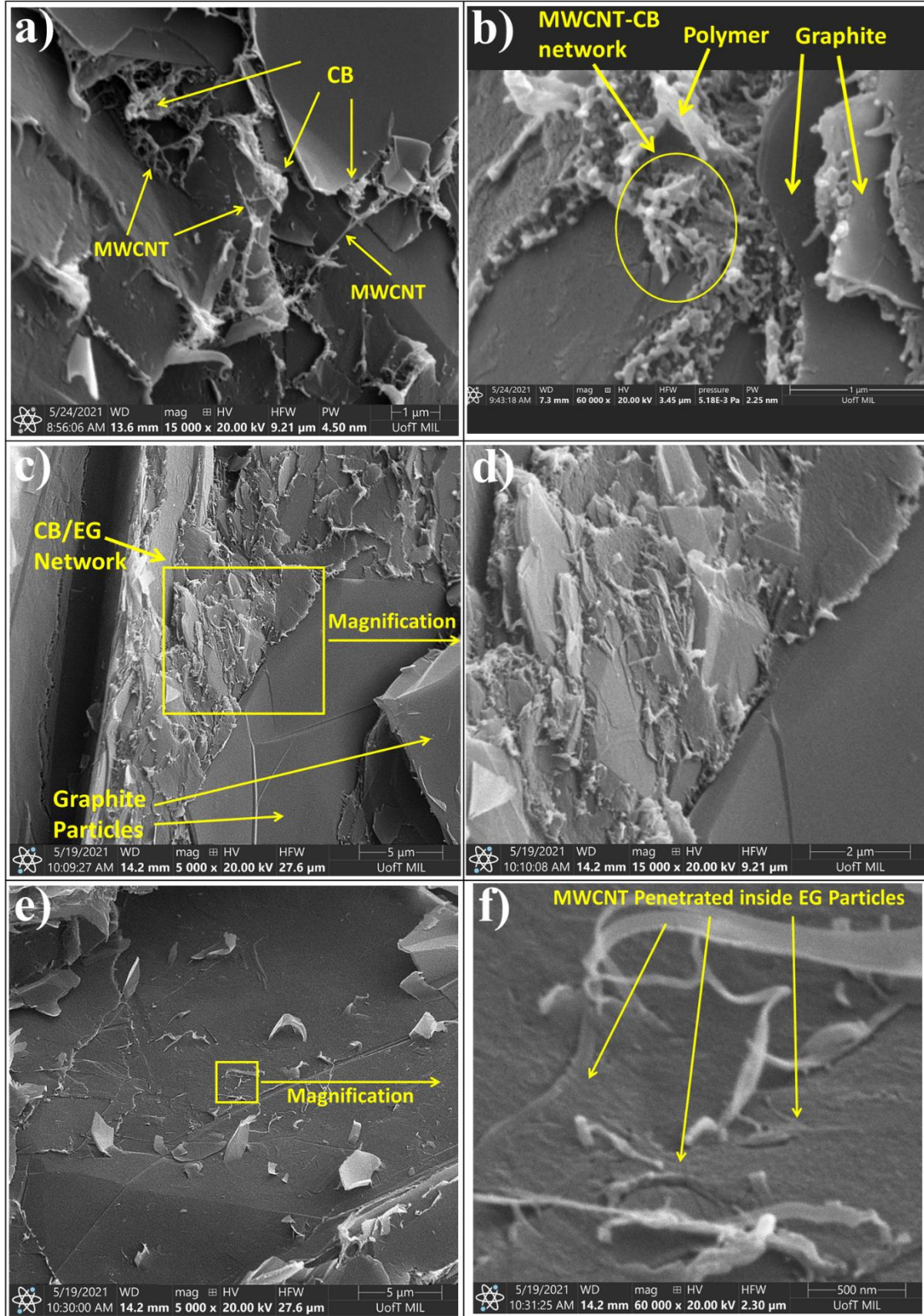
Figure 4.50: SEM micrographs ternary filler composites: (a-b) PP/graphite/MWCNT/CB, (c-d) PP/graphite/EG/CB, and (e-f) PP/graphite/MWCNT/EG.

The interaction between MWCNT and EG particles was improved with the addition of CB particles. The interaction of graphite, MWCNT, EG, and CB inside the PP/graphite/MWCNT/EG/CB composites can be seen in Figure 4.51(a) and Figure 4.51(b). The conductive network that was formed by the combination of CB and MWCNT in PP/graphite/MWCNT/CB composites is further enhanced by the addition of EG particles. The combination of MWCNT, EG, and CB particles led to the formation of a complex conductive network that interlinked the graphite particles.
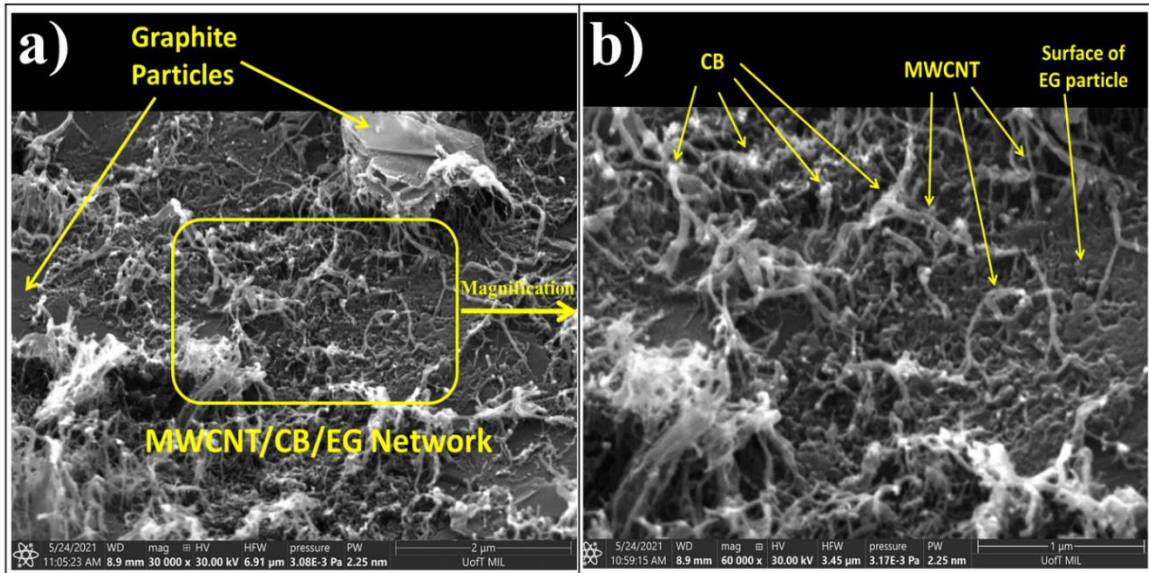
Figure 4.51: SEM micrographs of quaternary filler composites (a) 30,000x magnification, (b) 60000x magnification.

4.3.2 Effects of Filler Interaction on the Flexural Strength

The flexural strength of five specimens from each composition was tested, and the average values along with the standard deviation were reported in Table 4.12. Experimental runs involving 2.5 wt.% CB and 0 wt.% MWCNT demonstrated high flexural strength values. The highest flexural strength recorded in this study was 36.9 MPa at run number 2 with 0 wt.% MWCNT, 0 wt.% EG, and 2.5 wt.% CB. In contrast with the strength measurement, the electrical conductivity at run number 2 was observed to be 9.7 S/cm only.

The mechanical performance of the composites was improved by adding a small amount of CB. However, incorporating CB at high composition demonstrated negative effects on flexural strength. The flexural strength of PP/graphite composites increased from

30.3 to 36.9 MPa when 2.5 wt.% CB was added but reduced to 34.2 MPa when CB was added at 5 wt.%. A similar trend was observed when CB was added in ternary and quaternary filler formations in this study. The high surface area of CB results in better interfacial bonding with the resin, leading to better mechanical properties. On the other hand, the high content of CB inside the composite absorbed a large amount of resin, causing poor wetting of graphite and reducing overall mechanical properties [70]. This phenomenon was also observed in a research work investigated by Kang et al. [70], wherein the feasibility of using CB was studied for the development of a lightweight fuel cell stack. In the study, CB was added as a binary filler in the graphite-phenolic resin composites up to 5 wt.%. The flexural strength was observed to increase with the addition of 1 wt.% CB but started to decrease with the increase in the CB content to more than 3 wt.%.

The MWCNT exhibited adverse effects on the mechanical properties of the composites. The overall flexural strength of the composites was observed to decrease with the increase in MWCNT content. It may be attributed to improper filler mixing, causing the MWCNT to agglomerate. The melt-compounding technique is not very effective in handling the agglomeration issues of MWCNT [78,79]. Dhakate et al. [25] observed that adding 2 vol.% of MWCNT to polymer/graphite composites results in a reduction in the bending strength. The incorporation of EG has not been observed with any noticeable effects on the flexural strength of the composites. The flexural strength slightly decreased with increasing EG content in PP/graphite and PP/graphite/CB composites. It may be due to the weak interfacial bonding of the porous structure of EG with the resin [74]. However, a slight improvement in the flexural strength was observed when EG was mixed with MWCNT composites. The fluctuations in the values of flexural strength on changing EG content were not significant.

4.3.3 Analysis of Variance

The parametric evaluation of the experimental design was performed by ANOVA. The control factors were evaluated, and their significance was investigated. The mean output response for three control factors at each level is mentioned in Table 4.13 and Table 4.14. It was observed that the compositions of MWCNT (A) and CB (B) demonstrated

significant effects on the electrical conductivity and flexural strength of the composite. The corresponding values of the F-test demonstrated the high significance of MWCNT and CB at 99% confidence levels on both output responses. In contrast, the composition of the EG showed the least impact on the conductivity and strength measurements. The F-values of EG were observed to be 0.48 and 1.22 for electrical conductivity and flexural strength measurements, respectively, which were much lower than F)2.59 value@90%. Based on its minimum statistical summation of electrical conductivity and flexural strength, EG was deemed insignificant.

Table 4.13: ANOVA results for electrical conductivity.

Analysis of Variance (ANOVA)							
A1	105.6	B1	179	C1	86.6	SS)Total	3304.939
A2	187.5	B2	172.6	C2	174.3		
A3	244.4	B3	185.9	C3	276.6		
SSA	1081.876	SSB	9.831852	SSC	2009.503	SS)Error	203.7274
VA	540.9381	VB	4.915926	VC	1004.751	V)Error	10.18637
F)A	53.10411	F)B	0.482598	F)C	98.63685		
p)A	0.0001	p)B	0.6242	p)C	0.0001		
Signficant @ 90% C.L						2.59	
Signficant @ 95% C.L						3.49	
Signficant @ 99% C.L						5.85	

Table 4.14: ANOVA results for flexural strength.

Analysis of Variance (ANOVA)							
A1	291.9	B1	259.4	C1	246.54	SS)Total	344.8688
A2	259.24	B2	261.8	C2	283		
A3	245	B3	274.94	C3	266.6		
SSA	128.4838	SSB	15.55227	SSC	74.09982	SS)Error	126.7329
VA	64.24191	VB	7.776133	VC	37.04991	V)Error	6.336644
F)A	10.13816	F)B	1.227169	F)C	5.846929		
p)A	0.0009	p)B	0.3143	p)C	0.01		
Signficant @ 90% C.L						2.59	
Signficant @ 95% C.L						3.49	
Signficant @ 99% C.L						5.85	

4.3.4 Factorial Design Analysis

The factorial design analysis was performed to analyze the impact of each factor on the output responses. The analysis was carried out into two parts.

4.3.4.1 Electrical Conductivity

The summation values of the electrical conductivity for each input factor are shown in Figure 4.52(a). It was observed that the variations in CB and MWCNT content demonstrated a significant impact on the electrical conductivity. In contrast, the electrical conductivity summation values for EG did not show any significant fluctuations. It was found that increasing the composition level of MWCNT from A_1 to A_3 (0 wt.% to 4 wt.%) and CB from C_1 to C_3 (0 wt.% to 5 wt.%) significantly increased the value of electrical conductivity. Moreover, the difference between the lowest and highest summation values of electrical conductivity for the MWCNT and CB were found to be 138.8 and 190 S/cm, respectively, whereas this difference was only 13.3 S/cm in the case of EG. These results confirm that the composition of CB is the most significant factor with the highest variability effects on the electrical conductivity, whereas EG has the least effect on the electrical conductivity.

4.3.4.2 Flexural Strength

Figure 4.52(b) represents the summation values of Flexural Strength for each input factor. The summation values for the MWCNT compositions demonstrated the highest variation, whereas the EG composition showed the least variation. Summation values for CB were high when the composition level of CB increased from C_1 to C_2 (0 wt.% to 2.5 wt.%) but declined when the composition increased to C_3 (5 wt.%). The CB particles help in establishing strong interfacial bonding with the resin due to their large surface area, resulting in improved flexural strength. At the same time, the high surface area of the filler particle also absorbed large amounts of polymeric material. Thus, the increased content of CB absorbed a significant volume of the resin, leaving less polymer for the graphite wetting, which led to inefficient mixing and poor interfacial bonding between graphite and the polymer matrix [70]. The analysis showed that with the increase in the CB composition from C_1 to C_2 (0 wt.% to 2.5 wt.%) and the decrease in MWCNT composition from A_3 to A_1 (4 wt.% to 0 wt.%), the flexural strength increased and reached the highest value. The

difference between the highest and lowest summation values for MWCNT, CB, and EG was found to be 46.2, 13.14, and 35.46 MPa, respectively. These results confirm that the composition of CB is the most significant factor influencing electrical conductivity, and the EG has the least significant effect on electrical conductivity.
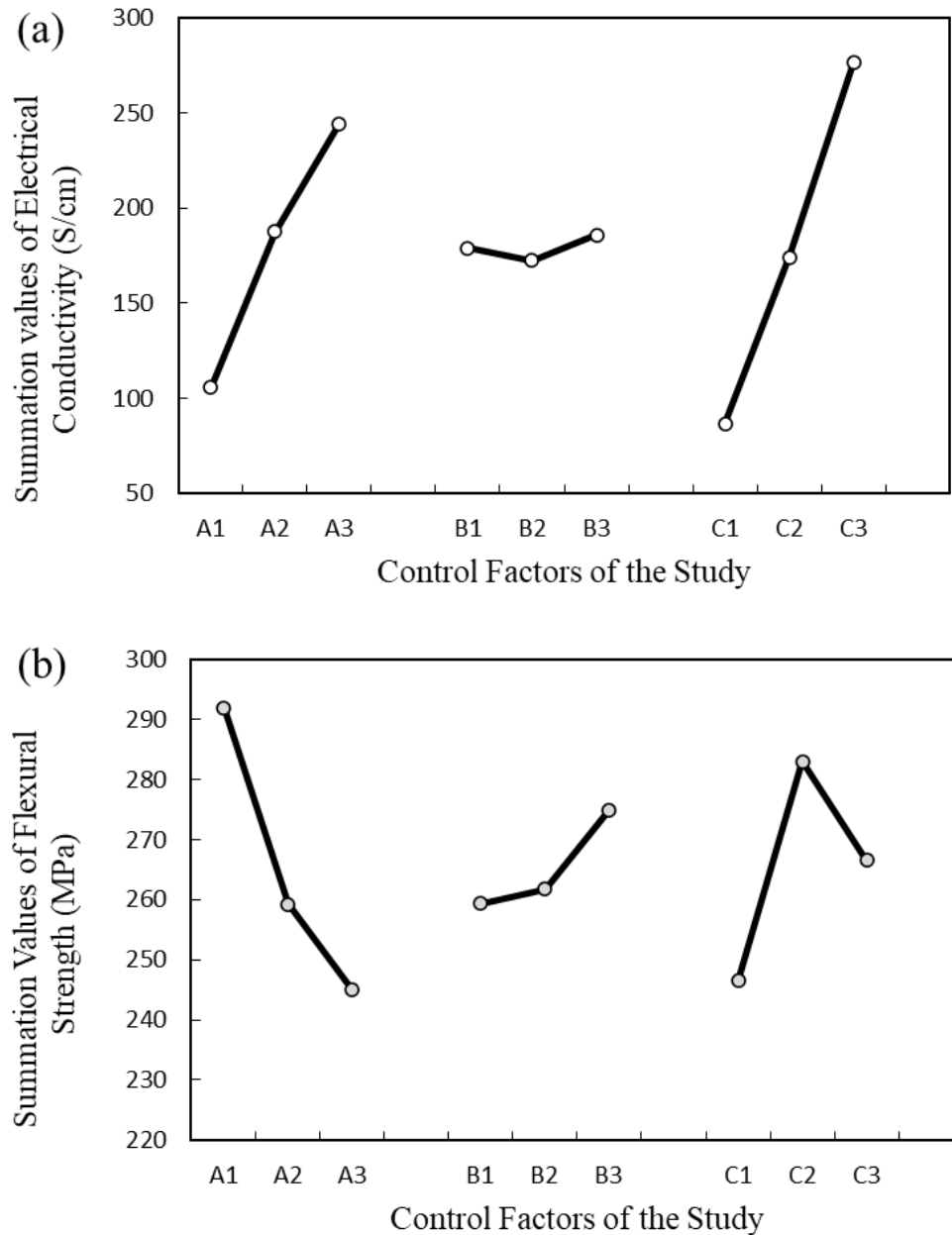
Figure 4.52: Summation values of the output responses: (a) Electrical conductivity (b) Flexural strength.

4.3.5 Response Surface Methodology

Multiple regression equations were generated to evaluate the significance of control factors on the electrical conductivity and flexural strength as output responses. The predictive mathematical modeling was performed on these output responses using the RSM technique to investigate the model accuracy of the melt-compounding process. The statistical study investigates the effect of three input factors, viz. MWCNT, EG, and CB with three-level variation leading to $3^3 = 27$ trials for the complete analysis, and the OA design involve a full-factorial design. The following equations give the mathematical modeling generated for the composite manufacturing process:

$$X = 1.4296 + (5.2444 * A) - (0.1204 * B) + (3.5733 * C) - (0.3472 \quad (4.1)$$
$$* A^2) + (0.0049 * B^2) + (0.1298 * C^2)$$

$$Y = 29.6756 - (2.3261 * A) - (0.022 * B) + (2.7951 * C) + (0.2558 \quad (4.2)$$
$$* A^2) + (0.0027 * B^2) - (0.4699 * C^2)$$

Where,

X is the predicted value of electrical conductivity,

Y is the predicted value of flexural strength,

A is the composition of MWCNT,

B is the composition of EG, and

C is the composition of CB.

The average model accuracy determined in Figure 4.53(a-b) differentiates between the experimental data and the predictive output response. The predictive model demonstrated an average model accuracy of 84% and 94% for the electrical conductivity (X) and flexural strength (Y), respectively, based on 27 experimental runs. The three-dimensional surface contour plots of the output responses have been demonstrated in Figure 4.54(a-b).
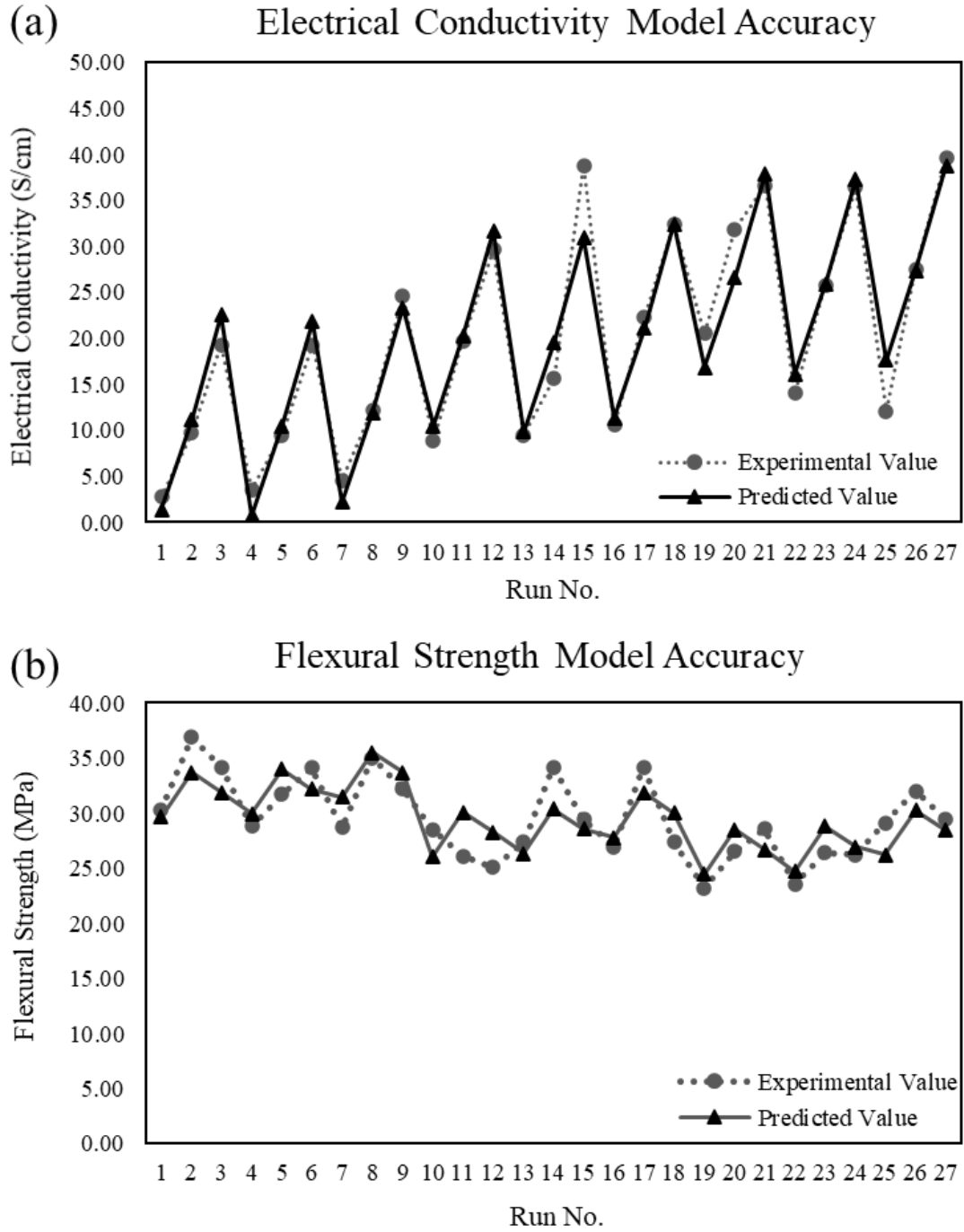
Figure 4.53: Comparison of predictive model outcomes with experimental outcomes (a) electrical conductivity (b) flexural strength.
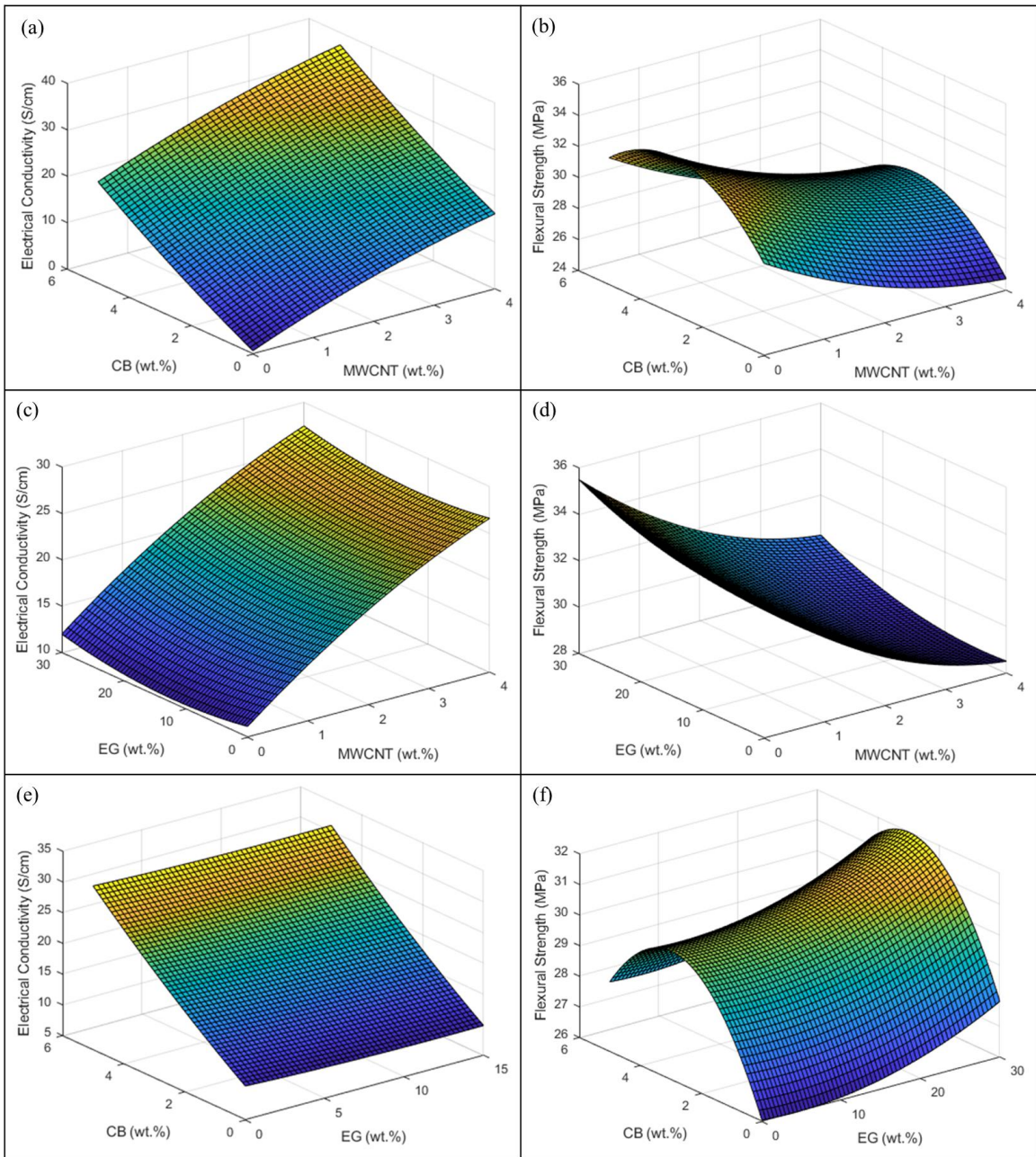
Figure 4.54 Three-dimensional surface contour plots for the following measurements: electrical conductivity (a-c) and flexural strength (d-f)

4.3.6 Cost optimization study

The experimental trials listed in Table 4.12 were further studied for the cost optimization of the composite materials. The material cost of electrically conductive thermoplastic composites depends on the polymer resin and conductive fillers incorporated into the polymer matrix. One factor that affects the material cost is the order quantity. The cost at which the polymer resin and conductive fillers were procured for the lab-scale experiments is listed in Table 4.15. The cost can be decreased by ordering the materials in larger quantities for industrial production.

Table 4.15: Cost of polymer resin and conductive fillers.

S.no	Material	Cost (US$/lb)
1	PP	1
2	Graphite	2
3	MWCNT	100
4	EG	6
5	CB	38

a) Cost of composite materials

The total filler content and polymer content were fixed at 75 wt.% and 25 wt.%, respectively. Graphite was used as a primary, and the composition of graphite was configured according to the compositions of MWCNT, EG, and CB for each experimental trial. By using the material cost information given in table 4.14, the material cost for each composite formulation used for the DOE can be calculated by equation (4.3). Table 4.16 provides the material cost, compositions, and properties of each composite formulation.

$$Z = 0.98 * A + 0.04 * B + 0.36 * C + 1.75 \qquad (4.3)$$

Where Z is the material cost of the composites, and A, B, and C are the weight percent compositions of MWCNT, EG, and CB, respectively.

Table 4.16: Material compositions, properties, and costs of the composite formulations.

| Run# | Graphite (wt.%) | Control Factors | | | TPEC (S/cm) | IPEC (S/cm) | Flexural Strength (MPa) | Material Cost (US$/lb) |
| | | A | B | C | | | | |
		MWCNT (wt.%)	EG (wt.%)	CB (wt.%)				
1	75.0	0	0	0	2.8 ± 0.2	8.2 ± 0.8	30.3 ± 1.3	1.75
2	72.5	0	0	2.5	9.7 ± 0.4	23.9 ± 4.1	36.9 ± 1.2	2.65
3	70.0	0	0	5	19.3 ± 1.2	42.4 ± 6.9	34.2 ± 2.8	3.55
4	60.0	0	15	0	3.6 ± 0.1	11.2 ± 0.2	28.8 ± 0.4	2.35
5	57.5	0	15	2.5	9.5 ± 0.2	24.9 ± 1.8	31.7 ± 2.3	3.25
6	55.0	0	15	5	19.3 ± 1.1	53.4 ± 15.7	34.1 ± 2.3	4.15
7	45.0	0	30	0	4.6 ± 0.1	16.7 ± 1.4	28.7 ± 1.4	2.95
8	42.5	0	30	2.5	12.2 ± 0.5	32.2 ± 3.7	35.0 ± 2.0	3.85
9	40.0	0	30	5	24.6 ± 1.5	52.7 ± 5.7	32.2 ± 2.8	4.75
10	73.0	2	0	0	8.9 ± 0.2	28.6 ± 4.9	28.5 ± 2.1	3.71
11	70.5	2	0	2.5	19.7 ± 0.5	43.1 ± 5.8	26.1 ± 3.1	4.61
12	68.0	2	0	5	29.6 ± 0.7	58.4 ± 9.2	25.1 ± 0.9	5.51
13	58.0	2	15	0	9.5 ± 0.2	33.1 ± 2.6	27.4 ± 2.6	4.31
14	55.5	2	15	2.5	15.7 ± 0.4	45.4 ± 3.9	34.2 ± 3.8	5.21
15	53.0	2	15	5	38.8 ± 0.9	74.8 ± 16.5	29.4 ± 1.8	6.11
16	43.0	2	30	0	10.6 ± 0.3	30.2 ± 2.6	26.9 ± 4.4	4.91
17	40.5	2	30	2.5	22.3 ± 1.1	48.7 ± 5.8	34.2 ± 1.9	5.81
18	38.0	2	30	5	32.4 ± 0.3	62.5 ± 6.3	27.4 ± 0.6	6.71
19	71.0	4	0	0	20.5 ± 1.3	49.2 ± 2.4	23.2 ± 1.9	5.67
20	68.5	4	0	2.5	31.9 ± 0.8	58.4 ± 8.5	26.5 ± 2.0	6.57
21	66.0	4	0	5	36.6 ± 0.6	67.5 ± 5.4	28.6 ± 3.2	7.47
22	56.0	4	15	0	14.0 ± 0.2	43.5 ± 2.8	23.6 ± 1.8	6.27
23	53.5	4	15	2.5	25.8 ± 0.6	58.0 ± 5.2	26.4 ± 2.9	7.17
24	51.0	4	15	5	36.4 ± 0.2	81.9 ± 2.6	26.2 ± 2.6	8.07
25	41.0	4	30	0	12.1 ± 0.6	46.5 ± 0.8	29.1 ± 2.7	6.87
26	38.5	4	30	2.5	27.5 ± 0.4	85.8 ± 0.1	32.0 ± 3.8	7.77
27	36.0	4	30	5	39.6 ± 1.1	124.7 ± 9.1	29.4 ± 1.7	8.67

b) Effects of control factors on the material cost

The summation values of the material cost for MWCNT, EG, and CB are shown in Figure 4.55. A comparison of Figure 4.52(a) with Figure 4.55 shows that the composition of MWCNT considerably increased the electrical conductivity and material cost of the composites, whereas adding CB increased the electrical conductivity significantly and had less impact on the material cost. On the other hand, EG had no significant impact on the properties of the composites when compared to its contribution to the material cost. Also, the processing of EG took place in multiple steps. The first step was the expansion process, in which the expandable graphite was placed in the furnace at 700 ℃ for 15 minutes. The second step involved preparing PP/EG masterbatch as EG cannot be dry mixed with graphite, unlike CB. The processing of EG will further increase the overall cost of the material. So, adding EG to the composite to enhance its properties is not cost-effective. By adjusting the compositions of MWCNT and CB, the targeted values of TPEC and flexural strength can be achieved at the minimum cost. Figure 4.56 shows the 3D surface plot of material cost. By comparing Figure 4.56 with Figure 4.54(a), it is evident that increasing CB content significantly increased electrical conductivity at a lower cost than increasing MWCNT content.
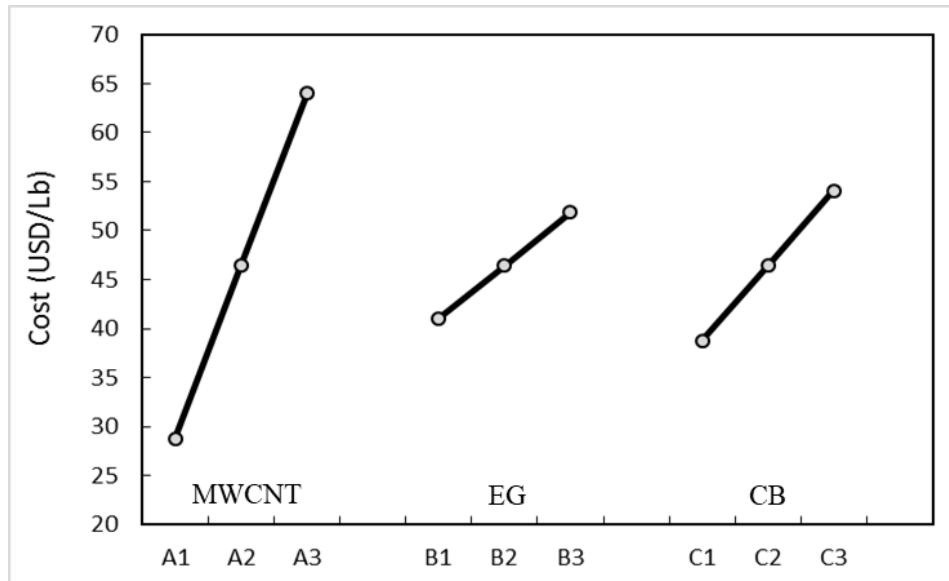
Figure 4.55: Main effects plot for material cost.
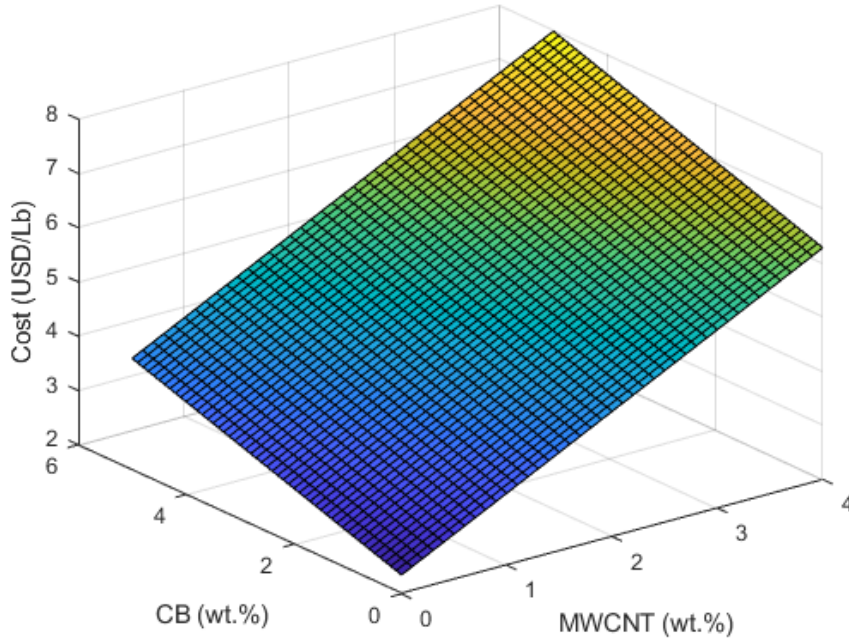
Figure 4.56: 3D surface plot for the material cost of the composites.

c) Material cost optimization

The statistical model developed using RSM to predict the values of electrical conductivity and flexural strength was used for the material cost optimization. Figure 4.57(a) and (b) plot the predicted values of TPEC and flexural strength of the composites against the CB content at different levels of MWCNT. These figures were plotted by using equations (4.1) and (4.2). Figure 4.57(c) presents the cost of the composite material as a function of CB content. Equation (4.3) was used to plot Figure 4.57(c). The target value for flexural strength was 25 MPa (Table 1.2). It can be seen from Table 2.2 that the bipolar plate with of 25 S/cm in the through-plane direction is suitable for fuel cell operation. Material cost can be minimized by selecting a composition that has TPEC and flexural strength equal to or higher than the targeted values with a minimum content of MWCNT. The data point with 5.5 wt.% CB and 0 wt.% MWCNT has TPEC and flexural strength values of 25 S/cm and 30.8 MPa with a material cost of 3.7 US$/lb. Hence the composite formulation with 25 wt.% PP, 69.5 wt.% graphite, and 5.5 wt.% CB has achieved the required levels of TPEC and flexural strength with the minimum material cost. However, the regression equations used to plot these curves were generated by the experimental data of DOE, and the range of CB in DOE was between 0 to 5 wt.%. The data point with 5.5 wt.% CB and 0 wt.% MWCNT is slightly outside the range of this study.
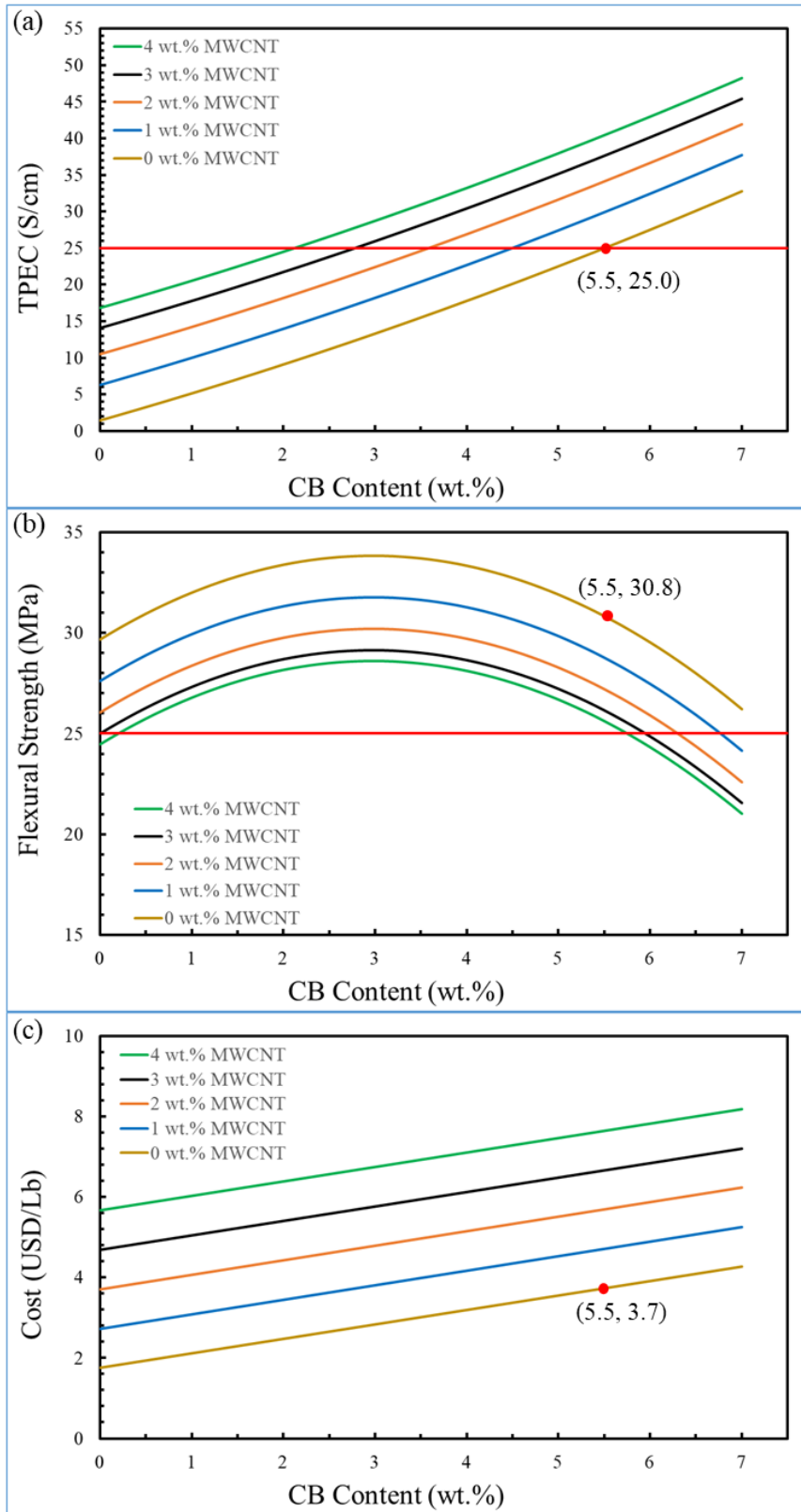
Figure 4.57: Properties of composite material plotted as a function of CB content (a) TPEC, (b) flexural Strength, and (c) material cost.

4.4 Miscellaneous Testing

To analyze performance of thermoplastic composites in the fuel cell operating environment, the thermoplastic composites were tested at different temperatures and loading conditions.

4.4.1 Fatigue Testing

The fatigue testing of the composite sheet was performed to investigate the effect of cyclic load on the strength of the material. The samples were tested under stress-controlled fatigue loading. The cyclic load was applied by using the DMA equipment, DMA Q800, by TA Instruments. The specimen was mounted on the dual-cantilever clamp, and the frequency of the cyclic load was set to 25 Hz. The flexural strength of the composite material was 33 MPa. Therefore, the first specimen was subjected to cyclic stress of 32.5 MPa. The test was continued until the specimen was fractured. The next specimen was subjected to cyclic stress of 30 MPa. Similarly, the stress loading was reduced with a step of 2.5 MPa to every specimen. Figure 4.58 shows the S-N curve for the fatigue testing of the composite sheet samples. The first specimen at 32.5 MPa was fractured within two cycles. The second specimen was broken after ten cycles. The specimen with the stress loading of 27.5 MPa was fractured after 10 seconds and completed 300 cycles. The specimen at 22.5 MPa was stable for 30 minutes and got fractured after 45,000 cycles. The last specimen was subjected to cyclic stress of 20 MPa, and the specimen was unbreakable even after 6 million cycles. The test was stopped after 70 hours.
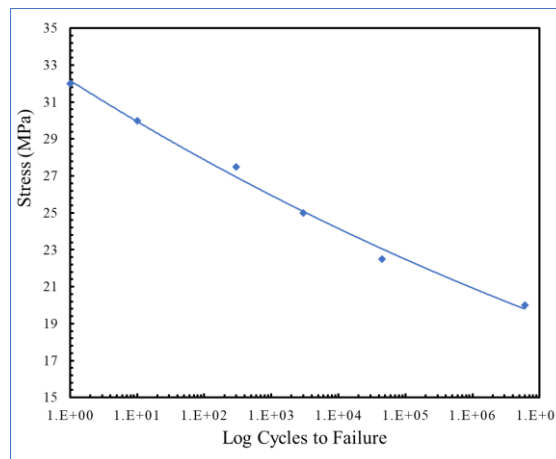
Figure 4.58: S-N curve for the composite material.

4.4.2 Effect of Temperature on the Electrical Conductivity

The effect of temperature on the electrical conductivity was investigated by measuring the TPEC of the composite material at different temperatures. This test was conducted to evaluate the composite material's performance under fuel cell operating conditions. PP/graphite composite with 55.5 wt.% graphite, 2.5 wt.% CB, 2 wt.%, and 15 wt.% EG (trail#14 of the optimization study in section 4.3) were chosen for this test. This composition was chosen to investigate the effect of temperature on all the conductive fillers. The TPEC testing setup was placed inside the lab furnace, while the power supply and voltmeter were placed outside the furnace. The furnace was heated to 100°C and then cooled down to room temperature. During both heating and cooling, the electrical conductivity of the sample was measured every 5°C. Table 4.17 shows the electrical conductivity of the composite at different temperatures. The electrical conductivity remained constant throughout the experiment at 15.4 S/cm. The conductivity of the composite material was not affected by temperature variations.

Figure 4.59: Electrical conductivity testing at variable temperature.

Table 4.17: Electrical Conductivity (through-plane) of the composite at different temperatures

S.no	Temperature (C)	TPEC (S/cm)	
		Heating	Cooling
1	25	15.4	15.4
2	30	15.4	15.4
3	35	15.4	15.4
4	40	15.4	15.4
5	45	15.4	15.4
6	50	15.4	15.4
7	55	15.4	15.4
8	60	15.4	15.4
9	65	15.4	15.4
10	70	15.4	15.4
11	75	15.4	15.4
12	80	15.4	15.4
13	85	15.4	15.4
14	90	15.4	15.4
15	95	15.4	15.4
16	100	15.4	15.4

4.4.3 Effect of Temperature on the Mechanical Strength

The effect of temperature on the mechanical performance was examined by performing the 3-point test of the composite at different temperatures. The purpose of the testing was to evaluate the mechanical performance of the composite material under the fuel cell operating temperature. PP/graphite composition with 36 wt.% graphite, 5 wt.% CB, 4 wt.%, and 30 wt.% EG (trail#27 of the optimization study in section 4.3) were chosen for this test. This composition includes all the conductive fillers that were used in the optimization study. The testing was performed by using Dynamic Mechanical Analyzer, DMA Q800 by TA instruments. Figure 4.60 shows the stress-strain curves of the composite at different temperatures. Due to the increase in temperature, the material became ductile and softer. At 30°C, the composite's flexural strength was 29.4 MPa, which decreased to 9.1 MPa at 120°C. On the other hand, the fracture toughness of the material increased due to an increase in the fracture strain. At 120 °C, the composite did not break, and testing was stopped when the strain value crossed 2.5 %. The overall mechanical performance of the material is adequate for fuel cell operation.
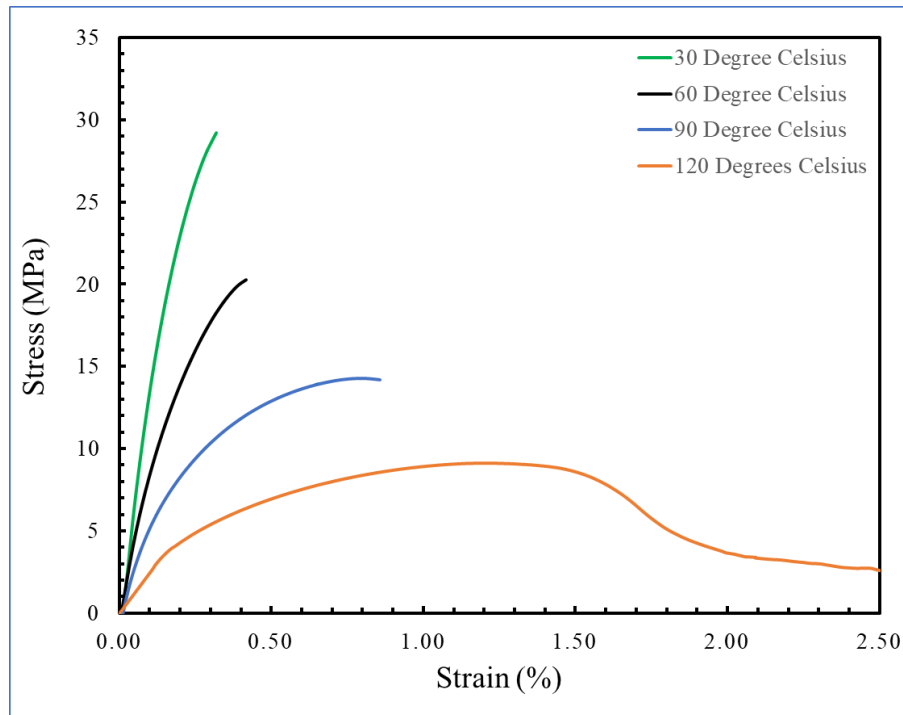
Figure 4.60: Stress-Strain curves of the composite at different temperatures.

4.5 Comparison With the Commercially Available Thermoset Composite Bipolar Plate Materials

The properties of the thermoplastic composites developed in this study were compared with those of commercially available thermoset bipolar plates (Table 4.18). TPEC values of the thermoplastic composites in Table 4.18 are similar to those of thermoset composites available on the market. BMC-940-15252A, produced by A. Schulman (LyondellBasell), has IPEC and TPEC values of 133 S/cm and 25 S/cm, respectively, with a flexural strength of 56 MPa. The flexural strength values of the thermoplastic composites are comparatively lower than the thermoset bipolar plates. However, the flexural strength values are above the criteria of the US department of energy mentioned in Table 1.2. Thermoset composites are stronger than thermoplastics, but their primary disadvantage is their low production rate. Thermoplastic composites bipolar plates can be produced through high production rate processes like sheet extrusion. As a result of using MWCNT, the first two thermoplastic composite formulations have better TPEC values, but their materials costs are comparatively higher. The third formulation is better in terms of material cost but low in TPEC value. Also, the polymer content of this formulation is only 15 wt.%, which results in a high melt viscosity during the melt-compounding and sheet extrusion process.

Table 4.18: Properties of bipolar plate materials.

Category	Manufacturer	Polymer	Filler Content (wt.%)	Filler types	Electrical Conductivity (S/cm)		Flexural Strength (MPa)	Material Cost (US$/lb)
					IPEC	TPEC		
Experimental Results	Thesis Section 4.3	PP	75	36 wt.% graphite 30 wt.% EG 5 wt.% CB 4 wt.% MWCNT	124.7	39.6	29.4	8.67
	Thesis Section 4.3	PP	75	53 wt.% graphite 15 wt.% EG 5 wt.% CB 2 wt.% MWCNT	74.8	38.8	29.4	6.11
	Thesis Section 4.1	PP	85	82.5 wt.% graphite and 2.5 wt.% CB	84.4	25.7	34.8	2.75
Commercially Available thermoset Bipolar Plates	BMC 940-15252A	Vinyl Ester	-	-	133	25	56	-
	Premix Inc. [43]	Vinyl Ester	68	Graphite	85	-	28.2	-
	Plug Power [44]	Vinyl Ester	68	Graphite	55	-	40	-
	DuPont [1]	Vinyl Ester	-	-	-	25-33	53	-
	SGL [1]	-	-	-	100	20	40	-

4.6 Chapter Summary

In the presented experimental study, the electrically conductive PP composites were produced by the melt-compounding technique in a twin-screw extruder. The conductive fillers were added to the polymer in binary, ternary, and quaternary formulations to synergistically enhance the electrical conductivity and flexural strength of the composites. The experimentation in this chapter is mainly divided into three sections. The effect of filler content on the properties of single filler and binary filler PP/graphite composites was investigated in the first section (section 4.1). Two different grades of PP were used to produce single filler PP/graphite composites. The homopolymer PP matrix demonstrated better electrical conductivity. In contrast, the copolymer PP matrix exhibited better mechanical properties at higher filler loading. The interaction of binary fillers with the graphite in the PP matrix has shown promising synergistic effects. The highest TPEC value was 49.25 S/cm and was observed in the case of 83 wt.% graphite and 2 wt.% MWCNT, whereas the highest flexural strength of 36.9 MPa was recorded at 72.5 wt.% graphite and 2.5 wt.% CB. However, in both above-mentioned cases, a compromise was observed in terms of flexural and conductivity properties, respectively. The most balanced PP/filler configuration in terms of electrical and mechanical properties was observed in the case of

82.5 wt.% graphite and 2.5 wt.% CB with the TPEC and flexural strength of 25.7 S/cm and 34.8 MPa, respectively.

The influence of the polymer matrix on the properties of the composites has been evaluated in the second section (section 4.2). PP, nylon, and TPU resins were used to produce thermoplastic composites with different graphite content. The CB was added as a binary filler to examine the interaction of binary filler in different polymer matrices. The electrical and mechanical properties of the single filler and binary filler composites were investigated. TPU composite with 69 wt.% graphite and 6 wt.% CB showed the highest values of electrical conductivity, which were 137.2 S/cm and 46.1 S/cm, respectively, in the in-plane and through-plane directions. However, the flexural strength of this formulation was only 16.7 MPa. A nylon composite formulation with 73 wt.% graphite and 2 wt.% CB exhibited the highest flexural strength of 56 MPa with the IPEC and TPEC values of 7.0 and 2.9 S/cm. TPU composites demonstrated better electrical properties at higher filler loading, while nylon composites demonstrated superior mechanical properties. PP composites offered balanced electrical and mechanical properties. A PP composite with 69 wt.% graphite and 6 wt.% CB had IPEC and TPEC values of 46.6 and 21.2 S/cm with a flexural strength of 28.5 MPa. Observations indicate that the electrical properties of composites depend mainly on the electrical network formed inside the polymer rather than on the inherent properties of the polymer matrix. However, the mechanical performance of the composites was highly influenced by the properties of the bonding matrix.

An optimization study has been performed in the third section (section 4.3) to obtain a balance value of electrical conductivity and flexural strength. The compositions of MWCNT, EG, and CB were the control factors of the optimization study. The effects of control factors with three-level variations were studied using a full-factorial design. The experimental run 27 with 4 wt.% MWCNT, 5 wt.% CB, and 30 wt.% EG demonstrated the optimum values of response parameters with the TPEC of 39.6 S/cm and flexural strength of 29.4 MPa. The IPEC value of this composition was 124.7 S/cm. The ANOVA study validates the significance of MWCNT and CB compositions at the high confidence level of 99% confidence level with a low-risk level. The RSM-generated mathematical model exhibits an average accuracy of 83.9% and 93.4% for TPEC and flexural strength,

respectively, for the range of selected process parameters. The last section of this chapter compared electrically conductive thermoplastic composites with commercially available thermoset bipolar plate materials. The electrical and mechanical properties of the thermoplastic composites formulated in this study are similar to the thermoset bipolar plates available on the market. The experimental data present a promising approach in the open literature to thoroughly understand the synergistic effects of conductive fillers on the electrical and mechanical properties of the electrically conductive thermoplastic composites. The comprehensive experimental study offers a detailed insight into the filler interactions inside the composites and provides potential guidelines for producing electrically conductive thermoplastic composites for the manufacturing of fuel cell bipolar plates.

Chapter 5: Sheet Extrusion of Electrically conductive thermoplastic composites

This chapter investigates the feasibility of fabricating thermoplastic composite bipolar plates by using the sheet extrusion process. The process of extruding sheets of highly filled thermoplastic composites, fabrication of gas flow channels on the surface of the composite sheets, and the implementation of this process in the industry have been described in detail.

5.1 Introduction

This study aims to introduce a method that can be implemented in industries for the faster production of bipolar plates. The first part of this study is to produce electrically conductive thermoplastic composites that can be used for the manufacturing of bipolar plates. Based on the experimental results of the previous chapters, a filler configuration was selected to produce an electrically conductive thermoplastic composite. The composite was produced by adding a combination of CB and graphite was added to the PP matrix. The melt-compounding of the composite material was carried out in a twin-screw extruder. The next step of this study was the sheet extrusion of the highly filled thermoplastic composite. A sheet die was attached with a single screw extruder for the sheet extrusion of the composite material. The melt-compounded material was inserted into the single screw extruder, and the sheets of the composite material were produced. The final step was to fabricate flow channels on the sheet. A mold plate with a flow channel design was used to produce flow channels on the surface of the composite sheets. This was by a pressure and heat mechanism in which the sheets of the composite material were heated and pressed against a mold plate. The gas flow channels were successfully produced on the surface of the composite sheets.

5.2 Material

It was observed in the previous chapters that the high loading of conductive filler increases the electrical conductivity of the composite but reduces the flexural strength. The filler formation with 82.5 wt.% graphite and 2.5 wt.% that was discussed in Section 4.1 had an electrical conductivity of 25.7 S/cm with a flexural strength of 35 MPa. However, the sheet extrusion of 85 wt.% filled material was challenging for the lab-scale extruder. Therefore, the composite material was prepared by mixing 80 wt.% graphite and 2.5 wt.% CB (82.5 wt.% total filler content) with the homopolymer PP matrix and used for the

producing composite sheets. This composite material has a TPEC value of 25.1 S/cm and flexural strength of 33 MPa.

5.3 Sheet Extrusion Process

The single-screw extruder (SSE) used for the sheet extrusion process was a 25.4mm diameter extruder with an L/D = 30:1 by Wayne Machine & Die Co. (USA). An 8-inch-wide sheet die was attached at the output of the single screw extruder. Figure 5.1 and Figure 5.2 show a single screw extruder and sheet die pictures. Sheet extrusion of the PP-graphite composites was carried out to test the sheet die with composites. The main purpose of the SSE was to melt the composite and build the required pressure to pump the suspension through the sheet die. Major pressure resistance was offered by the die. However, a breaker plate was not attached between the die and extruder, and thus no additional backpressure increase was expected. Due to this, a lower temperature profile in the SSE than in the twin-screw extruder was used, where the temperatures were comparable to the downstream zones of the twin-screw extruder. The sheet dies temperatures were lower than the extruder temperatures as recommended and also based on observations during melt-compounding of the composites. Different combinations of RPM and sheet die temperature were tested. Parameters were only changed after a steady state material flow was detected with the current set of parameters.

The material was also not showing a consistent flow and was prone to breakage after exiting the die. Highly filled composites exert very high melt pressure during extrusion. The motor speed was set below 40 RPM as the melt pressure reached 5000 psi. The sheet die was found to have flow imbalance during the extrusion of high filler content composite. An intermittent breakage was observed on the left side of the sheets. This might indicate higher flow speed and more shearing on the left side of the die. The flow imbalance became more noticeable as the sheet curved to the right as the left side of the extrudate was exiting the die at higher speeds, as shown in Figure 5.3. The temperature of the left side of the die was decreased to slow down to balance the material flow. However, decreasing the temperature of one side of the die did not show any significant effects. The sheet die did not equip with any oil or water-cooling mechanism. Measurement of the exact melt temperature was not possible; however, it is believed that the screw PRM would have

increased viscous heat dissipation raising the temperature of the melt. Changing the temperature of the left zone affects the other zone's temperature due to the heat conduction in the sheet die. A few good-quality samples of the sheets were collected by altering the parameters of the extrusion process [Figure 5.5].

Figure 5.1: Single screw extruder for the sheet extrusion process.

Figure 5.2: 8-inch-wide sheet die.
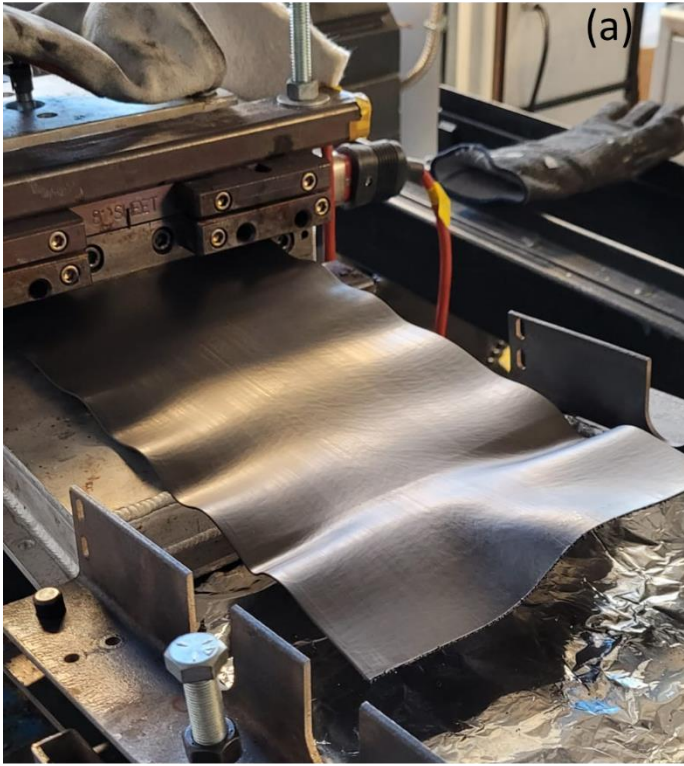
Figure 5.3: Flow imbalance during the sheet extrusion (a) sheet exiting from the die (b) collected sheet samples.

Figure 5.4: Sheet of the electrically conductive thermoplastic composites (a) coming out from sheet die (b) collected sample.

5.4 Fabrication of Bipolar Plates

Fabrication of the bipolar plates was done by embossing the gas flow channels on the surface of the composite sheets. It was done by applying heat and pressure to the extruded sheet samples. Gas flow channels were machined on the surface of the mold plate in order to emboss the design onto the composite sheets. A Carver press was used to apply heat and pressure to form flow channels on the sheet material. First, the extruded sheets were cut to 6 by 6 inches. At the beginning of the process, the press was preheated to 165°C, and the composite sheet was placed inside the press for five minutes without any pressure. The mold plate was placed on top of the preheated sheet, and the sheet was pressed against it with a pressure of 500 psi. The heat was provided for 5 minutes to maintain the temperature, then the mold was set for cooling, whereas the pressure was maintained until the mold temperature was cooled down to 100°C. The gas flow channel was successfully formed on the surface of the extruded sheets [Figure 5.5].

Figure 5.5: Fabrication of bipolar plates from composite sheet (a) bipolar plate (b) gas flow channels.

5.5 Industrial Scale Implementation

This study aimed to demonstrate the feasibility of fabricating bipolar plates using a fast production process, such as injection molding or sheet extrusion. The composite should have a high filler content in order to provide the conductivity required by bipolar plates. This increases the apparent viscosity of the molten material to such a degree that, in an injection mol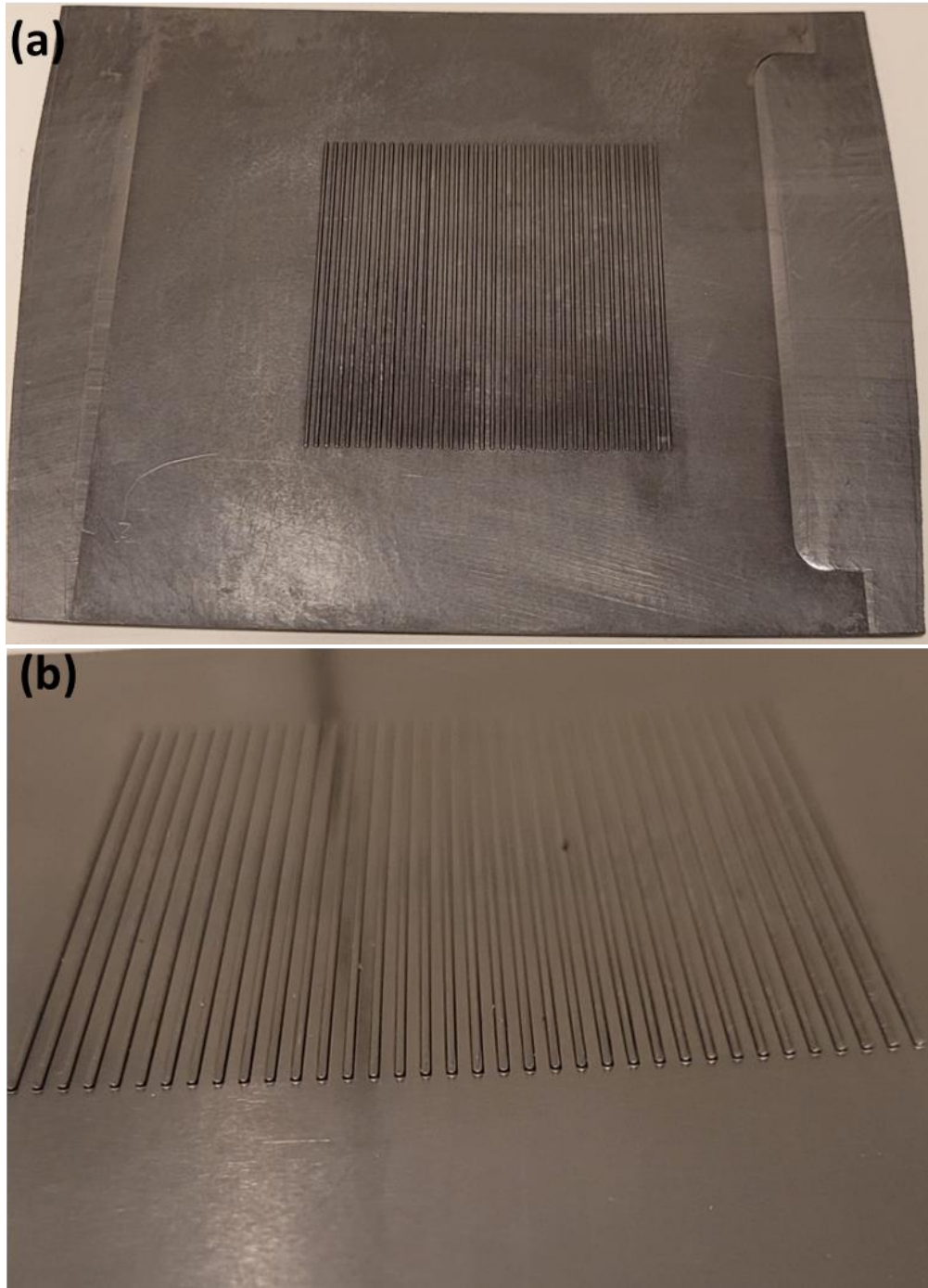ding process, it becomes impossible to properly fill the thin mold needed for the bipolar plates. Therefore, a more workable process based on sheet extrusion has been chosen for this research work. The development of a pilot production system was beyond the scope of this work. To demonstrate the feasibility of the above process, it was decided to show the viability of two key components of the process.

a. Demonstrate that the developed formulation can be extruded into sheets using a continuous extrusion and die system.

b. Demonstrate that the channel features required in bipolar plates can be embossed onto the surface of the fabricated sheets from the above extrusion system.

The assumption is that if these two processes work successfully, the rest of the continuous fabrication setup can be developed using the standard sheet extrusion, roller embossing, and other downstream processing equipment. To demonstrate the first process, melt-compounding of the composite material was carried out in a twin-screw extruder, and the extruded material was cut into pellets. These pellets were then processed in the single screw extruder fitted with a die capable of sheet extrusion. Sample composite sheets were successfully produced, fulfilling the first requirement. The sample sheets produced were then pressed against a hot metallic mold plate to successfully emboss flow channel profiles on the surface of these sheets, thus demonstrating the second process to be viable. Further modifications and industrial implementation can be achieved by designing downstream equipment and by integrating the sheet die with the twin-screw extruder. Figure 5.6 shows the schematic diagram of the thermoplastic composite bipolar plates production process. A positive displacement melt pump can be mounted in between a twin-screw extruder exit and the sheet die entrance to ensure a constant flow rate and hence produce consistent composite sheets. These can be directly fed into a sheet calendaring system in which roller surfaces can be machined to emboss the required gas flow channels

onto the surface of the hot extruded sheets. Roller embossing is a standardized industrial process and can easily be implemented in any continuous extrusion system. A final cutting stage can also be integrated with this system. Such a system can easily be built to produce bipolar plates with a production rate of more than 100 plates per hour.
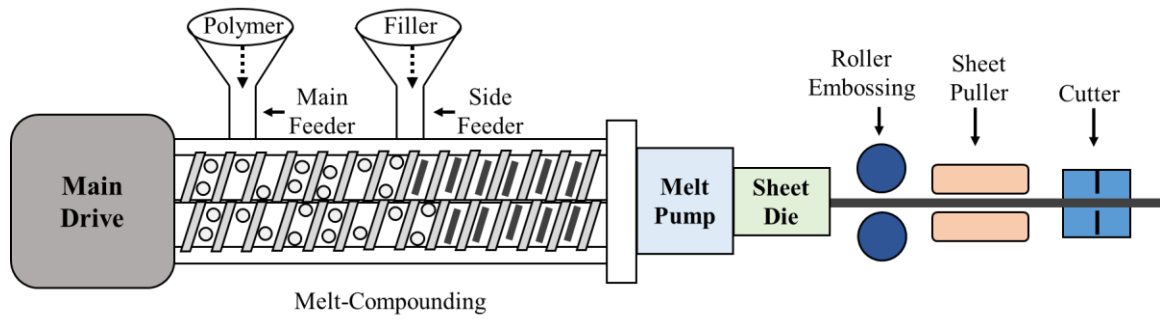

Figure 5.6: Schematic diagram of thermoplastic bipolar plates production process.

Chapter 6: Conclusions, Contributions, and Future Recommendations

The major outcomes, results, and findings obtained from this thesis are briefly described in this chapter. Recommendations for future research are provided.

6.1 Conclusions

The main findings of this study are summarized as follows:

- Electrically conductive thermoplastic composites were developed for bipolar plate applications.
- Thermoplastic composites have been developed by adding fillers to the PP, nylon, and TPU resins, and the influence of the bonding matrix on the properties of the composites has been investigated.
- TPU composites demonstrated better electrical properties at higher filler loading, while nylon composites demonstrated superior mechanical properties. PP composites offered balanced electrical and mechanical properties.
- Thermoplastic composites have been developed by adding graphite, MWCNT, EG, and CB in binary, ternary, and quaternary formulations, and the synergistic effects of filler interaction on the properties of thermoplastic composites have been investigated.
- The composite formulation with 36 wt.% graphite, 30 wt.% EG, 5 wt.% CB, 4 wt.%, and 25 wt.% PP has achieved the required properties and has the highest value of TPEC which was 39.6 S/cm.
- The formulation with 82.5 wt.% graphite, 2.5 wt.% CB, and 15 wt.% PP met the target values and had the minimum material cost.
- ANOVA test demonstrated the high significance of MWCNT and CB on electrical conductivity and flexural strength at a 99% confidence level.
- An empirical model was developed by using RSM to evaluate the effects of filler content and to achieve the optimum values of electrical conductivity and flexural strength of the composites.
- The empirical model demonstrated an average accuracy of 83.9% and 93.4% for predicting the values of electrical conductivity and flexural strength at different filler compositions.

- Thermoplastic composite bipolar plates have been fabricated by the sheet extrusion process, and the industrial implementation of this process has been described.
- The properties of thermoplastic composites developed in this study have been compared with commercially available bipolar plate materials, and it was found that they are suitable for manufacturing bipolar plates.

6.2 Thesis Contributions

The main thesis contributions of the experimental study can be outlined as follows:

- **Development of electrically conductive thermoplastic-based composite materials for the manufacturing of fuel cell bipolar plates.**

    The electrically conductive thermoplastic composites with different filler formulations were developed using a twin-screw extruder. Bipolar plates should have an adequate level of electrical conductivity in the through-plane direction so that electrons can travel from one cell to another during the fuel cell operation. The target of electrical conductivity for this research was a minimum of 25 S/cm in through-plane directions with a flexural strength of more than 25 MPa. Multiple conductive fillers, including graphite, CF, MWCNT, CB, and EG, were added to the polymer matrix in different formulations. A number of formulations meeting or exceeding the target values were successfully developed in this thesis and are listed in Table 4.18. The composite formulation with 36 wt.% graphite, 30 wt.% EG, 5 wt.% CB, 4 wt.%, and 25 wt.% PP has the TPEC value of 39.6 S/cm with a flexural strength of 29.4 MPa. This formulation is the best in terms of TPEC values. However, this formulation is also the most expensive in terms of material cost. The formulation with 82.5 wt.% graphite, 2.5 wt.%, and 15 wt.% PP has the TPEC and flexural strength values of 25.7 S/cm and 34.8 MPa, respectively. This composite formulation has the required properties with the lowest material cost and the highest flexural strength. The polymer content of this material, however, is only 15 weight percent, making processing difficult.

- **Development of composites by using different thermoplastic resins with different types of binary fillers to investigate the influence of matrix and filler bonding interaction on the properties of electrically conductive thermoplastic composites.**

The effects of filler compositions on the electrical and mechanical properties of the composites were investigated. Thermoplastic composites were produced with PP, nylon, and TPU resins containing different amounts of graphite and CB. Increasing the filler loading improved the conductivity network inside the composite but adversely affected its mechanical performance. TPU composites demonstrated better electrical properties at higher filler loading, while nylon composites demonstrated superior mechanical properties. PP composites offered balanced electrical and mechanical properties. The synergistic effects of filler interaction were examined by adding graphite, CB, CF, MWCNT, and EG to the PP matrix in binary, ternary, and quaternary filler formulations. CB and MWCNT demonstrated promising effects on the electrical conductivity of the composites. Surprisingly, MWCNT had an adverse effect on flexural strength. The main issue was the agglomeration of MWCNT particles which affected the mechanical performance of the composites. The addition of EG had no significant effect on the properties of the composites. The vermicular shape, porous structure, and high aspect ratio of EG particles generates the conductive path that increases electrical conductivity. The high shear force generated during the melt-compounding inside the twin-screw extruder damage the porous structure of EG and reduce the effectiveness of EG particles. CF was added to increase the flexural strength of the composites, but no significant effects were observed. An important factor affecting the properties of the CF reinforce composites is the length of CF particles. The length of CF was reduced from 6 mm to 200 microns during the melt mixing.

- **Development of a statistical model for evaluating the effects of filler contents in the composites to achieve the optimum values of electrical conductivity and flexural strength by utilizing ANOVA and RSM**

An optimization study was conducted in order to determine a filler formulation that can provide the most suitable values of electrical conductivity and flexural strength. MWCNT, EG, and CB compositions were the control input factors of the optimization study. A full factorial design of the L-27 orthogonal array was used as a design of experiments. Electrical conductivity and flexural strength of the composites were used as output responses. ANOVA was performed to examine the significance of each filler.

The significance of MWCNT and CB compositions was validated at a 99% confidence level. By processing the experimental results using Response Surface Methodology (RSM), an empirical model was developed that demonstrated an average accuracy of 83.9% and 93.4% for predicting the values of electrical conductivity and flexural strength, respectively.

- **Development of thermoplastic composite bipolar plates by sheet extrusion process.**

    Limited samples of bipolar plates were developed by fabricating (embossing) the gas flow channels on the surface of extruded composite sheets in order to ascertain the viability of the manufacturing process. A sheet die was attached to a 1-inch diameter single screw extruder, having an L/D ratio of 30, for the extrusion of the composite material sheet. The pellets of the composite material compounded on the twin-screw extruder were used in the single screw extruder as the feedstock for producing the composite sheets. A metallic mold plate was used to successfully emboss the flow channels on the surface of the extruded sheets using a heated plate compression molding system. This demonstrated the feasibility of fabricating bipolar plates from the electrically conductive thermoplastic composite. The purpose of this study was to present a method that can produce bipolar plates on an industrial scale. This process can be modified and implemented on an industrial scale to produce bipolar plates at a very high production rate. The industrial-scale implementation of this method has been described in Section 5.5.

6.3 Future Recommendations

Based on the findings of this thesis, the following are the recommendations for future studies:

- Development and manufacturing of a sheet die equipped with a downstream mechanism for the sheet extrusion that can emboss bipolar plate flow channels on the surfaces of hot extruded sheets.

- Development of a modified screw design for the twin-screw extruder to maintain the length of the carbon fiber particles during the melt-compounding process.

- Composite materials that have been produced and examined in this study should be used in a pilot fuel cell to investigate their effects on the performance of the fuel cell.

- Incorporation of toughness modifiers in the polymer resin and to improve the flexural strength and toughness of the composites. Also, investigation of the effect of wetting angles of the filler on the properties of the composites.

References

[1] B. Cunningham, J. Huang, D. Baird, Review of materials and processing methods used in the production of bipolar plates for fuel cells, International Materials Reviews. 52 (2007) 1–13.

[2] A. Hermann, T. Chaudhuri, P. Spagnol, Bipolar plates for PEM fuel cells: A review, International Journal of Hydrogen Energy. 30 (2005) 1297–1302.

[3] T. Wilberforce, O. Ijaodola, E. Ogungbemi, Z. El Hassan, J. Thompson, A.G. Olabi, Effect of bipolar plate materials on performance of fuel cells, in: Reference Module in Materials Science and Materials Engineering, Elsevier Inc., 2018: pp. 1–15.

[4] W. Daud, R. Rosli, E. Majlan, S. Hamid, R. Mohamed, T. Husaini, PEM fuel cell system control: A review, Renewable Energy. 113 (2017) 620–638.

[5] J. Larminie, A. Dicks, M.S. McDonald, Fuel cell systems explained, J. Wiley Chichester, UK, 2003.

[6] G. Karanfil, Importance and applications of DOE/optimization methods in PEM fuel cells: A review, International Journal of Energy Research. 44 (2020) 4–25.

[7] F.G. Boyaci San, G. Tekin, A review of thermoplastic composites for bipolar plate applications, International Journal of Energy Research. 37 (2013) 283–309.

[8] H. Kahraman, M.F. Orhan, Flow field bipolar plates in a proton exchange membrane fuel cell: Analysis & modeling, Energy Conversion and Management. 133 (2017) 363–384.

[9] R. Yeetsorn, M.W. Fowler, C. Tzoganakis, A review of thermoplastic composites for bipolar plate materials in PEM fuel cells, Nanocomposites with Unique Properties and Applications in Medicine and Industry. (2011).

[10] H. Tsuchiya, O. Kobayashi, Mass production cost of PEM fuel cell by learning curve, International Journal of Hydrogen Energy. 29 (2004) 985–990.

[11] F. Mighri, M.A. Huneault, M.F. Champagne, Electrically conductive thermoplastic blends for injection and compression molding of bipolar plates in the fuel cell application, Polymer Engineering & Science. 44 (2004) 1755–1765.

[12] R.L. Borup, N.E. Vanderborgh, Design and testing criteria for bipolar plate materials for PEM fuel cell applications, Los Alamos National Lab., NM (United States), 1995.

[13] V. Mehta, J.S. Cooper, Review and analysis of PEM fuel cell design and manufacturing, Journal of Power Sources. 114 (2003) 32–53.

[14] L.-T. Chang, T.-H. Yu, H.-H. Huang, Y.-Y. Su, C.-C. Tseng, H.-J. Tsai, W.-K. Hsu, Electrolyte adsorption improved thermoelectric power of non-conductive polymer/carbon nanotubes composites, Journal of Power Sources. 450 (2020) 227651.

[15] J.A. King, B.A. Johnson, M.D. Via, C.J. Ciarkowski, Electrical conductivity of carbon-filled polypropylene-based resins, Journal of Applied Polymer Science. 112 (2009) 425–433. https://doi.org/10.1002/app.29422.

[16] C. Chen, J. Kuo, Nylon 6/CB polymeric conductive plastic bipolar plates for PEM fuel cells, Journal of Applied Polymer Science. 101 (2006) 3415–3421.

[17] A. Heinzel, F. Mahlendorf, O. Niemzig, C. Kreuz, Injection moulded low cost bipolar plates for PEM fuel cells, Journal of Power Sources. 131 (2004) 35–40.

[18] J. Chen, Y. Zhu, Z. Guo, A.G. Nasibulin, Recent Progress on Thermo-electrical Properties of Conductive Polymer Composites and Their Application in

Temperature Sensors, Engineered Science. 12 (2020) 13–22. https://doi.org/10.30919/es8d1129.

[19] Utkarsh, H. Hegab, M. Tariq, N.A. Syed, G. Rizvi, R. Pop-Iliev, Towards Analysis and Optimization of Electrospun PVP (Polyvinylpyrrolidone) Nanofibers, Advances in Polymer Technology. 2020 (2020) 4090747. https://doi.org/10.1155/2020/4090747.

[20] N.A.M. Radzuan, A.B. Sulong, T. Husaini, E.H. Majlan, M.I. Rosli, M.F. Aman, Fabrication of multi-filler MCF/MWCNT/SG-based bipolar plates, Ceramics International. 45 (2019) 7413–7418.

[21] M. Tariq, Utkarsh, N.A. Syed, A. Baten, A.H. Behravesh, G. Rizvi, R. Pop-Iliev, Effect of Filler Content on the Electrical Conductivity of Graphite Based Composites, in: Proceedings of SPE ANTEC 2021, United States, 2021.

[22] B. Hu, F.-L. Chang, L.-Y. Xiang, G.-J. He, X.-W. Cao, X.-C. Yin, High performance polyvinylidene fluoride/graphite/multi-walled carbon nanotubes composite bipolar plate for PEMFC with segregated conductive networks, International Journal of Hydrogen Energy. (2021).

[23] B.D. Cunningham, D.G. Baird, Development of bipolar plates for fuel cells from graphite filled wet-lay material and a compatible thermoplastic laminate skin layer, Journal of Power Sources. 168 (2007) 418–425.

[24] O. Ayotunde Alo, I. Olatunji Otunniyi, Hc. Pienaar, E. Rotimi Sadiku, Electrical and mechanical properties of polypropylene/epoxy blend-graphite/carbon black composite for proton exchange membrane fuel cell bipolar plate, Materials Today: Proceedings. 38 (2021) 658–662. https://doi.org/10.1016/j.matpr.2020.03.642.

[25] S. Dhakate, S. Sharma, N. Chauhan, R. Seth, R. Mathur, CNTs nanostructuring effect on the properties of graphite composite bipolar plate, International Journal of Hydrogen Energy. 35 (2010) 4195–4200.

[26] A. Adloo, M. Sadeghi, M. Masoomi, H.N. Pazhooh, High performance polymeric bipolar plate based on polypropylene/graphite/graphene/nano-carbon black composites for PEM fuel cells, Renewable Energy. 99 (2016) 867–874.

[27] S.R. Dhakate, S. Sharma, M. Borah, R.B. Mathur, T.L. Dhami, Expanded graphite-based electrically conductive composites as bipolar plate for PEM fuel cell, International Journal of Hydrogen Energy. 33 (2008) 7146–7152. https://doi.org/10.1016/j.ijhydene.2008.09.004.

[28] W. Zheng, X. Lu, S. Wong, Electrical and mechanical properties of expanded graphite-reinforced high-density polyethylene, Journal of Applied Polymer Science. 91 (2004) 2781–2788.

[29] M. Wu, L.L. Shaw, A novel concept of carbon-filled polymer blends for applications in PEM fuel cell bipolar plates, International Journal of Hydrogen Energy. 30 (2005) 373–380.

[30] G. Hinds, E. Brightman, Towards more representative test methods for corrosion resistance of PEMFC metallic bipolar plates, International Journal of Hydrogen Energy. 40 (2015) 2785–2791.

[31] D.G. Baird, J. Huang, J.E. McGrath, Polymer electrolyte membrane fuel cells: Opportunities for polymers and composites, Plastics Engineering. 59 (2003) 46–55.

[32] B.S. Baker, H.G. Ghezel-Ayagh, Fuel cell system, (1985).

[33] R. Rosli, A. Sulong, W. Daud, M. Zulkifley, T. Husaini, M. Rosli, E. Majlan, M. Haque, A review of high-temperature proton exchange membrane fuel cell (HT-PEMFC) system, International Journal of Hydrogen Energy. 42 (2017) 9293–9314.

[34] A. Kulikovsky, Voltage loss in bipolar plates in a fuel cell stack, Journal of Power Sources. 160 (2006) 431–435.

[35] Z. Tao, Y. Yange, S. Yawei, M. Guozhe, W. Fuhui, Advances of the analysis methodology for electrochemical noise, Journal of Chinese Society for Corrosion and Protection. 34 (2014) 1–18.

[36] Y. Wang, Metallic bipolar plates for proton exchange membrane (PEM) fuel cells, (2008).

[37] J. Wind, R. Späh, W. Kaiser, G. Böhm, Metallic bipolar plates for PEM fuel cells, Journal of Power Sources. 105 (2002) 256–260.

[38] D. Davies, P. Adcock, M. Turpin, S. Rowen, Bipolar plate materials for solid polymer fuel cells, Journal of Applied Electrochemistry. 30 (2000) 101–105.

[39] R.C. Makkus, A.H. Janssen, F.A. de Bruijn, R.K. Mallant, Use of stainless steel for cost competitive bipolar plates in the SPFC, Journal of Power Sources. 86 (2000) 274–282.

[40] H. Wang, J.A. Turner, Ferritic stainless steels as bipolar plate material for polymer electrolyte membrane fuel cells, Journal of Power Sources. 128 (2004) 193–200.

[41] H. Wang, M.A. Sweikart, J.A. Turner, Stainless steel as bipolar plate material for polymer electrolyte membrane fuel cells, Journal of Power Sources. 115 (2003) 243–251.

[42] J.A. Heiser, J.A. King, J.P. Konell, L.L. Sutter, Electrical conductivity of carbon filled nylon 6, 6, Advances in Polymer Technology: Journal of the Polymer Processing Institute. 23 (2004) 135–146.

[43] M.S. Wilson, D.N. Busick, Composite bipolar plate for electrochemical cells, (2001).

[44] C.-Y. Yen, S.-H. Liao, Y.-F. Lin, C.-H. Hung, Y.-Y. Lin, C.-C.M. Ma, Preparation and properties of high performance nanocomposite bipolar plate for fuel cell, Journal of Power Sources. 162 (2006) 309–315.

[45] G.J. Koncar, L.G. Marianowski, Proton exchange membrane fuel cell separator plate, (1999).

[46] T.M. Besmann, T.D. Burchell, Bipolar plate/diffuser for a proton exchange membrane fuel cell, (2001).

[47] R. Leaversuch, Fuel cells jolt plastics innovation, Plastics Technology. 47 (2001) 48–53.

[48] M.K. Bisaria, P. Andrin, M. Abdou, Y. Cai, Injection moldable conductive aromatic thermoplastic liquid crystalline polymeric compositions, (2002).

[49] R.J. Lawrance, Low cost bipolar current collector-separator for electrochemical cells, (1980).

[50] E.N. Balko, R.J. Lawrance, Carbon fiber reinforced fluorocarbon-graphite bipolar current collector-separator, (1982).

[51] L. Xia, A. Li, W. Wang, Q. Yin, H. Lin, Y. Zhao, Effects of resin content and preparing conditions on the properties of polyphenylene sulfide resin/graphite composite for bipolar plate, Journal of Power Sources. 178 (2008) 363–367.

[52] R. Dweiri, J. Sahari, Electrical properties of carbon-based polypropylene composites for bipolar plates in polymer electrolyte membrane fuel cell (PEMFC), Journal of Power Sources. 171 (2007) 424–432.

[53] A. Bairan, M.Z. Selamat, S.N. Sahadan, S.D. Malingam, N. Mohamad, Effect of carbon nanotubes loading in multifiller polymer composite as bipolar plate for PEM fuel cell, Procedia Chemistry. 19 (2016) 91–97.

[54] X. Yan, J. Liu, M.A. Khan, S. Sheriff, S. Vupputuri, R. Das, L. Sun, D.P. Young, Z. Guo, Efficient solvent-free microwave irradiation synthesis of highly conductive polypropylene nanocomposites with lowly loaded carbon nanotubes, ES Materials & Manufacturing. 9 (2020) 21–33.

[55] C. Ramírez-Herrera, M. Tellez-Cruz, J. Pérez-González, O. Solorza-Feria, A. Flores-Vela, J. Cabañas-Moreno, Enhanced mechanical properties and corrosion behavior of polypropylene/multi-walled carbon nanotubes/carbon nanofibers nanocomposites for application in bipolar plates of proton exchange membrane fuel cells, International Journal of Hydrogen Energy. (2021).

[56] B. Krause, P. Pötschke, T. Hickmann, Improvement of electrical resistivity of highly filled graphite/PP composite based bipolar plates for fuel cells by addition of carbon black, in: AIP Publishing LLC, 2019: p. 110006.

[57] P. Rzeczkowski, B. Krause, P. Pötschke, Characterization of highly filled PP/graphite composites for adhesive joining in fuel cell applications, Polymers. 11 (2019) 462.

[58] M.Z. Selamat, J. Sahari, N. Muhamad, A. Muchtar, Simultaneous Optimization for Multiple Responses on the Compression Moulding Parameters of Composite Graphite – Polypropylene Using Taguchi Method, Key Engineering Materials. 471–472 (2011) 361–366. https://doi.org/10.4028/www.scientific.net/KEM.471-472.361.

[59] F. Roncaglia, M. Romagnoli, S. Incudini, E. Santini, M. Imperato, L. Spinelli, A. di Bona, R. Biagi, A. Mucci, Graphite-epoxy composites for fuel-cell bipolar plates: Wet vs dry mixing and role of the design of experiment in the optimization of molding parameters, International Journal of Hydrogen Energy. 46 (2021) 4407–4416. https://doi.org/10.1016/j.ijhydene.2020.10.272.

[60] F.G. Boyaci San, I. Isik-Gulsac, O. Okur, Analysis of the polymer composite bipolar plate properties on the performance of PEMFC (polymer electrolyte membrane fuel cells) by RSM (response surface methodology), Energy. 55 (2013) 1067–1075. https://doi.org/10.1016/j.energy.2013.03.076.

[61] Nylon (PA6)-1013NW8 by UBE®, (n.d.). https://www.ube.com/contents/en/chemical/nylon/chemical_injection/1013nw8.html .

[62] PP-3620WZ by Total Petrochemicals Inc., (n.d.). https://polymers.totalenergies.com/3620wz.

[63] Bapolene® PP5082 Polypropylene, (n.d.). http://lookpolymers.com/polymer_Bapolene-PP5082-Polypropylene-Injection-Grade.php.

[64] Testing protocol for composite bipolar plates, Fuel Cells Bulletin. 2003 (2003) 5. https://doi.org/10.1016/S1464-2859(03)01115-5.

[65] L.-C. Jia, D.-X. Yan, C.-H. Cui, X. Jiang, X. Ji, Z.-M. Li, Electrically conductive and electromagnetic interference shielding of polyethylene composites with

devisable carbon nanotube networks, Journal of Materials Chemistry C. 3 (2015) 9369–9378.

[66] O.A. Alo, I.O. Otunniyi, Hc. Pienaar, Development of graphite-filled polymer blends for application in bipolar plates, Polymer Composites. 41 (2020) 3364–3375.

[67] R.A. Antunes, M.C. De Oliveira, G. Ett, V. Ett, Carbon materials in composite bipolar plates for polymer electrolyte membrane fuel cells: A review of the main challenges to improve electrical performance, Journal of Power Sources. 196 (2011) 2945–2961.

[68] W. Thongruang, R.J. Spontak, C.M. Balik, Correlated electrical conductivity and mechanical property analysis of high-density polyethylene filled with graphite and carbon fiber, Polymer. 43 (2002) 2279–2286.

[69] S.-H. Liao, C.-Y. Yen, C.-C. Weng, Y.-F. Lin, C.-C.M. Ma, C.-H. Yang, M.-C. Tsai, M.-Y. Yen, M.-C. Hsiao, S.-J. Lee, Preparation and properties of carbon nanotube/polypropylene nanocomposite bipolar plates for polymer electrolyte membrane fuel cells, Journal of Power Sources. 185 (2008) 1225–1232.

[70] K. Kang, S. Park, S. Cho, K. Choi, H. Ju, Development of lightweight 200-W direct methanol fuel cell system for unmanned aerial vehicle applications and flight demonstration, Fuel Cells. 14 (2014) 694–700.

[71] P. Pötschke, A.R. Bhattacharyya, A. Janke, H. Goering, Melt mixing of polycarbonate/multi-wall carbon nanotube composites, Composite Interfaces. 10 (2003) 389–404.

[72] K. Wu, Y. Xue, W. Yang, S. Chai, F. Chen, Q. Fu, Largely enhanced thermal and electrical conductivity via constructing double percolated filler network in polypropylene/expanded graphite–Multi-wall carbon nanotubes ternary composites, Composites Science and Technology. 130 (2016) 28–35.

[73] K. Sever, I.H. Tavman, Y. Seki, A. Turgut, M. Omastova, I. Ozdemir, Electrical and mechanical properties of expanded graphite/high density polyethylene nanocomposites, Composites Part B: Engineering. 53 (2013) 226–233.

[74] A. Yasmin, J.-J. Luo, I.M. Daniel, Processing of expanded graphite reinforced polymer nanocomposites, Composites Science and Technology. 66 (2006) 1182–1189. https://doi.org/10.1016/j.compscitech.2005.10.014.

[75] B. Debelak, K. Lafdi, Use of exfoliated graphite filler to enhance polymer physical properties, Carbon. 45 (2007) 1727–1734. https://doi.org/10.1016/j.carbon.2007.05.010.

[76] Waseem Khan, Carbon Nanotube-Based Polymer Composites: Synthesis, Properties and Applications, in: Rahul Sharma (Ed.), Carbon Nanotubes, IntechOpen, Rijeka, 2016: p. Ch. 1. https://doi.org/10.5772/62497.

[77] A. Celzard, J. Mareche, G. Furdin, S. Puricelli, Electrical conductivity of anisotropic expanded graphite-based monoliths, Journal of Physics D: Applied Physics. 33 (2000) 3094.

[78] R. Haggenmueller, H. Gommans, A. Rinzler, J.E. Fischer, K. Winey, Aligned single-wall carbon nanotubes in composites by melt processing methods, Chemical Physics Letters. 330 (2000) 219–225.

[79] A.R. Bhattacharyya, T. Sreekumar, T. Liu, S. Kumar, L.M. Ericson, R.H. Hauge, R.E. Smalley, Crystallization and orientation studies in polypropylene/single wall carbon nanotube composite, Polymer. 44 (2003) 2373–2377.
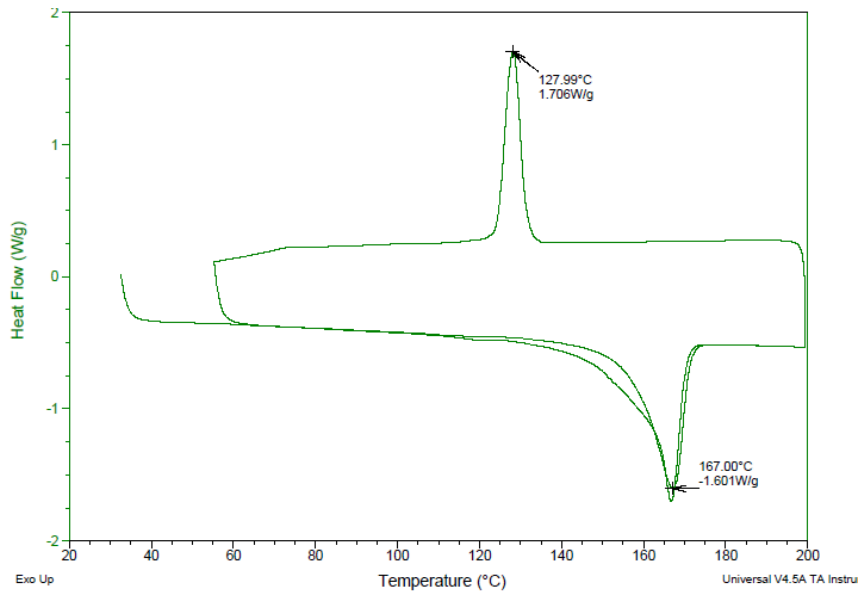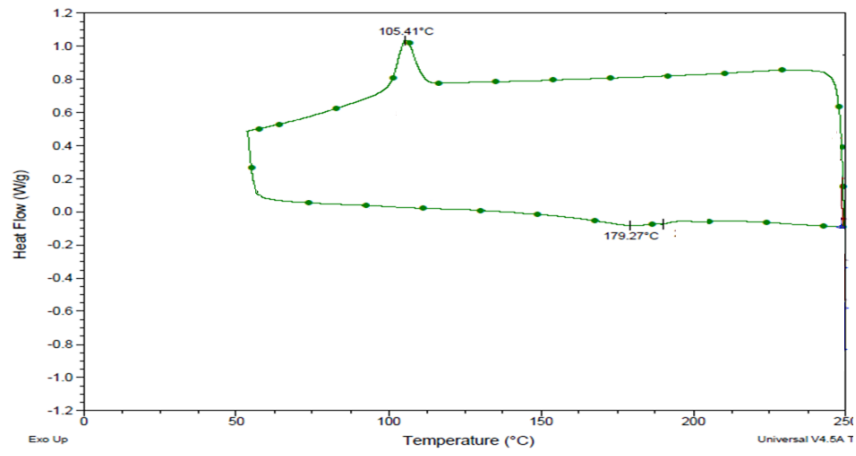
Appendices

Appendix A
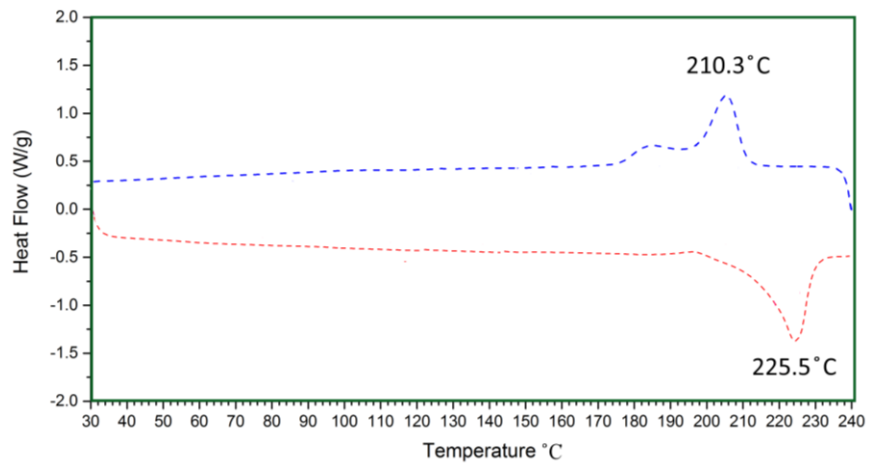
A1. DSC results for copolymer PP resin.
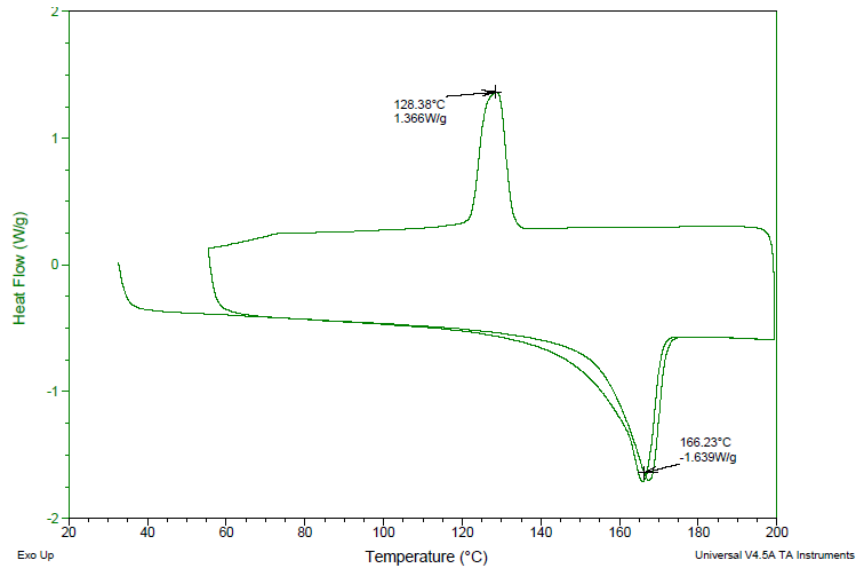
A2. DSC results for homopolymer PP resin.

A3. DSC results for TPU resin.

A4. DSC results for Nylon resin.

Appendix B

B1. Rights and permissions for the figures used in the thesis

CCC Marketplace™

Order Number: 1241516
Order Date: 28 Jun 2022

Payment Information

Muhammad Tariq
muhammad.tariq7@ontariotechu.net
Payment method: Invoice

Billing Address:
Mr. Muhammad Tariq
1820 Dalhousie Crescent
Oshawa, ON L1G8C5
Canada

+1 (289) 886-1692
muhammad.tariq7@ontariotechu.net

Customer Location:
Mr. Muhammad Tariq
1820 Dalhousie Crescent
Oshawa, ON L1G8C5
Canada

Order Details

1. International journal of hydrogen energy

Article: Bipolar plates for PEM fuel cells: A review

Billing Status:
Open

Order License ID	1241516-1	Type of use	Republish in a thesis/dissertation
Order detail status	Completed	Publisher	PERGAMON
ISSN	0360-3199	Portion	Chart/graph/table/figure

0.00 CAD
Republication Permission

LICENSED CONTENT

Publication Title	International journal of hydrogen energy	Rightsholder	Elsevier Science & Technology Journals
Article Title	Bipolar plates for PEM fuel cells: A review	Publication Type	Journal
Author/Editor	INTERNATIONAL ASSOCIATION FOR HYDROGEN ENERGY.	Start Page	1297
		End Page	1302
		Issue	12
Date	01/01/1976	Volume	30
Language	English		
Country	United Kingdom of Great Britain and Northern Ireland		

REQUEST DETAILS

Portion Type	Chart/graph/table/figure	Distribution	Worldwide

Number of charts / graphs / tables / figures requested	1	Translation	Original language of publication
Format (select all that apply)	Print, Electronic	Copies for the disabled?	No
Who will republish the content?	Academic institution	Minor editing privileges?	No
Duration of Use	Life of current edition	Incidental promotional use?	No
Lifetime Unit Quantity	Up to 499	Currency	CAD
Rights Requested	Main product		

NEW WORK DETAILS

Title	Development and Characterization of Electrically Conductive Thermoplastic Based Composite materials for Fuel Cell Bipolar Plates	Institution name	Ontario Tech University
		Expected presentation date	2022-07-04
Instructor name	Muhammad Tariq		

ADDITIONAL DETAILS

The requesting person / organization to appear on the license	Muhammad Tariq

REUSE CONTENT DETAILS

Title, description or numeric reference of the portion(s)	Fig. 1. Schematic diagram of a polymer electrolyte membrane fuel cell	Title of the article/chapter the portion is from	Bipolar plates for PEM fuel cells: A review
		Author of portion(s)	Hermann, Allen; Chaudhuri, Tapas; Spagnol, Priscila
Editor of portion(s)	Hermann, Allen; Chaudhuri, Tapas; Spagnol, Priscila		
		Issue, if republishing an article from a serial	12
Volume of serial or monograph	30		
		Publication date of portion	2005-09-01
Page or page range of portion	1297-1302		